Chaotic Maps of Discretized Memristor Circuit Equations

Makoto Itoh [1]
1-19-20-203, Arae, Jonan-ku,
Fukuoka, 814-0101 JAPAN
Email: itoh-makoto@jcom.home.ne.jp

Abstract
In this paper, we show that many well-known chaotic maps can be generated by discretizing the equations of memristor or nonlinear resistor circuits using the Euler method or the central difference method. These examples show that the dynamics of a wide variety of nonlinear maps, such as those found in engineering, physics, chemistry, biology, and ecological systems, are closely related to the discretized memristor or nonlinear resistor circuit equations. Furthermore, the discretized memristor circuit equations also propose the new modified or simplified version of the well-known chaotic maps. We also propose the generalized extended memristor with non-volatility property. To satisfy the non-volatility property, the $v-i$ characteristic of the generalized extended memristor is defined by two bounded functions, namely the resistive-fuse function and the saturation function. Using this element, the discretized two-element memristor circuits can generate any two-dimensional chaotic map. The computer simulations in this paper show that the discretization of the memristor or nonlinear resistor circuit equations is one of the most promising methods to find interesting chaotic maps. Furthermore, some of the discretized three-dimensional circuit equations clearly show the topological structure of the chaotic attractors.

Keywords
chaotic map; discretization; central difference metod; Euler method; memristor; extended memristor; two-terminal device; non-volatility; resistive-fuse function; saturation function; paper-sheet model; Hamiltonian circuit; Van der Pol equation; Chua circuit; Rössler equation; Lorenz equation; Rikitake dynamo system; Hamilton's equation; Hénon-Heiles equation; Hénon map; 2-D Lorenz map; predator-prey model; two-dimensional logistic map; Chossat-Golubitsky symmetry map; fold map; Lozi map; Tinkerbell map; three-dimensional Hénon map; Gumowski-Mira map; Ikeda map; Peter de Jong map; Kawakami map; logistic map; doubling map; Bernoulli shift map; Hopalong Map; Helleman map; Gingerbreadman Map; Yamaguti-Ushiki map; Chirikov standard map; tent map.

1 Introduction

It is well known that discretization of the logistic differential equation using the central difference method produces chaotic behavior for large time steps [1].

In this paper, we first show that many well-known two-dimensional chaotic maps can be obtained by applying the Euler method to discretize the equation of certain types of memristor circuits. We then show that any two-dimensional map can be related to the equation of the two-element memristor circuit with a generalized extended memristor circuit. That is, any two-dimensional map can be transformed into the equation of the memristor circuit using the Euler method. Furthermore, we show that in order for the

[1] He continues his research on the nonlinear dynamics of memristors, although he has no affiliation since his retirement.

generalized extended memristor circuits associated with the chaotic maps to have the non-volatility property, their $v-i$ characteristic curve must be defined by two bounded functions, namely the resistive-fuse function and the saturation function.

We also show that the discretized memristor circuit equations suggest the new modified or simplified version of the well-known chaotic maps. Furthermore, some other interesting two-dimensional chaotic maps can also be obtained by applying the Euler method to discretize the equations of the Hamiltonian circuits and the controlled circuits.

Many examples in this paper show that the dynamics of a wide variety of nonlinear maps, such as those found in engineering, physics, chemistry, biology, and ecological systems, are closely related to the discretized memristor or nonlinear resistor circuit equations. For example, the following maps are relate to the circuit equations: Hénon map, 2-D Lorenz map, predator-prey model, two-dimensional logistic map Chossat-Golubitsky symmetry map, fold map, Lozi map, Tinkerbell map, three-dimensional Hénon map Gumowski-Mira map, Ikeda map, Peter de Jong map, Kawakami map, logistic map, doubling map, Bernoulli shift map, Hopalong Map, Helleman map, Gingerbreadman Map, Yamaguti-Ushiki map, and their simplified or modified maps.

In addition, the memristor and nonlinear resistor circuits, whose discretized equations exhibit chaotic behavior, usually contain at least one active element. The computer simulations in this paper show that the discretization of the memristor or nonlinear resistor circuit equations is one of the most promising methods to find interesting chaotic maps. Furthermore, the chaotic maps of the discretized three-dimensional equations, such as the discretized Rikitake dynamo system, the discretized Lorenz equation, the discretized Rössler equation, and the discretized Chua circuit equation, clearly show the topological structures (paper-sheet models) of the chaotic attractors. That is, they give a different perspective from the one that can be obtained from the continuous-time trajectories.

Finally, we show that the well-known chaotic maps, such as the two-dimensional Yamaguti-Ushiki map, modified Chirikov standard map, and four kinds of Kawakami maps, can be obtained from the discretized Hamiltonian circuit equations. In particular, the discretized Hénon-Heiles equation exhibits very interesting chaotic behavior.

2 Memristors

The Memristor is a 2-terminal electronic device, which was postulated by Chua [2, 3, 4] and found by Strukov et al. [5]. An ideal memristor can be described by a constitutive relation between the charge q and the flux φ,

$$q = g(\varphi) \quad \text{or} \quad \varphi = f(q), \tag{1}$$

where $g(\cdot)$ and $f(\cdot)$ are differentiable scalar-valued functions. Its terminal voltage v and terminal current i are described by (see Fig. 1)

$$i = G(\varphi)v \quad \text{or} \quad v = R(q)i, \tag{2}$$

where

$$v = \frac{d\varphi}{dt} \quad \text{and} \quad i = \frac{dq}{dt}, \tag{3}$$

which represent Faraday's law of induction and its dual law, respectively. Note that the flux $\varphi(t)$, the voltage $v(t)$, the charge $q(t)$, and the current $i(t)$ satisfy the following universal relationships:

$$\varphi(t) = \int_{-\infty}^{t} v(\tau)d\tau \quad \text{and} \quad q(t) = \int_{-\infty}^{t} i(\tau)d\tau. \tag{4}$$

The nonlinear functions $G(\varphi)$ and $R(\varphi)$, called memductance and memristance, respectively, are defined by

$$G(\varphi) \triangleq \frac{dg(\varphi)}{d\varphi}, \quad \text{and} \quad R(q) \triangleq \frac{df(q)}{dq}. \tag{5}$$

They represent the slope of the scalar function $q = g(\varphi)$ and $\varphi = f(q)$, respectively (called the memristor constitutive relation).

Thus, the voltage-controlled ideal memristor is defined by Eq. (1) or the state-dependent Ohm's law and its associated state equation given by (see Fig. 1)

voltage-controlled ideal memristor

$$\left.\begin{aligned} i &= G(\varphi)v, \\ \frac{d\varphi}{dt} &= v. \end{aligned}\right\} \tag{6}$$

Similarly, those for the current-controlled ideal memristor are given by

current-controlled ideal memristor

$$\left.\begin{aligned} v &= R(q)i, \\ \frac{dq}{dt} &= i. \end{aligned}\right\} \tag{7}$$

The classification of the more generalized memristors is shown in Appendix (see also [6, 7]).

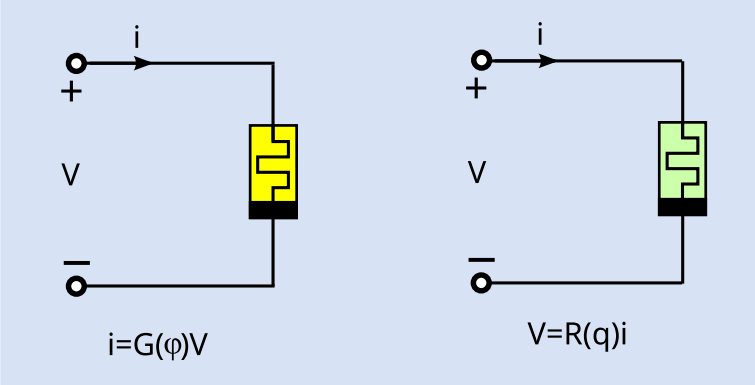

Figure 1: Flux-controlled memristor with the terminal current $i = G(\varphi)\, v$ (left). Charge-controlled memristor with the terminal voltage $v = R(q)\, i$ (right). Here v and i are the voltage across and the current through the ideal memristors, respectively, φ and q are the flux and the charge of the ideal memristors, respectively, and $G(\varphi)$ and $R(\varphi)$ are called the memductance and the memristance, respectively.

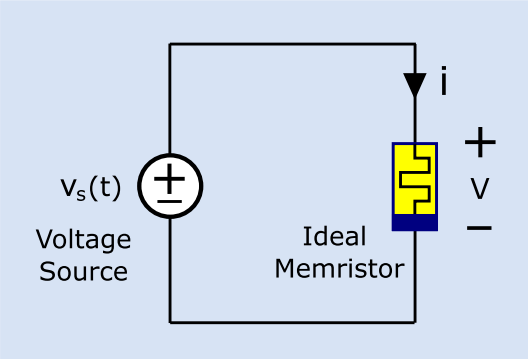

Figure 2: Voltage controlled ideal memristor driven by a voltage source $v_s(t)$, where v and i are the voltage across and the current through the voltage-controlled ideal memristor, respectively.

Let us apply the voltage source $v_s(t)$ to the voltage controlled ideal memristor (6) as shown in Fig. 2. Assume that the output of the voltage source $v_s(t)$ is set to zero for $t \geq t_0$[2], that is,

$$v_s(t) = v(t) = 0 \text{ for } t \geq t_0. \tag{8}$$

Then we obtain

$$\varphi(t) = \varphi(t_0) \quad \text{for} \quad t \geq t_0, \tag{9}$$

since the flux $\varphi(t)$ satisfies $\dfrac{d\varphi}{dt} = v = 0$ for $t \geq t_0$. Thus, if there is a real number $M > 0$ such that

$$\boxed{\mid G(\varphi(t_0)) \mid \leq M, \qquad (10)}$$

then we obtain

$$\boxed{i(t) = G(\varphi(t_0))\, v(t) = 0 \quad \text{for} \quad t \geq t_0, \qquad (11)}$$

since $v(t) = 0$ for $t \geq t_0$.

The charge $q(t)$ also holds the value $q(t_0) = g(\varphi(t_0))$ for $t \geq t_0$, since $\dfrac{dq}{dt} = i = 0$ for $t \geq t_0$. Thus the voltage-controlled ideal memristor (6) exhibits the following non-volatile state:

$$\boxed{\begin{array}{l}\text{non-volatile state} \\ \left.\begin{array}{rcl} v(t) & = & \dfrac{d\varphi(t)}{dt} = 0, \\ i(t) & = & \dfrac{q(t)}{dt} = 0, \\ \varphi(t) & = & \varphi(t_0), \\ q(t) & = & q(t_0), \end{array}\right\} (\text{ for } t \geq t_0). \quad (12)\end{array}}$$

That is, all state variables do not evolve for $t \geq t_0$, and the voltage-controlled ideal memristor (6) has the non-volatility property.

Similarly, if there is a real number $M > 0$ such that

[2]Equivalently, we can assume that the memristor is short-circuited for $t \geq t_0$, that is, $v(t) = 0$ for $t \geq t_0$ [8]).

$$| R(q(t_0)) | \leq M, \qquad (13)$$

then the current-controlled ideal memristor (7) driven by the current source $i_s(t)$ has the non-volatility property, where we set $i_s(t) = 0$ for $t \geq t_0$.

3 Memristor Circuits

It is well known that discretization of the logistic equation using the central difference method produces chaotic behavior for large time steps. In this section, we show that many well-known two-dimensional chaotic maps can be obtained by applying the Euler method to discretize the two-element memristor circuit equations.

3.1 Two-element extended memristor circuits

In this subsection, we use the voltage-controlled extended memristor defined in Appendix (see also [6, 7]). This element is an extended version of the ideal memristor shown in Sec. 2. That is, the $v - i$ characteristic of the voltage-controlled extended memristor is given by

$v - i$ characteristic of the extended memristor

$$\left.\begin{aligned} i &= \hat{G}(x,\ v)v, \\ \frac{dx}{dt} &= \tilde{g}(x,\ v), \end{aligned}\right\} \qquad (14)$$

where i, v, and x denote the terminal current, the terminal voltage, and the state variable of the voltage-controlled memristor, respectively, $\hat{G}(x,\ v)$, and $\hat{g}(x,\ v)$ are continuous scalar-valued functions of the state variables x and v. Thus, Eq. (14) is more complex than Eq. (6).

To study the non-volatility property of the memristors, we apply the voltage source $v_s(t)$ to the voltage controlled extended memristor (14). Assume that the output of the voltage source $v_s(t)$ is set to zero for $t \geq t_0$. Furthermore, we assume that there is a real number M such that

$$| \hat{G}(x,\ 0) | \leq M. \qquad (15)$$

Then $i(t) = \hat{G}(x(t),\ v(t))v(t) = 0$ for $t \geq t_0$ where we set $v_s(t) = v(t) = 0$ for $t \geq t_0$. We also assume that $\tilde{g}(x,\ v)$ satisfies

$$\tilde{g}(x,\ 0) = 0. \qquad (16)$$

Then we obtain

$$x(t) = x(t_0) \ \text{ for } \ t \geq t_0, \qquad (17)$$

since the state $x(t)$ satisfies $\dfrac{dx}{dt} = \tilde{g}(x,\ 0) = 0$ for $t \geq t_0$. That is, $v(t) = i(t) = 0$ and $x(t) = x(t_0)$ for $t \geq t_0$ where we assumed that $v_s(t) = v(t) = 0$ for $t \geq t_0$. In this case, the voltage-controlled extended memristor has the non-volatility property. However, if the condition (16) is not satisfied, then the state $x(t)$ may evolve with time even when the drive signal is set to zero.

Consider next the two-element memristor circuit in Fig. 3, where the $v-i$ characteristic of the voltage-controlled extended memristor (right) is given by Eq. (14). The dynamics of this circuit is given by

Dynamics of the extended memristor circuit

$$\left.\begin{aligned} C\frac{dv}{dt} &= -\hat{G}(x,\ v)v, \\ \frac{dx}{dt} &= \tilde{g}(x,\ v), \end{aligned}\right\} \tag{18}$$

where C is the capacitance of the capacitor, and i, v, and x denote the terminal current, the terminal voltage, and the state variable of the voltage-controlled extended memristor, respectively. For the sake of simplicity, let us set $C=1$. That is, we get

$$\left.\begin{aligned} \frac{dv}{dt} &= -\hat{G}(x,\ v)v, \\ \frac{dx}{dt} &= \tilde{g}(x,\ v). \end{aligned}\right\} \tag{19}$$

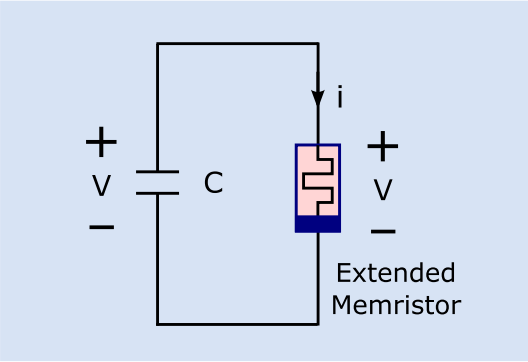

Figure 3: Two-element memristor circuit consisting of a capacitor (left) and a voltage-controlled extended memristor (right), where C is the capacitance of the capacitor and v and i are the voltage across and the current through the voltage-controlled extended memristor, respectively.

Since Eq. (19) is a two-dimensional autonomous system, we cannot expect any chaotic behavior of this system. However, as in the case of the logistic equation, we can expect the chaotic behavior by the discretizing the differential equation (19). So we discretize it using the Euler method defined by

Euler method

$$\left.\begin{aligned} \frac{dv}{dt} &\approx \frac{v(t+\Delta t)-v(t)}{\Delta t}, \\ \frac{dx}{dt} &\approx \frac{x(t+\Delta t)-x(t)}{\Delta t}, \end{aligned}\right\} \tag{20}$$

where Δt is the time step size. Then, we can approximate Eq. (19) by

$$\left.\begin{aligned} \frac{v(t+\Delta t)-v(t)}{\Delta t} &= -\hat{G}\big(x(t),\ v(t)\big)v(t), \\ \frac{x(t+\Delta t)-x(t)}{\Delta t} &= g\big(x(t),\ v(t)\big). \end{aligned}\right\} \tag{21}$$

If we set $\Delta t = 1$, $v_n \triangleq v(t + n\Delta t)$, and $x_n \triangleq x(t + n\Delta t)$ (where n is an integer), then we obtain

$$\left.\begin{array}{rcl} v_1 - v_0 &=& -\hat{G}\big(x_0,\ v_0\big)v_0, \\ x_1 - x_0 &=& g\big(x_0,\ v_0\big), \end{array}\right\}$$
$$\left.\begin{array}{rcl} v_2 - v_1 &=& -\hat{G}\big(x_1,\ v_1\big)v_1, \\ x_2 - x_1 &=& g\big(x_1,\ v_1\big), \end{array}\right\} \qquad (22)$$
$$\vdots \qquad\qquad \vdots$$
$$\left.\begin{array}{rcl} v_{n+1} - v_n &=& -\hat{G}\big(x_n,\ v_n\big)v_n, \\ x_{n+1} - x_n &=& g\big(x_n,\ v_n\big). \end{array}\right\}$$

We can simply write

Discretized equation

$$\left.\begin{array}{rcl} v_{n+1} - v_n &=& -\hat{G}\big(x_n,\ v_n\big)v_n, \\ x_{n+1} - x_n &=& g\big(x_n,\ v_n\big), \end{array}\right\} \qquad (23)$$

where $n = 0, 1, 2, \cdots$. We can rewrite Eq. (23) in the following form

Two-dimensional map

$$\left.\begin{array}{rcl} v_{n+1} &=& \Big\{-\hat{G}\big(x_n,\ v_n\big) + 1\Big\}\, v_n, \\ x_{n+1} &=& g\big(x_n,\ v_n\big) + x_n. \end{array}\right\} \qquad (24)$$

Note that if Δt is sufficiently small, then chaotic behavior is unlikely to be observed in a discretized two-dimensional autonomous system. Thus, we set $\Delta t = 1$.

3.2 Examples of the two-element memristor circuits generating chaotic maps

In this section we show some examples of two-element memristor circuits, which can be transformed into the two-dimensional chaotic maps. In this section, we show some examples of two-element memristor circuits that can be transformed into the two-dimensional chaotic maps. We also investigate whether the memristor circuits have at least one active element. We also study the non-volatility property of memristors.

3.2.1 2-D Lorenz map

Assume that the $v - i$ characteristic of the voltage-controlled extended memristor is given by

$v - i$ characteristic of the extended memristor

$$\left.\begin{array}{rcccl} i &=& \hat{G}(x,\ v)v &\triangleq& (bx - ab)v, \\ \dfrac{dx}{dt} &=& \tilde{g}(x,\ v) &\triangleq& -bx + bv^2, \end{array}\right\} \qquad (25)$$

that is, the two scaler functions $\hat{G}(x,\ v)$ and $\tilde{g}(x,\ v)$ are given by

$$\left.\begin{array}{rcl} \hat{G}(x,\ v) &=& bx - ab, \\ \tilde{g}(x,\ v) &=& -bx + bv^2, \end{array}\right\} \qquad (26)$$

where a and b are constants. The voltage-controlled extended memristor defined by Eq. (25) is an active element, since the instantaneous power consumed by the memristor satisfies

$$P(t) \triangleq v(t)\, i(t) = (bx(t) - ab)v(t)^2 < 0, \tag{27}$$

when $x(t)$ satisfies $bx(t) - ab < 0$.

To study the non-volatility property, we drive the voltage-controlled extended memristor (25) by the voltage source $v_s(t)$ where we set $v_s(t) = v(t) = 0$ for $t \geq t_0$ (as shown in Fig. 2). Then we obtain

$$\frac{dx}{dt} = \tilde{g}(x,\ 0) = -bx, \tag{28}$$

where $t \geq t_0$. If $b > 0$, then the origin, i.e. $x = 0$, becomes the asymptotically stable equilibrium point and $x(t) \to 0$. That is, if the initial condition $x(t_0)$ takes a finite value, then $x(t)$ also takes a finite value for $t \geq t_0$, and there is a real number M such that

$$|\ \hat{G}(x(t),\ 0)\ | = |\ bx(t) - ab\ | \leq M, \tag{29}$$

for $t \geq t_0$. Furthermore, we obtain from Eq. (25)

$$v(t) = i(t) = 0 \ \text{ and } \ x(t) \to 0 \ \text{ for } \ t \geq t_0. \tag{30}$$

Note that if $x(t_0) \neq 0$, then $x(t)$ changes with time. Thus, the voltage-controlled extended memristor (25) does not exhibit the non-volatility property, that is, it is the volatile memristor [9, 10].

The dynamics of the circuit in Fig. 3 is given by

Dynamics of the memristor circuit

$$\left.\begin{array}{rcl} C\dfrac{dv}{dt} &=& -(bx - ab)v, \\ \dfrac{dx}{dt} &=& -bx + bv^2. \end{array}\right\} \tag{31}$$

Assume that $C = 1$. Then from Eq. (23) we obtain

$$\left.\begin{array}{rcl} v_{n+1} - v_n &=& -(bx_n - ab)v_n, \\ x_{n+1} - x_n &=& -bx_n + b{v_n}^2. \end{array}\right\} \tag{32}$$

It can be recast into the 2-D Lorenz map [11, 12]

2-D Lorenz map

$$\left.\begin{array}{rcl} v_{n+1} &=& (1 + ab)v_n - bv_n x_n, \\ x_{n+1} &=& (1 - b)x_n + b{v_n}^2. \end{array}\right\} \tag{33}$$

Thus, we conclude that the 2-D Lorenz map (33) can be generated by discretizing the extended memristor circuit equation (31) using the Euler method. The chaotic behavior of the 2-D Lorenz map (33) is shown in Fig. 4.

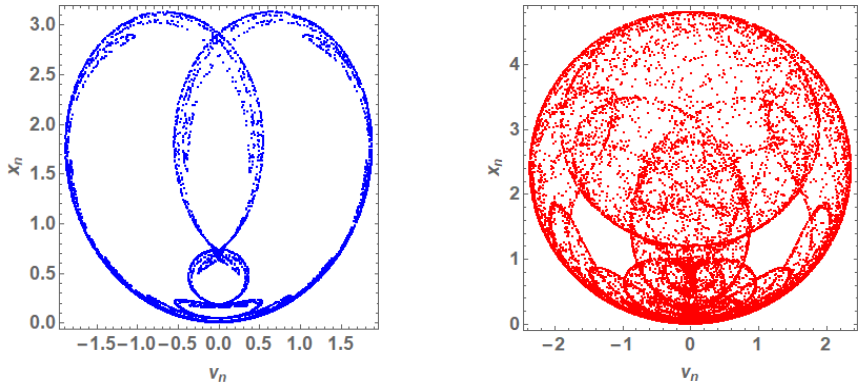

(a) (b)

Figure 4: Chaotic behavior of the 2-D Lorenz map (33) for two different parameters. (a) Parameters: $a = 1.05$, $b = 0.75$. Initial conditions: $v_0 = 0.1$, $x_0 = 0.1$. (b) Parameters: $a = 1.25$, $b = 0.75$. Initial conditions: $v_0 = 0.1$, $x_0 = 0.1$.

3.2.2 Predator-prey model A

Assume that the $v - i$ characteristic of the voltage-controlled extended memristor is given by

$v - i$ characteristic of the extended memristor

$$\left.\begin{array}{rcll} i & = & \hat{G}(x,\ v)v & \triangleq \{1 - a(1 - v - x)\}\, v, \\ \dfrac{dx}{dt} & = & \tilde{g}(x,\ v) & \triangleq \{b(1 + cv) - 1\}\, x, \end{array}\right\} \tag{34}$$

that is, the two scaler functions $\hat{G}(x,\ v)$ and $\tilde{g}(x,\ v)$ are given

$$\left.\begin{array}{rcl} \hat{G}(x,\ v) & = & \{1 - a(1 - v - z)\}\,, \\ \tilde{g}(x,\ v) & = & \{b(1 + cv) - 1\}\, x, \end{array}\right\} \tag{35}$$

where a, b, and c are constants. The voltage-controlled extended memristor defined by Eq. (34) is an active element, since the instantaneous power consumed by the memristor satisfies

$$P(t) \triangleq v(t)\, i(t) = \big\{1 - a\,(1 - v(t) - x(t))\big\} v(t)^2, \tag{36}$$

when $x(t)$ and $v(t)$ satisfy $a\,(1 - v(t) - x(t)) > 1$.

To study the non-volatility property, we drive the voltage-controlled extended memristor (34) by the voltage source $v_s(t)$ where we set $v_s(t) = v(t) = 0$ for $t \geq t_0$. Then we obtain

$$\frac{dx}{dt} = \tilde{g}(x,\ 0) = (b - 1)x, \tag{37}$$

where $t \geq t_0$. If $b < 1$, then the origin becomes the asymptotically stable equilibrium point and $x(t) \to 0$. That is, if the initial condition $x(t_0)$ takes a finite value, then $x(t)$ also takes a finite value for $t \geq t_0$, and there is a real number M such that

$$|\ \hat{G}(x(t),\ 0)\ | = |\ bx(t) - ab\ | \leq M, \tag{38}$$

for $t \geq t_0$. Furthermore, we obtain from Eq. (34)

$$v(t) = i(t) = 0 \quad \text{and} \quad x(t) \to 0 \quad \text{for} \quad t \geq t_0. \qquad (39)$$

If $x(t_0) \neq 0$, then $x(t)$ changes with time. Thus, the voltage-controlled extended memristor (34) does not exhibit the non-volatility property, that is, it is the volatile memristor [9, 10].

The dynamics of the circuit in Fig. 3 is given by

Dynamics of the memristor circuit

$$\left.\begin{aligned} C\frac{dv}{dt} &= \{a(1-v-x)-1\}\,v, \\ \frac{dx}{dt} &= \{b(1+cv)-1\}\,x, \end{aligned}\right\} \qquad (40)$$

where we assume that $C = 1$. From Eq. (24), we obtain

$$\left.\begin{aligned} v_{n+1} - v_n &= \{a(1-v_n-x_n)-1\}\,v_n, \\ x_{n+1} - x_n &= \{b(1+cv_n)-1\}\,x_n. \end{aligned}\right\} \qquad (41)$$

It can be recast into the predator-prey model A [13, 14, 15]

Predator-prey model A

$$\left.\begin{aligned} v_{n+1} &= av_n(1-v_n-x_n), \\ x_{n+1} &= bx_n(1+cv_n). \end{aligned}\right\} \qquad (42)$$

The chaotic behavior of the Predator-prey model A (42) is shown in Fig. 5.

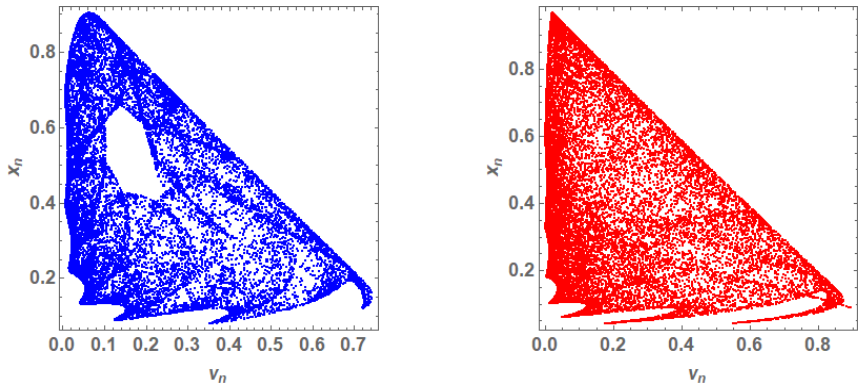

(a) (b)

Figure 5: Chaotic behavior of the predator-prey model A (42) for two different parameters. (a) Parameters: $a = 3.6$, $b = 0.55$, $c = 5.0$. Initial conditions: $v_0 = 0.1$, $x_0 = 0.1$. (b) Parameters: $a = 4$, $b = 0.55$, $c = 5.0$. Initial conditions: $v_0 = 0.1$, $x_0 = 0.1$.

3.2.3 Predator-prey model B

Assume that the $v-i$ characteristic of the voltage-controlled extended memristor is given by

$v-i$ characteristic of the extended memristor

$$\left.\begin{array}{rcll} i & = & \hat{G}(x,\ v)v & \triangleq & (1-bx)v, \\ \dfrac{dx}{dt} & = & \tilde{g}(x,\ v) & \triangleq & a(1-x)(1-v)-x, \end{array}\right\} \tag{43}$$

that is, the two scaler functions $\hat{G}(x,\ v)$ and $\tilde{g}(x,\ v)$ are given

$$\left.\begin{array}{rcl} \hat{G}(x,\ v) & = & 1-bx, \\ \tilde{g}(x,\ v) & = & a(1-x)(1-v)-x, \end{array}\right\} \tag{44}$$

where a and b are constants. The voltage-controlled extended memristor defined by Eq. (43) is an <u>active element</u>, since the instantaneous power consumed by the memristor satisfies

$$P(t) \triangleq v(t)\, i(t) = (1-bx(t))v(t)^2 < 0, \tag{45}$$

when $x(t)$ satisfies $bx(t) > 1$.

To study the non-volatility property, we drive the voltage-controlled extended memristor (43) by the voltage source $v_s(t)$ where we set $v_s(t) = v(t) = 0$ for $t \geq t_0$. Then we obtain

$$\begin{array}{rcl} \dfrac{dx}{dt} & = & \tilde{g}(x,\ 0) = a(1-x)-x \\ & = & -(a+1)\left(x - \dfrac{a}{a+1}\right), \end{array} \tag{46}$$

where $t \geq t_0$. If $a > 0$, then $x(t)$ tends to the asymptotically stable equilibrium point $\dfrac{a}{a+1}$, and there is a real number M such that

$$\mid \hat{G}(x(t),\ 0) \mid = \mid bx(t) - ab \mid \leq M, \tag{47}$$

for $t \geq t_0$. Therefore, we obtain from Eq. (43)

$$v(t) = i(t) = 0 \ \text{ and } \ x(t) \to \frac{a}{a+1} \ \text{ for } \ t \geq t_0. \tag{48}$$

If $x(t_0) \neq \dfrac{a}{a+1}$, then $x(t)$ changes with time. Thus, the voltage-controlled extended memristor (43) does not exhibit the non-volatility property. that is, it is the <u>volatile</u> memristor [9, 10].

The dynamics of the circuit in Fig. 3 is given by

Dynamics of the memristor circuit

$$\left.\begin{array}{rcl} C\dfrac{dv}{dt} & = & -(1-bx)v, \\ \dfrac{dx}{dt} & = & a(1-x)(1-v), \end{array}\right\} \tag{49}$$

where we assume that $C = 1$.

From Eq. (24), we obtain

$$\left.\begin{array}{rcl} v_{n+1} - v_n & = & -(1-bx_n)v_n, \\ x_{n+1} - x_n & = & a(1-x_n)(1-v_n) - x_n. \end{array}\right\} \tag{50}$$

It can be transformed into another kind of predator-prey model B [13]:

Predator-prey model B

$$\left.\begin{aligned} v_{n+1} &= b v_n x_n, \\ x_{n+1} &= a(1-x_n)(1+v_n). \end{aligned}\right\} \tag{51}$$

The chaotic behavior of the Predator-prey model B (51) is shown in Fig. 6.

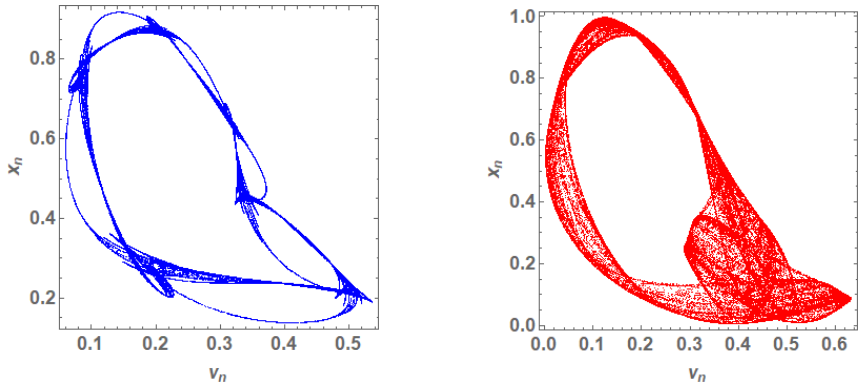

(a) (b)

Figure 6: Chaotic behavior of the predator-prey model B (51) for two different parameters. (a) Parameters: $a = 0.86$, $b = 4.28$. Initial conditions: $v_0 = 0.1$, $x_0 = 0.1$. (b) Parameters: $a = 0.86$, $b = 4.42$. Initial conditions: $v_0 = 0.1$, $x_0 = 0.1$.

3.2.4 Two-dimensional logistic map

Assume that the $v - i$ characteristic of the voltage-controlled extended memristor is given by

$v - i$ characteristic of the extended memristor

$$\left.\begin{aligned} i &= \hat{G}(x,\ v)v \ \triangleq\ -r(3x+1)(1-v)v - v, \\ \frac{dx}{dt} &= \tilde{g}(x,\ v) \ \triangleq\ r\Big[3r(3x+1)v(1-v)+1\Big](1-x)x - x, \end{aligned}\right\} \tag{52}$$

that is, the two scaler functions $\hat{G}(x,\ v)$ and $\tilde{g}(x,\ v)$ are given

$$\left.\begin{aligned} \hat{G}(x,\ v) &= -r(3x+1)(1-v) - 1, \\ \tilde{g}(x,\ v) &= r\Big[3r(3x+1)(1-v)v+1\Big](1-x)x - x, \end{aligned}\right\} \tag{53}$$

where $r = 1.19$.

The voltage-controlled extended memristor defined by Eq. (52) is an active element, since the instantaneous power consumed by the memristor satisfies

$$P(t) \triangleq v(t)\, i(t) = -\big\{r(3x(t)+1)(1-v(t))+1\big\}v(t)^2 < 0, \tag{54}$$

when $x(t)$ and $v(t)$ satisfy $\big\{r(3x(t)+1)(1-v(t))+1\big\} > 0$.

To study the non-volatility property, we drive the voltage-controlled extended memristor (52) by the voltage source $v_s(t)$ where we set $v_s(t) = v(t) = 0$ for $t \geq t_0$. Then we obtain

$$\frac{dx}{dt} = \tilde{g}(x,\ 0) = r(1-x)x - x = -rx\left(x - \frac{r-1}{r}\right). \tag{55}$$

It has two equilibrium points $p_1 = 0$ and $p_2 = \dfrac{r-1}{r} \approx 0.159664$. The equilibrium point p_1, that is, the origin is unstable and the equilibrium point p_2 is asymptotically stable. Therefore, we obtain

$$\left.\begin{array}{ll} \text{if } \; x(t_0) < 0 & x(t) \to -\infty, \\ \text{if } \; x(t_0) = 0 & x(t) = 0, \\ \text{if } \; x(t_0) > 0 & x(t) \to \dfrac{r-1}{r} > 0. \end{array}\right\} \tag{56}$$

That is, if $x(t_0) > 0$, then $x(t)$ is bounded for $t \geq t_0$, and there is a real number M such that

$$\mid \hat{G}(x(t),\ 0) \mid = \mid r(3x(t)+1)+1 \mid \leq M, \tag{57}$$

for $t \geq t_0$. Thus, we obtain from Eq. (52)

$$v(t) = i(t) = 0 \ \text{ and } \ x(t) \to \frac{r-1}{r} \ \text{ for } \ t \geq t_0, \tag{58}$$

where $v_s(t) = v(t) = 0$ for $t \geq t_0$.

If $x(t_0)$ is not at the equilibrium point, then $x(t)$ changes with time. However, since $x(t)$ satisfies Eq.(56), the sign of $x(t)$ remains unchanged, that is,

$$\text{sgn}(x(t)) = \left\{\begin{array}{rll} 1 & if & x(t_0) > 0, \\ 0 & if & x(t_0) = 0, \\ -1 & if & x(t_0) < 0, \end{array}\right. \tag{59}$$

even if $v_s(t) = v(t) = 0$ for $t \geq t_0$, where $\text{sgn}(\cdot)$ denotes a sign function. Thus, the voltage-controlled extended memristor (52) exhibits the discrete non-volatility (see [7, 17] for more details).

The dynamics of the circuit in Fig. 3 is given by

Dynamics of the memristor circuit

$$\left.\begin{array}{rcl} C\dfrac{dv}{dt} & = & r(3x+1)(1-v)v - v, \\ \dfrac{dx}{dt} & = & r\Big[3r(3x+1)(1-v)v+1\Big](1-x)x - x, \end{array}\right\} \tag{60}$$

where we assume that $C = 1$. From Eq. (24), we obtain

$$\left.\begin{array}{rcl} v_{n+1} - v_n & = & r(3x_n+1)(1-v_n)v_n - v_n, \\ x_{n+1} - x_n & = & r\Big[3r(3x_n+1)(1-v_n)v_n+1\Big](1-x_n)x_n - x_n. \end{array}\right\} \tag{61}$$

It can be written as

$$\left.\begin{array}{rcl} v_{n+1} & = & r(3x_n+1)(1-v_n)v_n, \\ x_{n+1} & = & r\Big[3r(3x_n+1)(1-v_n)v_n+1\Big](1-x_n)x_n. \end{array}\right\} \tag{62}$$

If we replace the term $3r(3x_n+1)(1-v_n)v_n$ by $3v_{n+1}$ in the right-hand side of the second equation, we obtain the two-dimensional logistic map [16]

Two-dimensional logistic map

$$\left.\begin{array}{rcl} v_{n+1} & = & r(3x_n+1)(1-v_n)v_n, \\ x_{n+1} & = & r(3v_{n+1}+1)(1-x_n)x_n. \end{array}\right\} \tag{63}$$

Note that we can obtain $3v_{n+1} = 3r(3x_n+1)(1-v_n)v_n$ from the first equation of Eqs. (62) and (63). The chaotic behavior of the two-dimensional logistic map (63) is shown in Fig. 7.

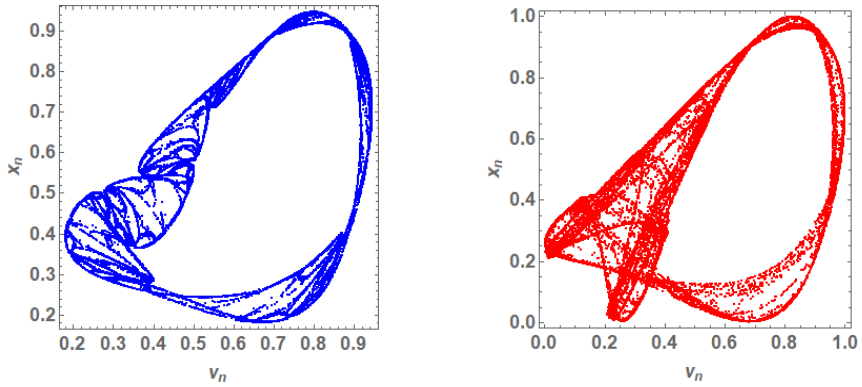

(a) (b)

Figure 7: Chaotic behavior of the two-dimensional logistic map (63) for two different parameters. (a) Parameter: $r = 1.1523$. Initial conditions: $v_0 = 0.8909$, $x_0 = 0.3342$. (b) Parameter: $r = 1.19$. Initial conditions: $v_0 = 0.8909$, $x_0 = 0.3342$.

3.2.5 Chossat-Golubitsky symmetry map

Assume that the $v - i$ characteristic of the voltage-controlled extended memristor is given by

$v - i$ characteristic of the extended memristor

$$\left.\begin{array}{rcll} i & = & \hat{G}(x,\ v)v & \triangleq & -\{(A-1) - 2dx\}v, \\ \dfrac{dx}{dt} & = & \tilde{g}(x,\ v) & \triangleq & (A-1)x + d\left(x^2 - v^2\right), \end{array}\right\} \tag{64}$$

where

$$A = a\left(x^2 + v^2\right) + bx\left(x^2 - 3v^2\right) + c, \tag{65}$$

and a, b, c and d are constants. The two scaler functions $\hat{G}(x,\ v)$ and $\tilde{g}(x,\ v)$ are given by

$$\left.\begin{array}{rcl} \hat{G}(x,\ v) & = & (A-1) - 2dx, \\ \tilde{g}(x,\ v) & = & (A-1)x + d\left(x^2 - v^2\right). \end{array}\right\} \tag{66}$$

The voltage-controlled extended memristor defined by Eq. (64) is an <u>active element</u>, since the instantaneous power consumed by the memristor satisfies

$$P(t) \triangleq v(t)\, i(t) = -\{(A-1) - 2dx(t)\}v(t)^2 < 0, \tag{67}$$

when $x(t)$ satisfies $\{(A-1) - 2dx(t)\} > 0$.

To study the non-volatility property, we drive the voltage-controlled extended memristor (64) by the voltage source $v_s(t)$ where we set $v_s(t) = v(t) = 0$ for $t \geq t_0$. Then we obtain

$$\begin{array}{rcl} \dfrac{dx}{dt} & = & \tilde{g}(x,\ 0) = (A-1)x + d\left(x^2 - v^2\right)\Big|_{v=0} \\ & = & \Big[\{ax^2 + bx^3 + c\} - 1\Big]x + dx^2 \\ & = & bx^4 + ax^3 + dx^2 + (c-1)x, \end{array} \tag{68}$$

where $t \geq t_0$.

(1) Volatility property

Assume that the parameters are given by

$$a = 1,\ b = 0,\ c = -1.9,\ d = 0.4. \qquad (69)$$

Then Eq. (68) has the two unstable equilibrium points $p_1 \approx -1.91$ and $p_2 \approx 1.51$, and it has also the asymptotically stable equilibrium point $p_0 = 0$. Thus, if the initial condition $x(t_0)$ satisfies $p_1 < x(t_0) < p_2$, then $x(t) \to 0$, that is, $x(t)$ is bounded for $t \geq t_0$. Since the function $\hat{G}(x,\ 0)$ is given by

$$\begin{aligned} \hat{G}(x,\ 0) &= \left\{a\left(x^2 + v^2\right) + bx\left(x^2 - 3v^2\right) + c - 1\right\} - 2dx\Big|_{v=0} \\ &= -2dx, \end{aligned} \qquad (70)$$

there exists a real number M such that

$$|\ \hat{G}(x(t),\ 0)\ | = |\ -2dx(t)\ | \leq M, \qquad (71)$$

where $p_1 < x(t_0) < p_2$ and $t \geq t_0$.

Considering that $v_s(t) = v(t) = 0$ for $t \geq t_0$, we obtain

$$i(t) = \hat{G}(x(t),\ v(t))\, v(t) = 0 \quad \text{for} \quad t \geq t_0. \qquad (72)$$

Thus, we conclude

$$v(t) = i(t) = 0 \quad \text{and} \quad x(t) \to 0 \quad \text{for} \quad t \geq t_0. \qquad (73)$$

If we take into account that the state $x(t)$ changes with time, the voltage-controlled extended memristor (64) does not possess the non-volatile property, making it a volatile memristor [9, 10].

(2) Discrete non-volatility property

Assume next that the parameters are given by

$$a = -1,\ b = 0.1,\ c = 1.6, d = -0.8. \qquad (74)$$

Then Eq. (68) has the two asymptotically stable equilibrium points $p_1 \approx -1.74$ and $p_2 \approx 0.478$. It has also the two unstable equilibrium points $p_0 = 0$ and $p_3 \approx 10.7$. Therefore, if $x(t_0) < 0$, then $x(t) \to p_1 < 0$, and if $0 < x(t_0) < p_3$, then $x(t) \to p_2 > 0$. If the initial condition $x(t_0)$ satisfies $0 < x(t_0) < p_3$, then $x(t)$ takes a finite value, and there exists a real number M such that

$$|\ \hat{G}(x(t),\ 0)\ | = |\ -2dx(t)\ | \leq M, \qquad (75)$$

for $t \geq t_0$. Thus, from Eq. (64), we obtain

$$\text{if} \quad x(t_0) < 0, \quad \text{then} \quad v(t) = i(t) = 0 \quad \text{and} \quad x(t) \to p_1 < 0, \qquad (76)$$

and

$$\text{if} \quad 0 < x(t_0) < p_3, \quad \text{then} \quad v(t) = i(t) = 0 \quad \text{and} \quad x(t) \to p_2 > 0, \qquad (77)$$

where $t \geq t_0$. That is, if $x(t_0) < p_3$, then the sign of $x(t)$ remains unchanged for $t \geq t_0$, even if $v_s(t) = v(t) = 0$ for $t \geq t_0$. It is shown that the voltage-controlled extended memristor (64) can exhibit the discrete non-volatility (see [17, 7] for more details).

The dynamics of the circuit in Fig. 3 is given by

Dynamics of the memristor circuit

$$\left.\begin{aligned} C\frac{dv}{dt} &= \{(A-1) - 2dx\}v, \\ \frac{dx}{dt} &= (A-1)x + d\left(x^2 - v^2\right), \end{aligned}\right\} \tag{78}$$

where we assume that $C = 1$ and A is given by Eq. (65).

From Eq. (24), we obtain

$$\left.\begin{aligned} v_{n+1} - v_n &= \{(A-1) - 2dx_n\}v_n, \\ x_{n+1} - x_n &= (A-1)x_n + d\left({x_n}^2 - {v_n}^2\right). \end{aligned}\right\} \tag{79}$$

It can be transformed into the Chossat-Golubitsky symmetry map [18]

Chossat-Golubitsky symmetry map

$$\left.\begin{aligned} v_{n+1} &= Av_n - 2dx_n v_n, \\ x_{n+1} &= Ax_n + d\left({x_n}^2 - {v_n}^2\right). \end{aligned}\right\} \tag{80}$$

The chaotic behavior of the Chossat-Golubitsky symmetry map (80) for two different parameters is shown in Fig. 8.

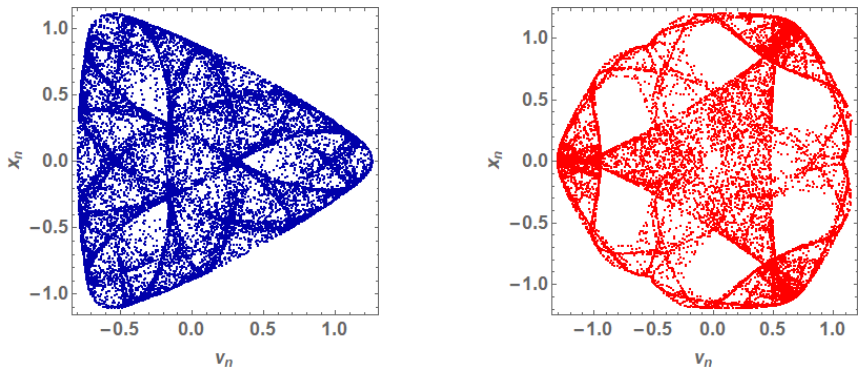

(a) (b)

Figure 8: Chaotic behavior of the Chossat-Golubitsky symmetry map (80) for two different parameters. (a) Parameters: $a = 1,\ b = 0,\ c = -1.9,\ d = 0.4$. Initial conditions: $v_0 = 0.1,\ x_0 = 0.1$. (b) Parameters: $a = -1,\ b = 0.1,\ c = 1.6, d = -0.8$. Initial conditions: $v_0 = 0.1,\ x_0 = 0.1$.

3.2.6 Memristor Hénon map

Assume that the $v - i$ characteristic of the voltage-controlled extended memristor is given by

$v-i$ characteristic of the extended memristor

$$\left.\begin{array}{rcll} i & = & \hat{G}(x,\ v)v & \triangleq \quad (av^2-x)v, \\ \dfrac{dx}{dt} & = & \tilde{g}(x,\ v), & \triangleq \quad bv^2-x, \end{array}\right\} \tag{81}$$

that is, the two scaler functions $\hat{G}(x,\ v)$ and $\tilde{g}(x,\ v)$ are given

$$\left.\begin{array}{rcl} \hat{G}(x,\ v) & = & av^2-x, \\ \tilde{g}(x,\ v) & = & bv^2-x, \end{array}\right\} \tag{82}$$

where a and b are constants. The voltage-controlled extended memristor defined by Eq. (81) is an active element, since the instantaneous power consumed by the memristor satisfies

$$P(t) \triangleq v(t)\, i(t) = \big(av(t)^2 - x(t)\big)v(t)^2 < 0, \tag{83}$$

when $x(t)$ and $v(t)$ satisfy $av(t)^2 - x(t) < 0$.

To study the non-volatility property, we drive the voltage-controlled extended memristor (81) by the voltage source $v_s(t)$ where we set $v_s(t) = v(t) = 0$ for $t \geq t_0$. Then we obtain

$$\frac{dx}{dt} = \tilde{g}(x,\ 0) = -x, \tag{84}$$

where $t \geq t_0$. The origin becomes the asymptotically stable equilibrium point and $x(t) \to 0$. That is, if the initial condition $x(t_0)$ takes a finite value, then $x(t)$ also takes a finite value for $t \geq t_0$, and there is a real number M such that

$$\mid \hat{G}(x(t),\ 0) \mid = \mid -x(t) \mid \leq M, \tag{85}$$

for $t \geq t_0$. Furthermore, we obtain from Eq. (81)

$$v(t) = i(t) = 0 \ \text{ and } \ x(t) \to 0 \ \text{ for } \ t \geq t_0. \tag{86}$$

If $x(t_0) \neq 0$, then $x(t)$ changes with time. Thus, the voltage-controlled extended memristor (81) does not exhibit the non-volatility property, that is, it is the volatile memristor [9, 10].

The dynamics of the circuit in Fig. 3 is given by

Dynamics of the memristor circuit

$$\left.\begin{array}{rcl} C\dfrac{dv}{dt} & = & -(av^2-x)v, \\ \dfrac{dx}{dt} & = & bv^2-x, \end{array}\right\} \tag{87}$$

where we assume that $C = 1$.

From Eq. (23), we obtain

$$\left.\begin{array}{rcl} v_{n+1}-v_n & = & -(av_n{}^2 - x_n)v_n, \\ x_{n+1}-x_n & = & bv_n{}^2 - x_n. \end{array}\right\} \tag{88}$$

It can be recast into the form

Memristor Hénon map

$$\left.\begin{array}{rcl} v_{n+1} & = & (1 - av_n{}^2 + x_n)v_n, \\ x_{n+1} & = & bv_n{}^2. \end{array}\right\} \tag{89}$$

This equation is similar to the Hénon map [19], which is defined by

Hénon map

$$\left.\begin{aligned} v_{n+1} &= 1 - a{v_n}^2 + x_n, \\ x_{n+1} &= b v_n. \end{aligned}\right\} \tag{90}$$

If we multiply v_n on the right side of Eq. (90), we obtain Eq. (89). We study the original Hénon map in Sec. 4.1.2. The chaotic behavior of the memristor Hénon map (89) and the original Hénon map (90) is shown in Fig. 9.

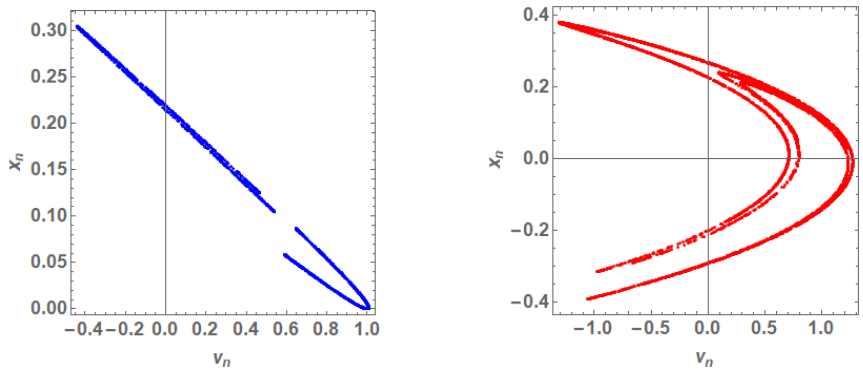

(a) (b)

Figure 9: (a) Chaotic behavior of the memristor Hénon map (89). (b) Chaotic behavior of the original Hénon map (90). Parameters for these two maps: $a = 1.42,\ b = 0.3$. Initial conditions: $v_0 = 0.2,\ x_0 = 0.2$.

3.2.7 Memristor Peter de Jong map

Assume that the $v - i$ characteristic of the voltage-controlled extended memristor is given by

$v - i$ characteristic of the extended memristor

$$\left.\begin{aligned} i &= \hat{G}(x,\ v)v \ \triangleq\ -\Big[\{\sin(a\pi x) - \cos(b\pi v)\} - 1\Big]v, \\ \frac{dx}{dt} &= \tilde{g}(x,\ v), \ \triangleq\ \{\sin(c\pi v) - \cos(d\pi x)\} - x, \end{aligned}\right\} \tag{91}$$

that is, the two scaler functions $\hat{G}(x,\ v)$ and $\tilde{g}(x,\ v)$ are given by

$$\left.\begin{aligned} \hat{G}(x,\ v) &= -\{\sin(a\pi x) - \cos(b\pi v)\} - 1, \\ \tilde{g}(x,\ v) &= \{\sin(c\pi v) - \cos(d\pi x)\} - x, \end{aligned}\right\} \tag{92}$$

where $a,\ b,\ c$ and d are constants. The voltage-controlled extended memristor is an active element, since the instantaneous power consumed by the memristor satisfies

$$P(t) \triangleq v(t)\, i(t) = -\Big[\{\sin(a\pi x(t)) - \cos(b\pi v(t))\} - 1\Big]v(t)^2 < 0, \tag{93}$$

when $x(t)$ and $v(t)$ satisfy $\{\sin(a\pi x(t)) - \cos(b\pi v(t))\} - 1 > 0$.

To study the non-volatility property, we drive the voltage-controlled extended memristor (91) by the voltage source $v_s(t)$ where we set $v_s(t) = v(t) = 0$ for $t \geq t_0$. Then we obtain

$$\frac{dx}{dt} = \tilde{g}(x,\ 0) = -\cos(d\pi x) - x = -\big\{1 + \cos(d\pi x)\big\}x, \tag{94}$$

where $t \geq t_0$. This equation has the equilibrium points at $x = \frac{2m+1}{d}$ $(m = 0,\ \pm 1,\ \pm 2,\ \cdots)$ and $x = 0$. The origin $x = 0$ is an asymptotically stable equilibrium poit. The other equilibrium points are not stable, since

$$\frac{d}{dt}\left(x^2\right) = -2\big\{1 + \cos(d\pi x)\big\}x^2 \leq 0, \tag{95}$$

for $t \geq t_0$, that is, $x(t)^2$ (or equivalently, $\mid x(t) \mid$) does not increase. Thus, if the initial condition satisfies

$$-\frac{1}{d} < x(0) < \frac{1}{d}, \tag{96}$$

that is, $x(0)$ is situated between the two equilibrium points $\pm\frac{1}{d}$, then $x(t) \to 0$. Thus, there is a real number M such that

$$\mid \hat{G}(x(t),\ 0) \mid = \mid bx(t) - ab \mid \leq M, \tag{97}$$

for $t \geq t_0$. Furthermore, we obtain from Eq. (91)

$$v(t) = i(t) = 0 \ \text{ and } \ x(t) \to 0 \ \text{ for } \ t \geq t_0. \tag{98}$$

If $x(t_0)$ is not situated at the equilibrium point, then $x(t)$ changes with time. Thus, the voltage-controlled extended memristor (91) does not exhibit the non-volatility property, that is, it is the volatile memristor [9, 10].

The dynamics of the circuit in Fig. 3 is given by

Dynamics of the memristor circuit

$$\left.\begin{array}{rcl} C\dfrac{dv}{dt} &=& \Big[\{\sin(a\pi x) - \cos(b\pi v)\} - 1\Big]v, \\ \dfrac{dx}{dt} &=& \{\sin(c\pi v) - \cos(d\pi x)\} - x, \end{array}\right\} \tag{99}$$

where we assume that $C = 1$.

From Eq. (23), we obtain

$$\left.\begin{array}{rcl} v_{n+1} - v_n &=& \Big[\{\sin(a\pi x_n) - \cos(b\pi v_n)\} - 1\Big]v_n, \\ x_{n+1} - x_n &=& \{\sin(c\pi v_n) - \cos(d\pi x_n)\} - x_n. \end{array}\right\} \tag{100}$$

It can be recast into the form

Memristor Peter de Jong map

$$\left.\begin{array}{rcl} v_{n+1} &=& \{\sin(a\pi x_n) - \cos(b\pi v_n)\}\, v_n, \\ x_{n+1} &=& \sin(c\pi v_n) - \cos(d\pi x_n). \end{array}\right\} \tag{101}$$

This equation is similar to the Peter de Jong map [20], which is defined by

Peter de Jong map

$$\left.\begin{aligned} v_{n+1} &= \sin(a\pi x_n) - \cos(b\pi v_n), \\ x_{n+1} &= \sin(c\pi v_n) - \cos(d\pi x_n). \end{aligned}\right\} \tag{102}$$

Multiplying v_n on the right side of the first equation of Eq. (102), we obtain Eq. (101). We study the original Peter de Jong map in Sec. 4.1.8. The chaotic behavior of the memristor Peter de Jong map (101) and the original Peter de Jong map (102) is shown in Fig. 10.

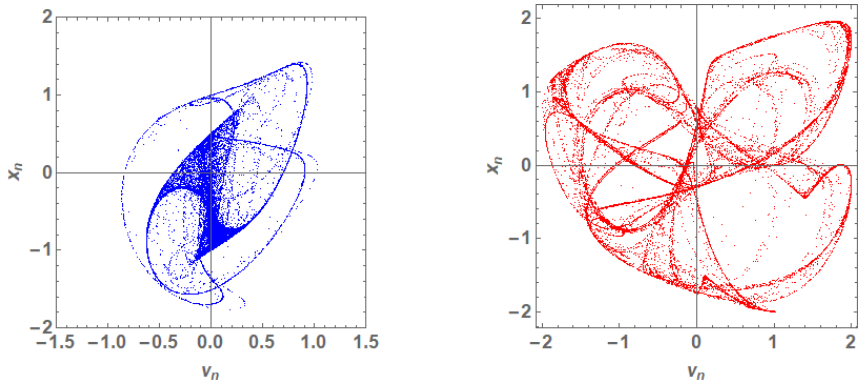

(a) (b)

Figure 10: (a) Chaotic behavior of the memristor Peter de Jong map (101). Parameters: $a = 0.43$, $b = 0.53$, $c = -0.274$, $d = 0.67$. Initial conditions: $v_0 = 1$, $x_0 = 1$. (b) Chaotic behavior of the original Peter de Jong map (102). Parameters: $a = 0.44$, $b = 0.53$, $c = -0.274$, $d = 0.67$. Initial conditions: $v_0 = 1$, $x_0 = 1$.

3.2.8 Memristor Rikitake dynamo system

Assume that the $v - i$ characteristic of the voltage-controlled extended memristor is given by

$v - i$ characteristic of the extended memristor

$$\left.\begin{aligned} i &= \hat{G}(y,\, z,\, v)\, v \;\triangleq\; -(1 - yz)\, v, \\ \frac{dy}{dt} &= \tilde{g}_1(y,\, z,\, v) \;\triangleq\; -by + zv, \\ \frac{dz}{dt} &= \tilde{g}_2(y,\, z,\, v) \;\triangleq\; -bz + yv - ay, \end{aligned}\right\} \tag{103}$$

that is, the scaler functions $\hat{G}(y,\, z,\, v)$ is given by

$$\hat{G}(y,\, z,\, v) = -(1 - yz), \tag{104}$$

where a and b are positive constants. The voltage-controlled extended memristor is an active element, since the instantaneous power consumed by the memristor satisfies

$$P(t) \triangleq v(t)\, i(t) = -\Big(1 - y(t)z(t)\Big)v(t)^2 < 0, \tag{105}$$

when $y(t)$ and $z(t)$ satisfy $y(t)z(t) < 1$.

To study the non-volatility property, we drive the voltage-controlled extended memristor (91) by the voltage source $v_s(t)$ where we set $v_s(t) = v(t) = 0$ for $t \geq t_0$. Then we obtain

$$\begin{aligned} \frac{dy}{dt} &= \tilde{g}_1(y,\, z,\, v) &= -by, \\ \frac{dz}{dt} &= \tilde{g}_2(y,\, z,\, v) &= -bz - ay, \end{aligned} \tag{106}$$

where $t \geq t_0$. This equation has the asymptotically stable equilibrium points at the origin, and therefore $y(t) \to 0$ and $z(t) \to 0$. Thus, there is a real number M such that

$$|\, \hat{G}(y(t),\, z(t),\, 0)\, | = \left|-(1 - y(t)z(t))\right| \leq M, \tag{107}$$

for $t \geq t_0$. Furthermore, we obtain from Eq. (103)

$$v(t) = i(t) = 0 \ \text{ and } \ y(t),\, z(t) \to 0 \ \text{ for } \ t \geq t_0. \tag{108}$$

If $y(t_0)$ and $z(t_0)$is not situated at the origin, then $y(t)$ and $z(t)$ change with time. Thus, the voltage-controlled extended memristor (91) does not exhibit the non-volatility property, that is, it is the volatile memristor [9, 10].

The dynamics of the circuit in Fig. 3 is given by

Dynamics of the memristor Rikitake circuit

$$\left.\begin{aligned} C\frac{dv}{dt} &= (1 - yz)\, v, \\ \frac{dy}{dt} &= -by + zv, \\ \frac{dz}{dt} &= -bz + yv - ay, \end{aligned}\right\} \tag{109}$$

where we assume that $C = 1$. Note that the Rikitake dynamo system is given by

Dynamics of the Rikitake dynamo system

$$\left.\begin{aligned} \frac{dv}{dt} &= 1 - yz, \\ \frac{dy}{dt} &= -by + zv, \\ \frac{dz}{dt} &= -bz + yv - ay. \end{aligned}\right\} \tag{110}$$

Multiplying v on the right side of the first equation of Eq. (110), we obtain Eq. (109).

Using the Euler method, we obtain from Eq. (109)

$$\left.\begin{aligned} v_{n+1} - v_n &= \{(1 - y_n z_n)\, v_n\}\, \Delta t, \\ y_{n+1} - y_n &= (-by_n + z_n v_n)\Delta t, \\ z_{n+1} - z_n &= (-bz_n + y_n v_n - ay_n)\Delta t. \end{aligned}\right\} \tag{111}$$

It can be recast into the form

Discretized memristor Rikitake dynamo equation

$$\left.\begin{aligned} v_{n+1} &= \{(1-y_n z_n)\, v_n\}\Delta t + v_n, \\ y_{n+1} &= (-b y_n + z_n v_n)\Delta t + y_n, \\ z_{n+1} &= (-b z_n + y_n v_n - a y_n)\Delta t + z_n. \end{aligned}\right\} \tag{112}$$

We show the chaotic behavior of the discretized memristor Rikitake dynamo equation (112) in Fig. 11, which clearly shows the topological structure (see the paper-sheet model of Ref. [24]) of the chaotic behavior. We show the chaotic behavior of the discretized Rikitake dynamo equation in Fig. 12, which is given by

Discretized Rikitake dynamo equation

$$\left.\begin{aligned} v_{n+1} &= (1-y_n z_n)\Delta t + v_n, \\ y_{n+1} &= (-b y_n + z_n v_n)\Delta t + y_n, \\ z_{n+1} &= (-b z_n + y_n v_n - a y_n)\Delta t + z_n. \end{aligned}\right\} \tag{113}$$

The topological structure of the chaotic attractor (see the paper-sheet model of Ref. [24]) is clearly observed in Figure 12(a).

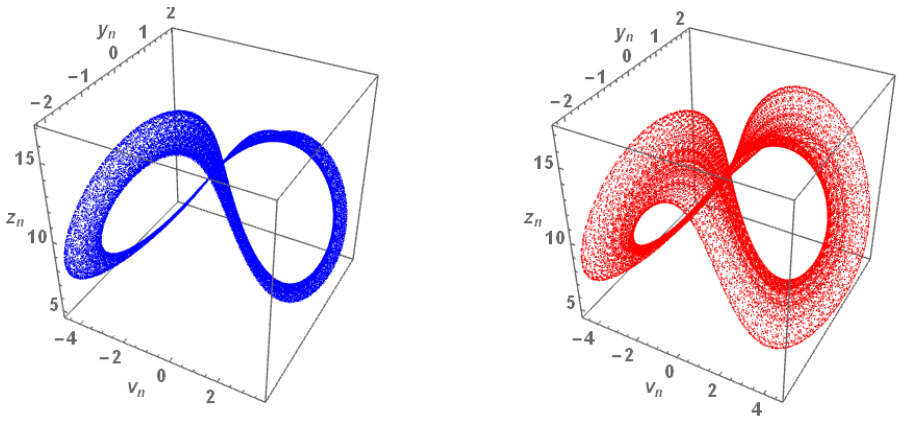

(a) (b)

Figure 11: Chaotic behavior of the discretized memristor Rikitake dynamo equation (112) for two different parameters. (a) Parameters: $a = 10$, $b = 2$, $\Delta t = 0.019$. Initial conditions: $v_0 = 3$, $y_0 = 1$, $z(0) = 6$. (b) Parameters: $a = 10$, $b = 2$, $\Delta t = 0.018$. Initial conditions: $v_0 = 3$, $y_0 = 1$, $z(0) = 6$.

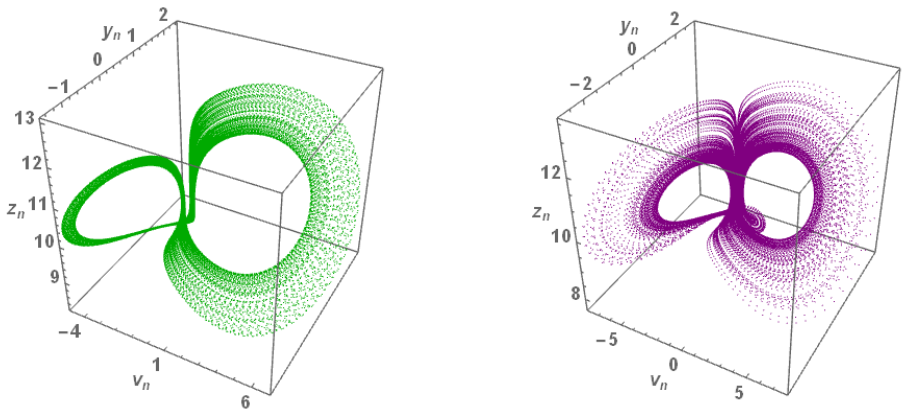

(a) (b)

Figure 12: Chaotic behavior of the discretized Rikitake dynamo equation (113) for two different parameters. (a) Parameters: $a = 10$, $b = 2.52$, $\Delta t = 0.02$. Initial conditions: $v_0 = 3$, $y_0 = 1$, $z(0) = 6$. (b) Parameters: $a = 10$, $b = 2.5$, $\Delta t = 0.02$. Initial conditions: $v_0 = 3$, $y_0 = 1$, $z(0) = 6$.

3.2.9 Memristor Lorenz equation

Assume that the $v - i$ characteristic of the voltage-controlled extended memristor is given by

$v - i$ characteristic of the two-terminal element

$$\left.\begin{array}{rcll} i & = & \hat{G}(x,\, y,\, v)v & \triangleq & -(xy - \beta v)v, \\ \dfrac{dx}{dt} & = & \tilde{g}_1(x,\, y,\, v) & \triangleq & \sigma(y - x)\, v, \\ \dfrac{dy}{dt} & = & \tilde{g}_1(x,\, y,\, v) & \triangleq & \{x(\rho - v) - y\}\, v, \end{array}\right\} \tag{114}$$

that is, the scaler functions $\hat{G}(y,\, z,\, v)$ is given by

$$\hat{G}(y,\, z,\, v) = xy - \beta v, \tag{115}$$

where σ, ρ and β are positive constants. The two-terminal element (114) is an active element, since the instantaneous power consumed by this element satisfies

$$P(t) \triangleq v(t)\, i(t) = -\{x(t)y(t) - \beta v(t)\}\, v(t)^2 < 0, \tag{116}$$

when $x(t)y(t) > \beta v(t)$.

Let us drive the two-terminal element (114) by the voltage source $v_s(t)$ where we set $v_s(t) = v(t) = 0$ for $t \geq t_0$. Then we obtain

$$\left.\begin{array}{rcl} \dfrac{dx}{dt} & = & 0, \\ \dfrac{dy}{dt} & = & 0, \end{array}\right\} \tag{117}$$

where $t \geq t_0$. Thus, $x(t) = x(t_0)$ and $y(t) = y(t_0)$ for $t \geq t_0$, that is, $x(t)$ and $y(t)$ holds the values $x(t_0)$ and $y(t_0)$, respectively. The current $i(t)$ is given by

$$i(t)\,\Big|_{v(t)=0} = -\big\{x(t)y(t) - \beta v(t)\big\}v(t)\,\Big|_{v(t)=0} = 0, \tag{118}$$

for $t \geq t_0$ since $x(t)$ and $y(t)$ is bounded for $t \geq t_0$. Therefore, the voltage-controlled extended memristor (114) has the non-volatility property.

The dynamics of the circuit in Fig. 3 is given by

Dynamics of the memristor Lorenz circuit

$$\left.\begin{aligned} \frac{dv}{dt} &= (xy - \beta v)\, v, \\ \frac{dx}{dt} &= \sigma(y - x)\, v, \\ \frac{dy}{dt} &= \{x(\rho - v) - y\}\, v, \end{aligned}\right\} \tag{119}$$

where we assume that $C = 1$. Note that the original Lorenz equation is given by

Dynamics of the memristor Lorenz circuit

$$\left.\begin{aligned} \frac{dv}{dt} &= xy - \beta v, \\ \frac{dx}{dt} &= \sigma(y - x), \\ \frac{dy}{dt} &= x(\rho - v) - y. \end{aligned}\right\} \tag{120}$$

Multiplying v on the right side of Eq. (120), we obtain Eq. (119).

Using the Euler method, we obtain from Eq. (119):

$$\left.\begin{aligned} v_{n+1} - v_n &= (x_n y_n - \beta v_n) v_n \Delta t, \\ x_{n+1} - y_n &= \sigma(y_n - x_n) v_n \Delta t, \\ y_{n+1} - z_n &= \{x_n(\rho - v_n) - y_n\}\, v_n \Delta t. \end{aligned}\right\} \tag{121}$$

It can be recast into the form

Discretized memristor Lorenz equation

$$\left.\begin{aligned} v_{n+1} &= (x_n y_n - \beta v_n) v_n \Delta t + v_n, \\ x_{n+1} &= \sigma(y_n - x_n) v_n \Delta t + y_n, \\ y_{n+1} &= \{x_n(\rho - v_n) - y_n\}\, v_n \Delta t + z_n. \end{aligned}\right\} \tag{122}$$

The chaotic behavior of the discretized Lorenz equation (121) is shown in Fig. 13, which clearly shows the topological structure of the chaotic behavior (see the paper-sheet model of Ref. [24]). We also show the chaotic behavior of the discretized Lorenz equation in Fig. 14, which is given by

Discretized Lorenz equation

$$\left.\begin{aligned} v_{n+1} &= (x_n y_n - \beta v_n) \Delta t + v_n, \\ x_{n+1} &= \sigma(y_n - x_n) \Delta t + y_n, \\ y_{n+1} &= \{x_n(\rho - v_n) - y_n\}\, \Delta t + z_n. \end{aligned}\right\} \tag{123}$$

We can also clearly observe the topological structure of the chaotic attractor (see the paper-sheet model of Ref. [24]).

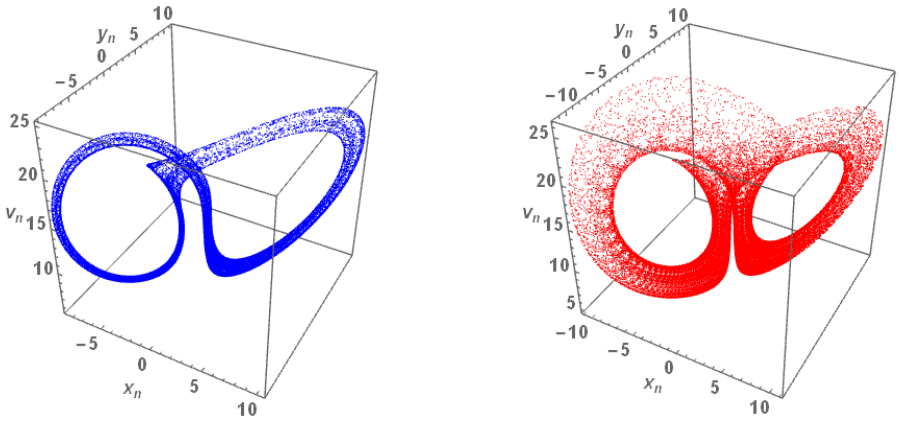

(a) (b)

Figure 13: Chaotic behavior of the discretized memristor Lorenz equation (122) for two different parameters.
(a) Parameters: $\sigma = 13$, $\rho = 15$, $\beta = 1.5$, $\Delta t = 0.002$. Initial conditions: $v_0 = 10$, $x_0 = 10$, $y_0 = 10$.
(b) Parameters: $\sigma = 13$, $\rho = 15$, $\beta = 1.56$, $\Delta t = 0.002$. Initial conditions: $v_0 = 10$, $x_0 = 10$, $y_0 = 10$.

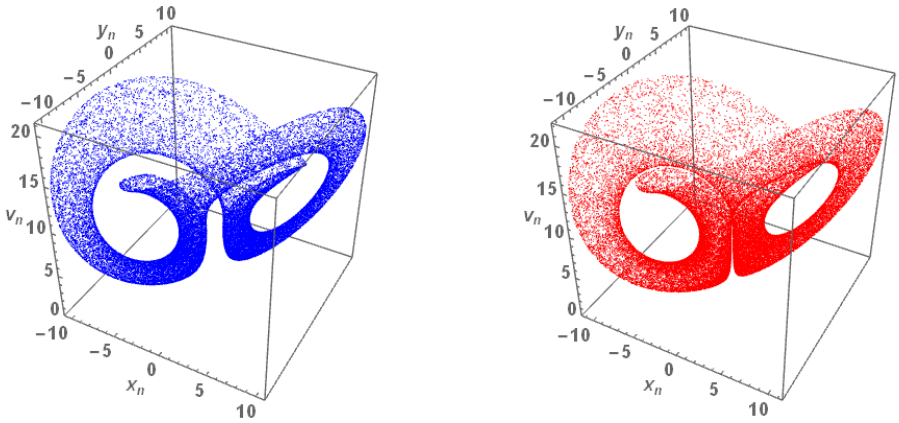

(a) (b)

Figure 14: Chaotic behavior of the discretized Lorenz equation (123) for two different parameters.
(a) Parameters: $\sigma = 13$, $\rho = 10$, $\beta = \dfrac{8}{3}$, $\Delta t = 0.075$. Initial conditions: $v_0 = 0.1$, $x_0 = 0.1$, $y_0 = 0.1$.
(b) Parameters: $\sigma = 13$, $\rho = 10$, $\beta = \dfrac{8}{3}$, $\Delta t = 0.068$. Initial conditions: $v_0 = 0.1$, $x_0 = 0.1$, $y_0 = 0.1$.

3.3 Three-element extended memristor circuit

In this section, the three-element memristor circuit in Fig. 15 is considered by adding a current source to the circuit in Fig. 3. We show two examples of the three-element memristor circuits that can be transformed into the two-dimensional chaotic maps.

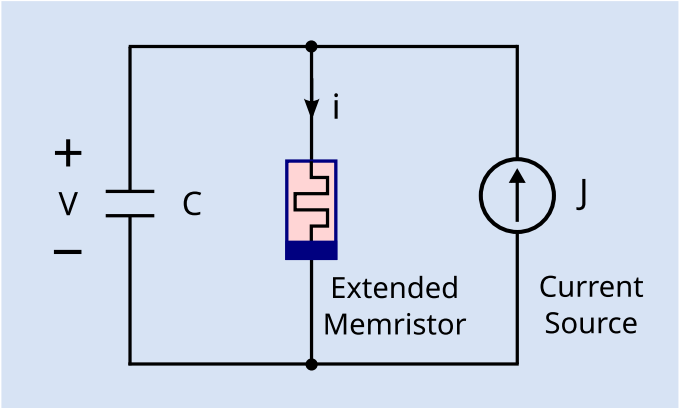

Figure 15: Three-element memristor circuit, which consists of a capacitor, a voltage-controlled extended memristor, and a current source, where v is the voltage across the capacitor with the capacitance C, i is the current through voltage-controlled extended memristor, and J is the output current of the current source.

3.3.1 Simplified Ikeda map

Assume that the $v-i$ characteristic of the voltage-controlled extended memristor is given by

$v-i$ characteristic of the extended memristor

$$\left.\begin{array}{rcll} i & = & \hat{G}(x,\ v)v & \triangleq & -\big\{b\cos(\xi)-1\big\}v, \\ \dfrac{dx}{dt} & = & \tilde{g}(x,\ v) & \triangleq & b\big\{v\sin(\xi)+x\cos(\xi)\big\}-x, \end{array}\right\} \tag{124}$$

where

$$\xi = c - \frac{d}{1+v^2+x^2}, \tag{125}$$

and $b,\ c$ and d are constants. The two scaler functions $\hat{G}(x,\ v)$ and $\tilde{g}(x,\ v)$ are given by

$$\left.\begin{array}{rcl} \hat{G}(x,\ v) & = & -\big\{b\cos(\xi)-1\big\}, \\ \tilde{g}(x,\ v) & = & b\big\{v\sin(\xi)+x\cos(\xi)\big\}-x. \end{array}\right\} \tag{126}$$

The voltage-controlled extended memristor is an passive element, since the instantaneous power consumed by the memristor satisfies

$$P(t) \triangleq v(t)\,i(t) = -\big\{b\cos(\xi)-1\big\}v(t)^2 \geq 0, \tag{127}$$

since $x(t)$ satisfies $b\cos(\xi)-1<0$ where we assume that $0<b<1$. Note that the current source in Fig. 15 is the active element.

To study the non-volatility property, we drive the voltage-controlled extended memristor (124) by the voltage source $v_s(t)$ where we set $v_s(t)=v(t)=0$ for $t \geq t_0$. Then we obtain

$$\left.\begin{array}{rcl} \dfrac{dx}{dt} & = & \tilde{g}(x,\ 0) = b\Big\{x\cos\Big(c-\dfrac{d}{1+x^2}\Big)\Big\}-x \\ & = & -x\left\{1-b\cos\left(c-\dfrac{d}{1+x^2}\right)\right\}, \end{array}\right\} \tag{128}$$

where $t \geq t_0$. If $0 < b < 1$, then the origin is the asymptotically stable equilibrium point. That is, if the initial condition $x(t_0)$ takes a finite value, then $x(t)$ also takes a finite value for $t \geq t_0$, and there is a real number M such that

$$\left|\hat{G}(x,\ 0)\right| = \left|-\left\{b\cos\left(c - \frac{d}{1+x^2}\right) - 1\right\}\right| \leq M, \tag{129}$$

for $t \geq t_0$. Furthermore, we obtain from Eq. (124)

$$v(t) = i(t) = 0 \ \text{ and } \ x(t) \to 0 \ \text{ for } \ t \geq t_0. \tag{130}$$

If $x(t_0) \neq 0$, then $x(t)$ changes with time. Thus, the voltage-controlled extended memristor (124) does not exhibit the non-volatility property, that is, it is the volatile memristor [9, 10].

The dynamics of the circuit in Fig. 15 is given by

Dynamics of the memristor circuit

$$\left.\begin{aligned} C\frac{dv}{dt} &= J + \big\{b\cos(\xi) - 1\big\}v, \\ \frac{dx}{dt} &= b\big\{v\sin(\xi) + x\cos(\xi)\big\} - x, \end{aligned}\right\} \tag{131}$$

where we assume that $C = 1$ and $J = a$. From Eq. (24), we obtain

$$\left.\begin{aligned} v_{n+1} - v_n &= a + \big\{b\cos(\xi_n) - 1\big\}v_n, \\ x_{n+1} - x_n &= b\big\{v_n\sin(\xi_n) + x_n\cos(\xi_n)\big\} - x_n, \end{aligned}\right\} \tag{132}$$

where

$$\xi = c - \frac{d}{1 + {v_n}^2 + v{x_n}^2}. \tag{133}$$

It can be recast into the form

Simplified Ikeda map

$$\left.\begin{aligned} v_{n+1} &= a + b\cos(\xi_n)v_n, \\ x_{n+1} &= b\big\{v_n\sin(\xi_n) + x_n\cos(\xi_n)\big\}. \end{aligned}\right\} \tag{134}$$

This equation is the simplified version of the Ikeda map [22, 23]. It is defined by

Ikeda map

$$\left.\begin{aligned} v_{n+1} &= a + b\big\{\cos(\xi_n)v_n - x_n\cos(\xi_n)\big\}, \\ x_{n+1} &= b\big\{v_n\sin(\xi_n) + x_n\cos(\xi_n)\big\}. \end{aligned}\right\} \tag{135}$$

Compare the first equation of Eq. (134) and Eq. (135). That is, Eq. (134) does not have the term $-bx_n\cos(\xi_n)$. We study the original Ikeda map in Sec. 4.1.7. The chaotic behavior of the simplified Ikeda map (134) and the original Ikeda map (135) is shown in Fig. 16.

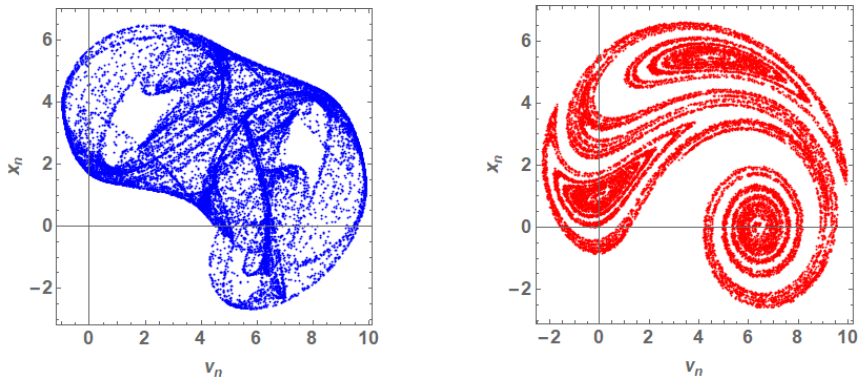

(a) (b)

Figure 16: (a) Chaotic behavior of the simplified Ikeda map (134). (b) Chaotic behavior of the original Ikeda map (135). Parameters for these two maps: $a = 6.41$, $b = 0.9$, $c = 3.02$, $d = 47.74$. Initial conditions: $v_0 = 0$, $x_0 = 0$.

3.3.2 Discretized Rössler equation

Assume that the $v - i$ characteristic of the voltage-controlled extended memristor (left) is given by

$v - i$ characteristic of the extended memristor

$$\left.\begin{array}{rcccl} i & = & \hat{G}(x,\ v)v & \triangleq & -(x-c)v, \\ \dfrac{dx}{dt} & = & \tilde{g}_1(x,\ v) & \triangleq & -y-v, \\ \dfrac{dy}{dt} & = & \tilde{g}_1(x,\ v) & \triangleq & x+ay, \end{array}\right\} \tag{136}$$

where a, b, and c are constants ($0 < a < 2$). The voltage-controlled extended memristor is an active element, since the instantaneous power consumed by the memristor satisfies

$$P(t) \triangleq v(t)\, i(t) = -(x(t) - c)v(t)^2 < 0, \tag{137}$$

when $x(t) > c$.

To study the non-volatility property, we drive the voltage-controlled extended memristor (124) by the voltage source $v_s(t)$ where we set $v_s(t) = v(t) = 0$ for $t \geq t_0$. Then we obtain

$$\left.\begin{array}{l} \dfrac{dx}{dt} = -y, \\ \dfrac{dy}{dt} = x + ay, \end{array}\right\} \tag{138}$$

where $t \geq t_0$. The origin is the unstable equilibrium point with an outward spiral on the (x, y)-plane, and therefore $x(t)$ and $y(t)$ change with time if the initial values for $x(t)$ and $y(t)$ are not at the origin. Thus the voltage-controlled extended memristor (124) does not exhibit the non-volatility property, that is, it is the volatile memristor [9, 10], although $v(t)$ and $i(t)$ satisfy

$$v(t) = i(t) = 0 \quad \text{for} \quad t \geq t_0, \tag{139}$$

if $|\, x(t)\, |$ is finite. This is because from Eq. (136), $i(t)$ can be written as

$$i(t) = \hat{G}(x(t),\ v(t))v(t) = -(x(t) - c)v(t). \tag{140}$$

Thus, if $\mid x(t) \mid$ is finite, then $i(t) = 0$ for $v(t) = 0$ where $v_s(t) = v(t) = 0$ for $t \geq t_0$.

The dynamics of the circuit in Fig. 15 is given by

Dynamics of the memristor circuit

$$\left.\begin{aligned} C\frac{dv}{dt} &= J + (x-c)v, \\ \frac{dx}{dt} &= -y - v, \\ \frac{dy}{dt} &= x + ay. \end{aligned}\right\} \tag{141}$$

If we assume that $C = 1$ and $J = b$, then Eq. (141) can be written as

Rössler equation

$$\left.\begin{aligned} \frac{dv}{dt} &= b + (x-c)v, \\ \frac{dx}{dt} &= -y - v, \\ \frac{dy}{dt} &= x + ay, \end{aligned}\right\} \tag{142}$$

which is equivalent to the Rössler equation [24].

From Eq. (142), we obtain

$$\left.\begin{aligned} v_{n+1} - v_n &= \{b + (x_n - c)v_n\}\,\Delta t, \\ x_{n+1} - x_n &= (-y_n - v_n)\Delta t, \\ y_{n+1} - y_n &= (x_n + ay_n)\Delta t. \end{aligned}\right\} \tag{143}$$

It can be recast into the form

Discretized Rössler equation

$$\left.\begin{aligned} v_{n+1} &= \{b + (x_n - c)v_n\}\,\Delta t + v_n, \\ x_{n+1} &= (-y_n - v_n)\Delta t + x_n, \\ y_{n+1} &= (x_n + ay_n)\Delta t + y_n. \end{aligned}\right\} \tag{144}$$

We show the chaotic behavior of the discretized Rössler equation (144) in Fig. 17, which clearly shows the topological structure of the chaotic attractor (see the paper-sheet model of Ref. [24]). Note that in the computer simulations, Eq. (142) has no chaotic attractor, but has a limit cycle when we use the parameter values shown in Fig. 17.

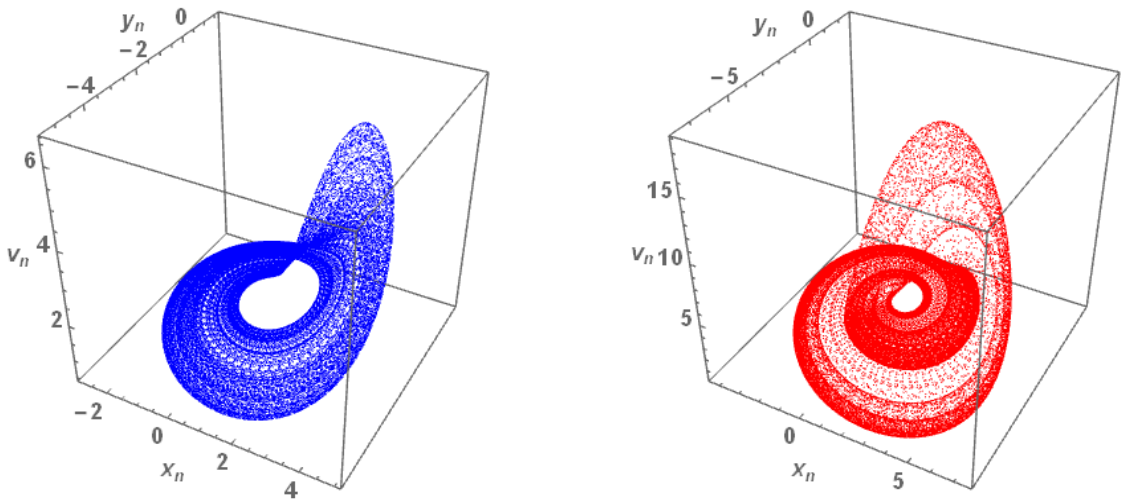

(a) (b)

Figure 17: Chaotic behavior of the discretized Rössler equation (144) for two different parameters.
(a) Parameters: $a = 0.398$, $b = 3.8$, $c = 4.5$, $\Delta t = 0.11$. Initial conditions: $v_0 = 0.01$, $x_0 = 0.01$, $y(0) = 0.01$.
(b) Parameters: $a = 0.4$, $b = 3.8$, $c = 5.0$, $\Delta t = 0.147$. Initial conditions: $v_0 = 0.01$, $x_0 = 0.01$, $y(0) = 0.01$.

4 Generalized Extended Memristor Circuits

Consider the two-element circuit in Fig. 18. The $v-i$ characteristic of the two-terminal device (left) is given by

$v-i$ characteristic of the two-terminal device

$$\left.\begin{array}{rcl} i &=& \hat{G}(x,\ v)v \ \triangleq\ -\big\{h\big(x,\ \ln\mid v\mid\big) - \ln\mid v\mid\big\}\, v, \\ \dfrac{dx}{dt} &=& \tilde{g}(x,\ v) \ \triangleq\ g\big(x,\ \ln\mid v\mid\big) - x, \end{array}\right\} \tag{145}$$

where i, v and y are the terminal current, the terminal voltage, and the state variable, respectively, and $h(x,\ \ln\mid v\mid)$ and $g(x,\ \ln\mid v\mid)$ are scalar-valued functions of x and $\ln\mid v\mid$.

The dynamics of the circuit in Fig. 18 is given b y

Dynamics of the two-element circuit

$$\left.\begin{array}{rcl} C\dfrac{dv}{dt} &=& \big\{h\big(x,\ \ln\mid v\mid\big) - \ln\mid v\mid\big\}\, v, \\ \dfrac{dx}{dt} &=& g\big(x,\ \ln\mid v\mid\big) - x, \end{array}\right\} \tag{146}$$

where C is the capacitance of the capacitor. If $C = 1$, then Eq. (146) can be recast into the form

$$\left.\begin{array}{rcl} \dfrac{d(\ln\mid v\mid)}{dt} &=& \big\{h\big(x,\ \ln\mid v\mid\big) - \ln\mid v\mid\big\}\, v, \\ \dfrac{dy}{dt} &=& g\big(x,\ \ln\mid v\mid\big) - x. \end{array}\right\} \tag{147}$$

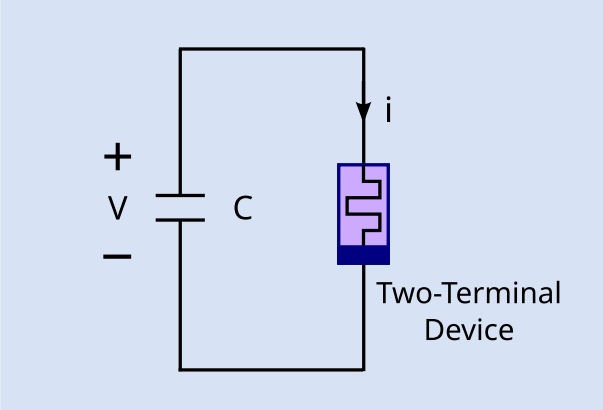

Figure 18: Two-element circuit, which consists of a capacitor and a two-terminal device, where v is the voltage of the capacitor with the capacitance C and i is the current through the two-terminal device.

Setting $y \triangleq \ln \mid v \mid$, we obtain

$$\left.\begin{array}{rcl} \dfrac{dy}{dt} &=& h\big(x,\ y\big) - y, \\ \dfrac{dx}{dt} &=& g\big(x,\ y\big) - x. \end{array}\right\} \tag{148}$$

Applying the Euler method:

Euler method

$$\left.\begin{array}{rcl} \dfrac{dy}{dt} &\approx& \dfrac{y(t+\Delta t) - y(t)}{\Delta t}, \\ \dfrac{dx}{dt} &\approx& \dfrac{x(t+\Delta t) - x(t)}{\Delta t}, \end{array}\right\} \tag{149}$$

we obtain the approximate equation from Eq. (148)

$$\left.\begin{array}{rcl} \dfrac{y(t+\Delta t) - y(t)}{\Delta t} &=& h\big(x(t),\ y(t)\big) - y(t), \\ \dfrac{x(t+\Delta t) - x(t)}{\Delta t} &=& g\big(x(t),\ y(t)\big) - x(t), \end{array}\right\} \tag{150}$$

where the time step size Δt is usually set sufficiently small. In this paper, we set $\Delta t = 1$ and define $y_n \triangleq y(t + n\Delta t)$ and $x_n \triangleq x(t + n\Delta t)$. Then we obtain

$$\left.\begin{array}{rcl} y_{n+1} - y_n &=& h\big(x_n,\ y_n\big) - y_n, \\ x_{n+1} - x_n &=& g\big(x_n,\ y_n\big) - x_n, \end{array}\right\} \tag{151}$$

where $n = 0, 1, 2, \cdots$. It can be transformed into the two-dimensional map

Two-dimensional map

$$\left.\begin{array}{rcl} y_{n+1} &=& h\big(x_n,\ y_n\big), \\ x_{n+1} &=& g\big(x_n,\ y_n\big). \end{array}\right\} \tag{152}$$

Note that Eq. (145 may not necessarily satisfy the conditions (15) and (16), since $\lim_{v\to 0} \ln \mid v \mid \to -\infty$.

Let us modify $v-i$ characteristic of the two-terminal device in Fig. 18 as follows:

$v-i$ characteristic of the two-terminal device

$$\left.\begin{array}{rcll} i & = & \hat{G}(x,\ v)v & \triangleq & -\rho\Big(h\big(x,\ \ln \mid v \mid\big) - \ln \mid v \mid\Big)v, \\ \dfrac{dx}{dt} & = & \tilde{g}(x,\ v) & \triangleq & \mu\left(g\big(x,\ \ln \mid v \mid\big) - x\right), \end{array}\right\} \tag{153}$$

where the saturation function $\rho(s)$ and the resistive-fuse function $\mu(s)$[3] are the bounded functions defined by

$$\rho(s) \triangleq \left\{ \begin{array}{cc} M & s > M, \\ s & \mid s \mid \leq M, \\ -M & s < -M, \end{array}\right. \tag{154}$$

and

$$\mu(s) \triangleq \left\{ \begin{array}{cc} 0 & s > L, \\ s & \mid s \mid \leq L, \\ 0 & s < -L, \end{array}\right. \tag{155}$$

respectively, where M and L are sufficiently large positive constants.

Let us drive the voltage-controlled extended memristor (153) by the voltage source $v_s(t)$ where we set $v_s(t) = v(t) \to 0$ for $t \geq t_0$. Since $\mid \hat{G}(x,\ v) \mid$ is bounded, that is,

$$\mid \hat{G}(x,\ v) \mid = \rho\Big(\ h\big(x,\ \ln \mid v \mid\big) - \ln \mid v \mid\ \Big) \mid \leq M, \tag{156}$$

we obtain

$$\lim_{v\to 0} i = \lim_{v\to 0} \hat{G}(x,\ v)\, v \to 0. \tag{157}$$

Thus, we can define without loss of generality

$$i \ \Big|_{v=0} = \hat{G}(x,\ v)\, v\Big|_{v=0} = 0. \tag{158}$$

It follows that the two-terminal device defined by Eq. (153) is considered to be an extended memristor [25]. Note that if the function $\tilde{g}(x,\ v)$ is not specified, then the non-volatility property cannot be examined. That is, the two-terminal device (153) may not necessarily satisfy the condition (16).

The dynamics of the circuit in Fig. 18 is given by

Dynamics of the two-element circuit

$$\left.\begin{array}{rcl} C\dfrac{dv}{dt} & = & \rho\left(h\big(x,\ \ln \mid v \mid\big) - \ln \mid v \mid\right) v, \\ \dfrac{dx}{dt} & = & \mu\left(g\big(x,\ \ln \mid v \mid\big) - x\right), \end{array}\right\} \tag{159}$$

where $C = 1$. Note that in the region satisfying the inequalities:

$$\left.\begin{array}{rcl} -M \leq & h\big(x,\ \ln \mid v \mid\big) - \ln \mid v \mid & \leq M, \\ -L \leq & g\big(x,\ \ln \mid v \mid\big) - x & \leq L, \end{array}\right\} \tag{160}$$

[3]The nonlinear element is called a resistive-fuse if its $v-i$ characteristic is defined by $i = \mu(v)$.

Eq. (159) can be written as

$$\left.\begin{aligned} C\frac{dv}{dt} &= \big\{h\big(x,\ \ln \mid v \mid\big) - \ln \mid v \mid\big\}\, v, \\ \frac{dx}{dt} &= g\big(x,\ \ln \mid v \mid\big) - x, \end{aligned}\right\} \tag{161}$$

which is identical to Eq. (146). Similarly, using the Euler method and setting $y \triangleq \ln \mid v \mid$, Eq. (161) can be transformed into the two-dimensional map:

Two-dimensional map

$$\left.\begin{aligned} y_{n+1} &= h\big(x_n,\ y_n\big), \\ x_{n+1} &= g\big(x_n,\ y_n\big), \end{aligned}\right\} \tag{162}$$

where we assumed that $C = 1$. Equation (162) is identical to Eq.(152).

Conversely, if the two-dimensional map (162) is given, then we can reconstruct the $v - i$ characteristic of the two-terminal device (145) or the extended memristor (153), and its corresponding two-element circuit equation (146) or (159). We conclude as follows:

Any two-dimensional map can be obtained by applying the Euler method to discretize the equation of certain types of two-element memristor circuits. Conversely, any two-dimensional map can be associated with the two-element memristor circuit equation.

4.1 Examples of the generalized extended memristor circuits generating chaotic maps

In this section we show some examples of generalized extended memristor circuits. They can be transformed into two-dimensional chaotic maps.

4.1.1 Fold map

Assume that the $v - i$ characteristic of the voltage-controlled extended memristor is given by

$v - i$ characteristic of the extended memristor

$$\left.\begin{aligned} i &= -\rho\Big(h\big(x,\ \ln \mid v \mid\big) - \ln \mid v \mid\Big)v, \\ \frac{dx}{dt} &= \mu\Big(g\big(x,\ \ln \mid v \mid\big) - x\Big), \end{aligned}\right\} \tag{163}$$

where

$$\left.\begin{aligned} h(x,\ \ln \mid v \mid) &= x + a \ln \mid v \mid, \\ g(x,\ \ln \mid v \mid) &= \ln \mid v \mid^2 + b, \end{aligned}\right\} \tag{164}$$

and a and b are constants. Substituting Eq. (164) into Eq. (163), we obtain

$$\left.\begin{aligned} i &= -\rho\Big(x + a \ln \mid v \mid - \ln \mid v \mid\Big)v, \\ \frac{dx}{dt} &= \mu\Big((\ln \mid v \mid)^2 + b - x\Big). \end{aligned}\right\} \tag{165}$$

The voltage-controlled extended memristor (165) is an active element, since the instantaneous power consumed by the memristor satisfies

$$P(t) \triangleq v(t)\, i(t) = -\rho\Big(x(t) + a \ln \mid v(t) \mid - \ln \mid v(t) \mid\Big) v(t)^2 < 0, \tag{166}$$

if $x(t) + a \ln \mid v(t) \mid - \ln \mid v(t) \mid > M$. This is because from Eq. (154) we obtain

$$\rho\Big(x(t) + a \ln \mid v(t) \mid - \ln \mid v(t) \mid\Big) = M > 0. \tag{167}$$

To study the non-volatility property, we drive the voltage-controlled extended memristor (165) by the voltage source $v_s(t)$ where we set $v_s(t) = v(t) \to 0$ for $t \geq t_0$. If $0 <\mid v \mid \ll 1$, then $(\ln \mid v \mid)^2$ is sufficiently large. Thus, from Eq. (155), we obtain $\mu\Big((\ln \mid v \mid)^2 + b - x\Big) = 0$, and therefore

$$\frac{dx}{dt} = \mu\Big((\ln \mid v \mid)^2 + b - x\Big) = 0. \tag{168}$$

Thus, Eq. (168) has the solution $x(t) = c$, where c is a constant. Similarly, we get

$$\lim_{v \to 0} i = \lim_{v \to 0} -\rho\Big(x + a \ln \mid v \mid - \ln \mid v \mid\Big) v \to 0. \tag{169}$$

Therefore, without loss of generality, we can define

$$i \,\Big|_{v=0} = 0. \tag{170}$$

Considering that the state $x(t)$ is a constant when $\mid v \mid$ is sufficiently small, the behavior of the two-terminal device (163) is similar to that of non-volatile memristors.

The dynamics of the circuit in Fig. 18 is given by

The dynamics of the circuit

$$\left.\begin{array}{rcl} C\dfrac{dv}{dt} & = & \rho\Big(x + a \ln \mid v \mid - \ln \mid v \mid\Big) v, \\ \dfrac{dx}{dt} & = & \mu\left(\ln \mid v \mid^2 + b - x\right), \end{array}\right\} \tag{171}$$

where $C = 1$. If $\mid v \mid$ is not sufficiently small, then this equation is recast into the form

$$\left.\begin{array}{rcl} \dfrac{d \ln \mid v \mid}{dt} & = & \big(x + a \ln \mid v \mid - \ln \mid v \mid\big), \\ \dfrac{dx}{dt} & = & \ln \mid v \mid^2 + b - x. \end{array}\right\} \tag{172}$$

Setting $y \triangleq \ln \mid v \mid$, we obtain

$$\left.\begin{array}{rcl} \dfrac{dy}{dt} & = & x + ay - y, \\ \dfrac{dx}{dt} & = & y^2 + b - x. \end{array}\right\} \tag{173}$$

Using Euler method, we obtain from Eq. (173)

$$\left.\begin{array}{rcl} y_{n+1} - y_n & = & x_n + a y_n - y_n, \\ x_{n+1} - x_n & = & {y_n}^2 + b - x_n. \end{array}\right\} \tag{174}$$

It can be recast into the fold map [26]

$$\boxed{\begin{array}{l}\text{Fold map}\\ \left.\begin{array}{rcl} y_{n+1} &=& x_n + a y_n, \\ x_{n+1} &=& {y_n}^2 + b. \end{array}\right\}\end{array}} \tag{175}$$

The chaotic behavior of the fold map (175) is shown in Fig. 19.

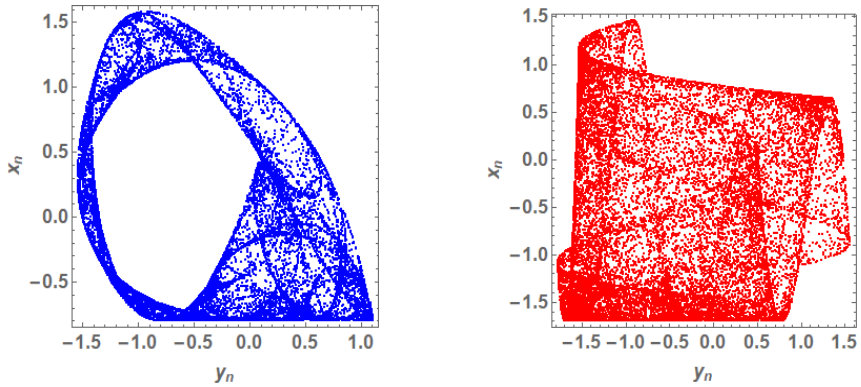

(a) (b)

Figure 19: Chaotic behavior of the fold map (175) for two different parameters. (a) Parameters: $a = -0.1$, $b = -1.7$. Initial conditions: $y_0 = 0$, $x_0 = 0$. (b) Parameters: $a = 0.8$, $b = -0.8$. Initial conditions: $y_0 = 0$, $x_0 = 0$.

4.1.2 Hénon map

Assume that the $v - i$ characteristic of the voltage-controlled extended memristor is given by

$$\boxed{\begin{array}{l}v - i \text{ characteristic of the extended memristor}\\ \left.\begin{array}{rcl} i &=& -\rho\Big(h\big(x,\ \ln \mid v \mid\big) - \ln \mid v \mid\Big) v, \\ \dfrac{dx}{dt} &=& \mu\Big(g\big(x,\ \ln \mid v \mid\big) - x\Big), \end{array}\right\}\end{array}} \tag{176}$$

where

$$\left.\begin{array}{rcl} h(x,\ \ln \mid v \mid) &=& bx, \\ g(x,\ \ln \mid v \mid) &=& 1 - ax^2 + \ln \mid v \mid, \end{array}\right\} \tag{177}$$

and a and b are constants. Substituting Eq. (177) into Eq. (176), we obtain

$$\left.\begin{array}{rcl} i &=& -\rho\Big(bx - \ln \mid v \mid\Big) v, \\ \dfrac{dx}{dt} &=& \mu\Big(1 - ax^2 + \ln \mid v \mid - x\Big). \end{array}\right\} \tag{178}$$

The voltage-controlled extended memristor (178) is an active element, since the instantaneous power consumed by the memristor satisfies

$$P(t) \triangleq v(t)\, i(t) = -\rho\Big(bx(t) - \ln \mid v(t) \mid\Big) v(t)^2 < 0, \tag{179}$$

when $bx(t) - \ln \mid v(t) \mid$ is sufficiently large, and therefore $\rho\Big(bx(t) - \ln \mid v(t) \mid\Big) = M > 0$.

To study the non-volatility property, we drive the voltage-controlled extended memristor (178) by the voltage source $v_s(t)$ where we set $v_s(t) = v(t) \to 0$ for $t \geq t_0$. If $0 <\mid v \mid \ll 1$, then $\Big|\ln \mid v \mid\Big|$ is sufficiently large. Furthermore, considering that the resistive-fuse function $\mu(s)$ satisfies Eq. (155), we obtain

$$\frac{dx}{dt} = \mu\Big(1 - ax^2 + \ln \mid v \mid -x\Big) = 0. \tag{180}$$

Equation (180) has the solution $x(t) = c$, where c is a constant. Similarly, we get

$$\lim_{v\to 0} i = \lim_{v\to 0} -\rho\Big(x + a \ln \mid v \mid - \ln \mid v \mid \Big)v \to 0, \tag{181}$$

for the solution $x(t) = c$ and $0 <\mid v \mid \ll 1$. Thus, without loss of generality, we can define

$$i \,\Big|_{v=0} = 0. \tag{182}$$

Considering that the state $x(t)$ is a constant in the neighborhood of $v = 0$, the behavior of the two-terminal device (176) is similar to that of non-volatile memristors.

The dynamics of the circuit in Fig. 18 is given by

The dynamics of the circuit

$$\left.\begin{array}{rcl} C\dfrac{dv}{dt} &=& \rho\Big(bx - \ln \mid v \mid\Big)v, \\ \dfrac{dx}{dt} &=& \mu\Big(1 - ax^2 + \ln \mid v \mid -x\Big), \end{array}\right\} \tag{183}$$

where $C = 1$. If $\mid v \mid$ is not sufficiently small, this equation is recast into the form

$$\left.\begin{array}{rcl} \dfrac{d \ln \mid v \mid}{dt} &=& bx - \ln \mid v \mid, \\ \dfrac{dx}{dt} &=& 1 - ax^2 + \ln \mid v \mid -x. \end{array}\right\} \tag{184}$$

Setting $y \triangleq \ln \mid v \mid$, we obtain

$$\left.\begin{array}{rcl} \dfrac{dy}{dt} &=& bx - y, \\ \dfrac{dx}{dt} &=& 1 - ax^2 + y - x. \end{array}\right\} \tag{185}$$

Using Euler method, we obtain from Eq. (185):

$$\left.\begin{array}{rcl} \dfrac{y_{n+1} - y_n}{\Delta t} &=& bx_n - y_n, \\ \dfrac{x_{n+1} - x_n}{\Delta t} &=& 1 - a{x_n}^2 + y_n - x_n. \end{array}\right\} \tag{186}$$

It can be written as

$$\left.\begin{array}{rcl} y_{n+1} &=& (bx_n - y_n)\Delta t + y_n, \\ x_{n+1} &=& (1 - a{x_n}^2 + y_n - x_n)\Delta t + x_n. \end{array}\right\} \tag{187}$$

If $\Delta t = 1$, then Eq. (187) can be recast into the Hénon map [19]

Hénon map

$$\left.\begin{aligned} y_{n+1} &= bx_n, \\ x_{n+1} &= 1 - a{x_n}^2 + y_n. \end{aligned}\right\} \tag{188}$$

The chaotic behavior of the discretized equation (187) and the Hénon map (188) is shown in Fig. 20. Note that the chaotic attractors of Eqs. (187) and (188) are quite different, even though the parameter value of a is different.

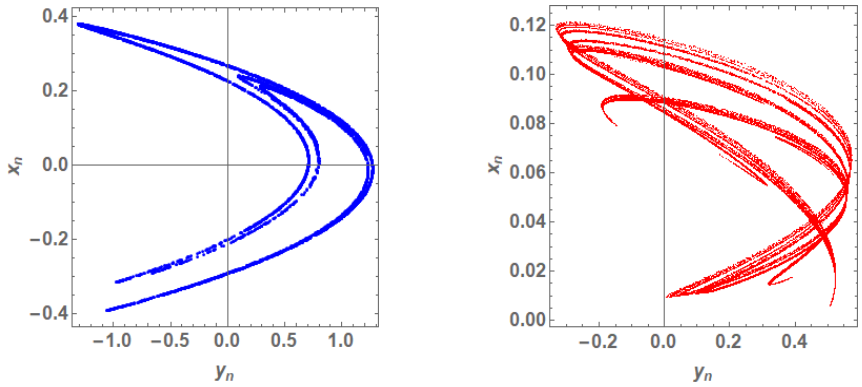

(a) (b)

Figure 20: (a) Chaotic behavior of the Hénon map (188). Parameters: $a = 1.42$, $b = 0.3$. Initial conditions: $y_0 = 0.2$, $x_0 = 0.2$. (b) Chaotic behavior of the discretized equation (187). Parameters: $a = 7$, $b = 0.3$, $\Delta t = 0.5$. Initial conditions: $y_0 = 0.2$, $x_0 = 0.2$.

4.1.3 Lozi map

Assume that the $v - i$ characteristic of the voltage-controlled extended memristor is given by

$v - i$ characteristic of the extended memristor

$$\left.\begin{aligned} i &= -\rho\Big(h\big(x,\ \ln \mid v \mid\big) - \ln \mid v \mid\Big)v, \\ \frac{dx}{dt} &= \mu\Big(g\big(x,\ \ln \mid v \mid\big) - x\Big), \end{aligned}\right\} \tag{189}$$

where

$$\left.\begin{aligned} h(x,\ \ln \mid v \mid) &= 1 - a\big|\ln \mid v \mid\big| + x, \\ g(x,\ \ln \mid v \mid) &= b \ln \mid v \mid, \end{aligned}\right\} \tag{190}$$

and $a \neq \pm 1$ and $b \neq 0$ are constants. Substituting Eq. (190) into Eq. (189), we obtain

$$\left.\begin{aligned} i &= -\rho\Big(1 - a\big|\ln \mid v \mid\big| + x - \ln \mid v \mid\Big)v, \\ \frac{dx}{dt} &= \mu\Big(b \ln \mid v \mid - x\Big). \end{aligned}\right\} \tag{191}$$

The voltage-controlled extended memristor (191) is an active element, since the instantaneous power consumed by the memristor satisfies

$$P(t) \triangleq v(t)\, i(t) = -\rho\Big(1 - a\big|\ln \mid v(t) \mid\big| + x(t) - \ln \mid v(t) \mid\Big)v(t)^2 < 0, \tag{192}$$

when $1 - a\big|\ln \mid v(t) \mid\big| + x(t) - \ln \mid v(t) \mid$ is sufficiently large.

To study the non-volatility property, we drive the voltage-controlled extended memristor (191) by the voltage source $v_s(t)$ where we set $v_s(t) = v(t) \to 0$ for $t \geq t_0$. If $0 <\mid v \mid \ll 1$, then $\big|\ln \mid v \mid\big|$ is sufficiently large. Furthermore, considering that the resistive-fuse function $\mu(s)$ satisfies Eq. (155), we obtain

$$\frac{dx}{dt} = 0, \tag{193}$$

where $t \geq t_0$ and $b \neq 0$. Equation (193) has the solution $x(t) = c$, where c is a constant. Similarly, we get

$$\lim_{v\to 0} i = \lim_{v\to 0} -\rho\Big(1 - a\big|\ln \mid v \mid\big| + x - \ln \mid v \mid\Big)v \to 0, \tag{194}$$

for $x(t) = c$ and $0 <\mid v \mid \ll 1$, where we assume that $a \neq \pm 1$. Thus, without loss of generality, we can define

$$i\ \Big|_{v=0} = 0. \tag{195}$$

Considering that the state $x(t)$ is a constant in the neighborhood of $v = 0$, the behavior of the two-terminal device (189) is similar to that of non-volatile memristors.

The dynamics of the circuit in Fig. 18 is given by

The dynamics of the circuit

$$\left.\begin{array}{rcl} C\dfrac{dv}{dt} &=& \rho\Big(1 - a\big|\ln \mid v \mid\big| + x - \ln \mid v \mid\Big)v, \\ \dfrac{dx}{dt} &=& \mu\Big(b\ln \mid v \mid -x\Big), \end{array}\right\} \tag{196}$$

where $C = 1$. If $\mid v \mid$ is not sufficiently small, this equation is recast into the form

$$\left.\begin{array}{rcl} \dfrac{d\ln \mid v \mid}{dt} &=& 1 - a\big|\ln \mid v \mid\big| + x - \ln \mid v \mid, \\ \dfrac{dx}{dt} &=& b\ln \mid v \mid -x. \end{array}\right\} \tag{197}$$

Setting $y \triangleq \ln \mid v \mid$, we obtain

$$\left.\begin{array}{rcl} \dfrac{dy}{dt} &=& 1 - a \mid y \mid + x - y, \\ \dfrac{dx}{dt} &=& by - x. \end{array}\right\} \tag{198}$$

Using Euler method, we obtain from Eq. (198)

$$\left.\begin{array}{rcl} \dfrac{y_{n+1} - y_n}{\Delta t} &=& 1 - a \mid y_n \mid + x_n - y_n, \\ \dfrac{x_{n+1} - x_n}{\Delta t} &=& by_n - x_n. \end{array}\right\} \tag{199}$$

It can be written as

$$\left.\begin{array}{rcl} y_{n+1} &=& (1 - a \mid y_n \mid + x_n - y_n)\Delta t + y_n, \\ x_{n+1} &=& (by_n - x_n)\Delta t + x_n. \end{array}\right\} \tag{200}$$

If $\Delta t = 1$, then Eq. (200) can be recast into the Lozi map [27]

Lozi map

$$\left.\begin{aligned} y_{n+1} &= 1 - a \mid y_n \mid + x_n, \\ x_{n+1} &= b y_n. \end{aligned}\right\} \tag{201}$$

The chaotic behavior of the discretized equation (200) and the Lozi map(201) is shown in Fig. 21. Note that the chaotic attractors of Eqs. (200) and (201) are quite different, even though the parameter value of a is different.

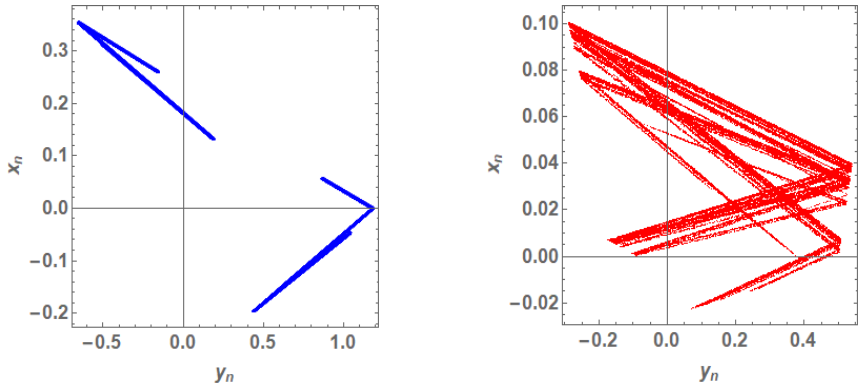

(a) (b)

Figure 21: (a) Chaotic behavior of the Lozi map (201). Parameters: $a = 1.4$, $b = 0.3$. Initial conditions: $y_0 = 0.2$, $x_0 = 0.2$. (b) Chaotic behavior of the discretized equation (200). Parameters: $a = 4$, $b = 0.3$, $\Delta t = 0.5$. Initial conditions: $y_0 = 0.2$, $x_0 = 0.2$.

4.1.4 Tinkerbell map

Assume that the $v - i$ characteristic of the voltage-controlled extended memristor is given by

$v - i$ characteristic of the extended memristor

$$\left.\begin{aligned} i &= -\rho\Big(h\big(x,\ \ln \mid v \mid\big) - \ln \mid v \mid\Big) v, \\ \frac{dx}{dt} &= \mu\Big(g\big(x,\ \ln \mid v \mid\big) - x\Big), \end{aligned}\right\} \tag{202}$$

where

$$\left.\begin{aligned} h\big(x,\ \ln \mid v \mid\big) &= 2x \ln \mid v \mid + cx + d \ln \mid v \mid, \\ g\big(x,\ \ln \mid v \mid\big) &= x^2 - (\ln \mid v \mid)^2 + ax + b \ln \mid v \mid, \end{aligned}\right\} \tag{203}$$

and a, b, c and d are positive constants. Substituting Eq. (203) into Eq. (202), we obtain

$$\left.\begin{aligned} i &= -\rho\Big(2x \ln \mid v \mid + cx + d \ln \mid v \mid - \ln \mid v \mid\Big) v, \\ \frac{dx}{dt} &= \mu\Big(x^2 - (\ln \mid v \mid)^2 + ax + b \ln \mid v \mid - x\Big). \end{aligned}\right\} \tag{204}$$

The voltage-controlled extended memristor (204) is an active element, since the instantaneous power consumed by the memristor satisfies

$$P(t) \triangleq v(t)\, i(t) = -\rho\Big(2x(t) \ln \mid v(t) \mid + cx(t) + d \ln \mid v(t) \mid - \ln \mid v(t) \mid\Big) v(t)^2 < 0, \tag{205}$$

when $x(t) = 0$ and $0 <\mid v(t) \mid \ll 1$, where we assumed that $0 < d < 1$.

To study the non-volatility property, we drive the voltage-controlled extended memristor (204) by the voltage source $v_s(t)$ where we set $v_s(t) = v(t) \to 0$ for $t \geq t_0$. If $0 <\mid v \mid \ll 1$, then $\Big|\ln \mid v \mid\Big|$ is sufficiently large. Furthermore, considering that the resistive-fuse function $\mu(s)$ satisfies Eq. (155), we obtain

$$\frac{dx}{dt} = \mu\Big(x^2 - (\ln \mid v \mid)^2 + ax + b \ln \mid v \mid -x\Big) = 0. \tag{206}$$

It has the solution $x(t) = c$, where c is a constant. Similarly, we get

$$\lim_{v \to 0} i = \lim_{v \to 0} -\rho\Big(2x \ln \mid v \mid +cx + d \ln \mid v \mid - \ln \mid v \mid\Big)v \to 0, \tag{207}$$

since $\Big|\ln \mid v \mid\Big|$ is sufficiently large. Thus, without loss of generality, we can define

$$i \Big|_{v=0} = 0. \tag{208}$$

Considering that the state $x(t)$ is a constant in the neighborhood of $v = 0$, the behavior of the two-terminal device (202) is similar to that of non-volatile memristors.

The dynamics of the circuit in Fig. 18is given by

The dynamics of the circuit

$$\left.\begin{array}{rcl} C\dfrac{dv}{dt} &=& \rho\Big(2x \ln \mid v \mid +cx + d \ln \mid v \mid - \ln \mid v \mid\Big)v, \\ \dfrac{dx}{dt} &=& \mu\Big(x^2 - (\ln \mid v \mid)^2 + ax + b \ln \mid v \mid -x\Big), \end{array}\right\} \tag{209}$$

where $C = 1$.

If $\mid v \mid$ is not sufficiently small, this equation is recast into the form

$$\left.\begin{array}{rcl} \dfrac{d \ln \mid v \mid}{dt} &=& 2x \ln \mid v \mid +cx + d \ln \mid v \mid - \ln \mid v \mid, \\ \dfrac{dx}{dt} &=& x^2 - (\ln \mid v \mid)^2 + ax + b \ln \mid v \mid -x. \end{array}\right\} \tag{210}$$

Setting $y \triangleq \ln \mid v \mid$, we obtain

$$\left.\begin{array}{rcl} \dfrac{dy}{dt} &=& 2xy + cx + dy - y, \\ \dfrac{dx}{dt} &=& x^2 - y^2 + ax + by - x. \end{array}\right\} \tag{211}$$

Using Euler method, we obtain from Eq. (211)

$$\left.\begin{array}{rcl} y_{n+1} - y_n &=& 2x_n y_n + cx_n + dy_n - y_n, \\ x_{n+1} - x_n &=& {x_n}^2 - {y_n}^2 + ax_n + by_n - x_n. \end{array}\right\} \tag{212}$$

It can be recast into the Tinkerbell map [28]

Tinkerbell map

$$\left.\begin{array}{rcl} y_{n+1} &=& 2x_n y_n + cx_n + dy_n, \\ x_{n+1} &=& {z_n}^2 - {y_n}^2 + ax_n + by_n. \end{array}\right\} \tag{213}$$

The chaotic behavior of the Tinkerbell map (213) is shown in Fig. 22.

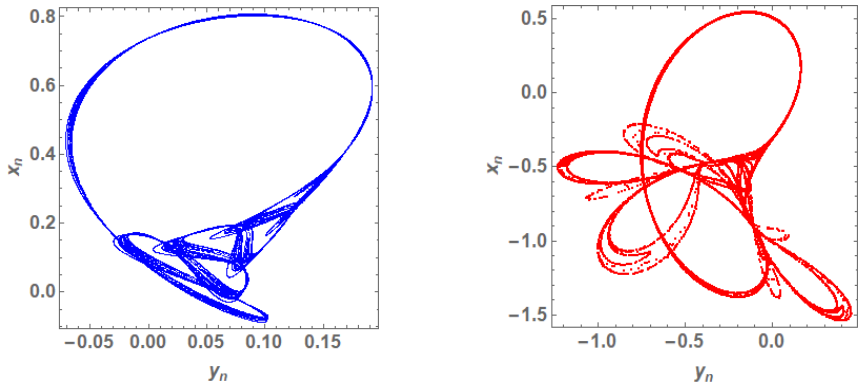

(a) (b)

Figure 22: Chaotic behavior of the Tinkerbell map (213) for two different parameters. (a) Parameters: $a = 0.3$, $b = 0.6845$, $c = 2.0$, $d = 0.27$. Initial conditions: $y_0 = 0.1$, $x_0 = 0.1$. (b) Parameters: $a = 0.9$, $b = -0.6013$, $c = 2.0$, $d = 0.5$. Initial conditions: $y_0 = 0.1$, $x_0 = 0.1$.

4.1.5 Three-dimensional Hénon map

Assume that the $v - i$ characteristic of the voltage-controlled extended memristor is given by

$v - i$ characteristic of the extended memristor

$$\left.\begin{aligned} i &= -\rho\Big(h\big(y,\ z,\ \ln \mid v \mid\big) - \ln \mid v \mid\Big)v, \\ \frac{dy}{dt} &= g\big(y,\ z,\ \ln \mid v \mid\big) - y, \\ \frac{dz}{dt} &= \mu\Big(f\big(y,\ z,\ \ln \mid v \mid\big) - z\Big), \end{aligned}\right\} \tag{214}$$

where

$$\left.\begin{aligned} h\big(y,\ z,\ \ln \mid v \mid\big) &= y, \\ g\big(y,\ z,\ \ln \mid v \mid\big) &= z, \\ f\big(y,\ z,\ \ln \mid v \mid\big) &= a + b\ln \mid v \mid + cy + dy^2 - z^2, \end{aligned}\right\} \tag{215}$$

and a, b, c, and d are constants. Substituting Eq. (215) into Eq. (214), we obtain

$$\left.\begin{aligned} i &= -\rho\Big(y - \ln \mid v \mid\Big)v, \\ \frac{dy}{dt} &= z - y, \\ \frac{dz}{dt} &= \mu\Big(a + b\ln \mid v \mid + cy + dy^2 - z^2 - z\Big). \end{aligned}\right\} \tag{216}$$

The voltage-controlled extended memristor (216) is an active element, since the instantaneous power consumed by the memristor satisfies

$$P(t) \triangleq v(t)\, i(t) = -\rho\Big(y(t) - \ln \mid v(t) \mid\Big)v(t)^2 < 0, \tag{217}$$

when $y(t) - \ln \mid v(t) \mid$ is sufficiently large.

To study the non-volatility property, we drive the voltage-controlled extended memristor (216) by the voltage source $v_s(t)$ where we set $v_s(t) = v(t) \to 0$ for $t \geq t_0$. If $0 <\mid v \mid \ll 1$, then $\big|\ln \mid v \mid\big|$ is sufficiently

large. Furthermore, the resistive-fuse function $\mu(s)$ satisfies Eq. (155). Thus we obtain from Eq. (216)

$$\left.\begin{array}{rcl} \dfrac{dy}{dt} &=& z-y, \\ \dfrac{dz}{dt} &=& \mu\Big(a+b\ln\mid v\mid +cy+dy^2-z^2-z\Big)=0. \end{array}\right\} \tag{218}$$

It has the solution $z(t)=c$, and $y(t)\to c$, where c is a constant. Similarly, we get

$$\lim_{v\to 0} i=\lim_{v\to 0}-\rho\Big(y-\ln\mid v\mid\Big)v\to 0, \tag{219}$$

since $\Big|\ln\mid v\mid\Big|$ is sufficiently large. Thus, without loss of generality, we can define

$$i\,\Big|_{v=0}=0. \tag{220}$$

Considering that the state $x(t)$ is a constant and $y(t)\to c$ in the neighborhood of $v=0$, the behavior of the two-terminal device (214) is similar to that of non-volatile memristors.

The dynamics of the circuit in Fig. 18 is given by

The dynamics of the circuit

$$\left.\begin{array}{rcl} C\dfrac{dv}{dt} &=& \rho\Big(y-\ln\mid v\mid\Big)v, \\ \dfrac{dz}{dt} &=& z-y, \\ \dfrac{dz}{dt} &=& \mu\Big(a+b\ln\mid v\mid +cy+dy^2-ez^2-z\Big), \end{array}\right\} \tag{221}$$

where $C=1$. If $\mid v\mid$ is not sufficiently small, this equation is recast into the form

The dynamics of the circuit

$$\left.\begin{array}{rcl} \dfrac{d\ln\mid v\mid}{dt} &=& \Big(y-\ln\mid v\mid\Big)v, \\ \dfrac{dz}{dt} &=& z-y, \\ \dfrac{dz}{dt} &=& a+b\ln\mid v\mid +cy+dy^2-ez^2-z. \end{array}\right\} \tag{222}$$

Setting $x\triangleq\ln\mid v\mid$, we obtain

The dynamics of the circuit

$$\left.\begin{array}{rcl} \dfrac{dx}{dt} &=& y-x, \\ \dfrac{dz}{dt} &=& z-y, \\ \dfrac{dz}{dt} &=& a+bx+cy+dy^2-ez^2-z. \end{array}\right\} \tag{223}$$

Using Euler method, we obtain from Eq. (223)

$$\left.\begin{aligned} x_{n+1} - x_n &= y_n - x_n, \\ y_{n+1} - y_n &= z_n - y_n, \\ z_{n+1} - z_n &= a + bx_n + cy_n + d{y_n}^2 - e{z_n}^2 - z_n. \end{aligned}\right\} \tag{224}$$

It can be recast into the form:

Three-dimensional Hénon map

$$\left.\begin{aligned} x_{n+1} &= y_n, \\ y_{n+1} &= z_n, \\ z_{n+1} &= a + bx_n + cy_n + d{y_n}^2 - e{z_n}^2. \end{aligned}\right\} \tag{225}$$

When $c = d = 0$ and $e = 1$, it is equivalent to the generalized Hénon map, which is shown in [29]:

Generalized Hénon map

$$\left.\begin{aligned} x_{n+1} &= y_n, \\ y_{n+1} &= z_n, \\ z_{n+1} &= a + bx_n - {z_n}^2. \end{aligned}\right\} \tag{226}$$

The chaotic behavior of the three-dimensional Hénon map (225) is shown in Fig. 23.

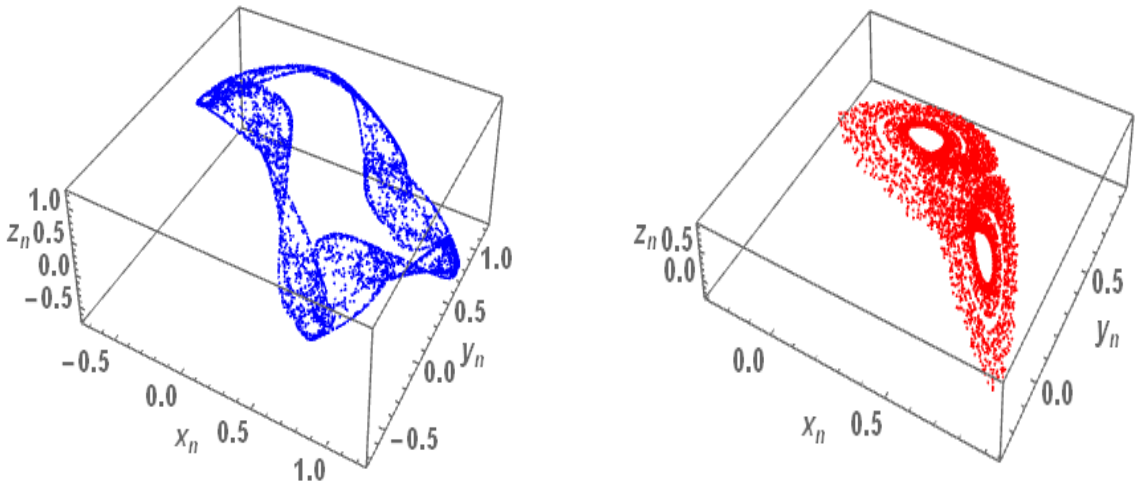

(a) (b)

Figure 23: Chaotic behavior of the three-dimensional Hénon map (225) for two different parameters. (a) Parameters: $a = 0.7281$, $b = 0.5$, $c = 0$, $d = 0$, $e = 1$. Initial conditions: $x_0 = 0$, $y_0 = 0$, $z_0 = 1$. (b) Parameters: $a = 0.002$, $b = 0.7$, $c = 0.87$, $d = 1$, $e = 0$. Initial conditions: $x_0 = 1$, $y_0 = 0$, $z_0 = 0$.

4.1.6 Gumowski-Mira map

Assume that the $v-i$ characteristic of the voltage-controlled extended memristor is given by

$v-i$ characteristic of the extended memristor

$$\left.\begin{array}{rcl} i &=& -\rho\Big(h\big(x,\ \ln\mid v\mid\big)-\ln\mid v\mid\Big)v, \\ \dfrac{dx}{dt} &=& \mu\Big(g\big(x,\ \ln\mid v\mid\big)-x\Big), \end{array}\right\} \tag{227}$$

where

$$\left.\begin{array}{rcl} h(x,\ \ln\mid v\mid) &=& x+b(1-0.05x^2)x+F\big(\ln\mid v\mid\big), \\ g(x,\ \ln\mid v\mid) &=& -\ln\mid v\mid+F\big(\,h(x,\ \ln\mid v\mid)\,\big), \\ F(y) &=& ay+\dfrac{2(1-a)y^2}{1+y^2}, \end{array}\right\} \tag{228}$$

and a and b are constants. Substituting Eq. (228) into Eq. (227), we obtain

$$\left.\begin{array}{rcl} i &=& -\rho\Big(x+b(1-0.05x^2)x+F(\ln\mid v\mid)-\ln\mid v\mid\Big)v, \\ \dfrac{dx}{dt} &=& \mu\Big(-\ln\mid v\mid+F\big(\,h(\,x,\ \ln\mid v\mid)\,\big)\,-x\Big). \end{array}\right\} \tag{229}$$

The voltage-controlled extended memristor (229) is an active element, since the instantaneous power consumed by the memristor satisfies

$$P(t)\triangleq v(t)\,i(t)=-\rho\Big(x(t)+b(1-0.05x(t)^2)x+F(\ln\mid v(t)\mid)-\ln\mid v(t)\mid\Big)v(t)^2<0, \tag{230}$$

since we can choose $x(t)$ and $v(t)$ such that $x(t)+b(1-0.05x(t)^2)x+F(\ln\mid v(t)\mid)-\ln\mid v(t)\mid$ is sufficiently large.

To study the non-volatility property, we drive the voltage-controlled extended memristor (229) by the voltage source $v_s(t)$ where we set $v_s(t)=v(t)\to 0$ for $t\geq t_0$. If $0<\mid v\mid\ll 1$, then $\big\mid\ln\mid v\mid\big\mid$ is sufficiently large. Furthermore, the resistive-fuse function $\mu(s)$ satisfies Eq. (155). Thus, without loss of generality, we can define

$$\frac{dx}{dt}=0. \tag{231}$$

It has the solution $x(t)=c$, where c is a constant. Similarly, we get

$$\lim_{v\to 0} i=\lim_{v\to 0}-\rho\Big(x+b(1-0.05x^2)x+F(\ln\mid v\mid)-\ln\mid v\mid\Big)v\to 0. \tag{232}$$

Thus we can define

$$i\,\Big|_{v=0}=0. \tag{233}$$

Considering that the state $x(t)$ is a constant in the neighborhood of $v=0$, the behavior of the two-terminal device (227) is similar to that of non-volatile memristors.

The dynamics of the circuit in Fig. 18 is given by

The dynamics of the circuit

$$\left.\begin{array}{rcl} C\dfrac{dv}{dt} &=& \rho\Big(x+b(1-0.05x^2)x+F(\ln\mid v\mid)-\ln\mid v\mid\Big)v, \\ \dfrac{dx}{dt} &=& \mu\Big(-\ln\mid v\mid+F\big(\,h(\,x,\ \ln\mid v\mid)\,\big)\,-x\Big), \end{array}\right\} \tag{234}$$

where $C = 1$. If $\mid v \mid$ is not sufficiently small, this equation is recast into the form

$$\left.\begin{array}{rcl} \dfrac{d\ln \mid v \mid}{dt} &=& x + b(1 - 0.05x^2)x + F(\ln \mid v \mid) - \ln \mid v \mid, \\ \dfrac{dx}{dt} &=& -\ln \mid v \mid + F\big(\, h(\, x,\ \ln \mid v \mid)\,\big) - x. \end{array}\right\} \tag{235}$$

Setting $y \triangleq \ln \mid v \mid$, we obtain

$$\left.\begin{array}{rcl} \dfrac{dy}{dt} &=& x + b(1 - 0.05x^2)x + F(y) - y, \\ \dfrac{dx}{dt} &=& -y + F\big(\, h(\, x,\ y\,)\,\big) - x. \end{array}\right\} \tag{236}$$

Using Euler method, we obtain from Eq. (236)

$$\left.\begin{array}{rcl} y_{n+1} - y_n &=& x_n + b(1 - 0.05{x_n}^2)x + F(y_n) - y_n, \\ x_{n+1} - x_n &=& -y_n + F\big(\, h(\, x_n,\ y_n\,)\,\big) - x_n. \end{array}\right\} \tag{237}$$

It is written as

$$\boxed{\left.\begin{array}{rcl} y_{n+1} &=& x_n + b(1 - 0.05{x_n}^2)x + F(y_n), \\ x_{n+1} &=& -y_n + F\big(\, h(\, x_n,\ y_n\,)\,\big). \end{array}\right\}} \tag{238}$$

From Eqs. (228) and (238), $h(\, x_n,\ y_n\,)$ satisfies the following relation

$$h(x_n,\ y_n) = x_n + b(1 - 0.05{x_n}^2)x_n + F(y_n) = y_{n+1}. \tag{239}$$

Thus, Eq. (237) can be recast into the Gumowski-Mira Map [30]

Gumowski-Mira map

$$\left.\begin{array}{rcl} y_{n+1} &=& x_n + b(1 - 0.05{x_n}^2)x_n + F(y_n), \\ x_{n+1} &=& -y_n + F(y_{n+1}). \end{array}\right\} \tag{240}$$

The chaotic behavior of the Gumowski-Mira Map (240) is shown in Fig. 24.

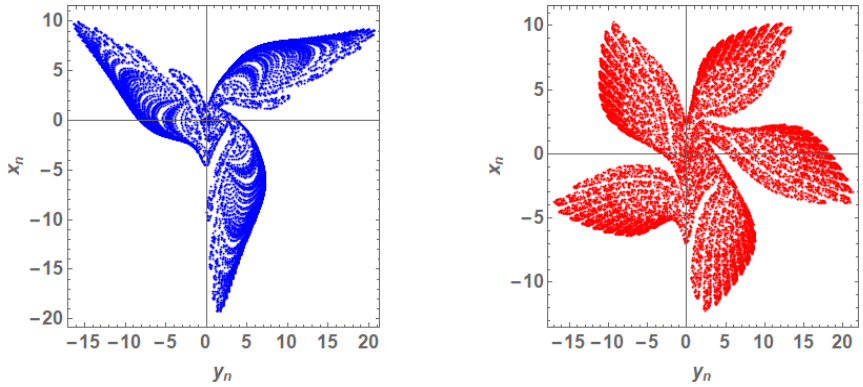

(a) (b)

Figure 24: Chaotic behavior of the Gumowski-Mira map (240) for two different parameters. (a) Parameters: $a = -0.8$, $b = 0.008$. Initial conditions: $y_0 = 0.1$, $x_0 = 0.1$. (b) Parameters: $a = -0.495$, $b = 0.005$. Initial conditions: $y_0 = 0.1$, $x_0 = 0.1$

(1) Simplified Gumowski-Mira map A

Let us obtain a somewhat simplified version of the equation (238). If we replace $g(x,\ \ln\ |\ v\ |)$ in Eq. (228) with

$$g(x,\ \ln\ |\ v\ |) = -\ln\ |\ v\ |, \tag{241}$$

then the dynamics of the circuit is given by

$$\left.\begin{aligned} C\frac{dv}{dt} &= \rho\Big(x + b(1-0.05x^2)x + F(\ln\ |\ v\ |) - \ln\ |\ v\ |\Big)v, \\ \frac{dx}{dt} &= \mu\Big(-\ln\ |\ v\ | - x\Big), \end{aligned}\right\} \tag{242}$$

where $C = 1$. Suppose that v is not sufficiently small and set $y \triangleq \ln\ |\ v\ |$. Then we obtain from Eq. (242)

$$\left.\begin{aligned} \frac{dy}{dt} &= x + b(1-0.05x^2)x + F(y) - y, \\ \frac{dx}{dt} &= -y - x. \end{aligned}\right\} \tag{243}$$

Its discretized equation is given by the simplified Gumowski-Mira map A:

Simplified Gumowski-Mira map A

$$\left.\begin{aligned} y_{n+1} &= x_n + b(1-0.05{x_n}^2)x_n + F(y_n), \\ x_{n+1} &= -y_n. \end{aligned}\right\} \tag{244}$$

The chaotic behavior of the simplified Gumowski-Mira Map A (244) is shown in Fig. 25(a).

(2) Simplified Gumowski-Mira map B

Similarly, if we replace $h(x,\ \ln|v|)$ and $g(x,\ \ln|v|)$ in Eq. (228) with

$$\left.\begin{aligned} h(x,\ \ln|v|) &= x, \\ g(x,\ \ln|v|) &= -\ln|v| + F\big(h(x,\ \ln|v|)\big), \end{aligned}\right\} \tag{245}$$

then the dynamics of the circuit is given by

$$\left.\begin{aligned} C\frac{dv}{dt} &= \rho\Big(x - \ln|v|\Big)v, \\ \frac{dx}{dt} &= \mu\Big(-\ln|v| + F\big(h(x,\ \ln|v|)\big) - x\Big), \end{aligned}\right\} \tag{246}$$

where $C = 1$. Suppose that v is not sufficiently small and set $y \triangleq \ln|v|$. Then we obtain from Eq. (246)

$$\left.\begin{aligned} \frac{dy}{dt} &= x, \\ \frac{dx}{dt} &= -y + F\big(h(x,\ y)\big) - x. \end{aligned}\right\} \tag{247}$$

Its discretized equation is given by the simplified Gumowski-Mira map B:

Simplified Gumowski-Mira map B

$$\left.\begin{aligned} y_{n+1} &= x_n, \\ x_{n+1} &= -y_n + F(y_{n+1}). \end{aligned}\right\} \tag{248}$$

The chaotic behavior of the simplified Gumowski-Mira map B (248 is shown in Fig. 25(b).

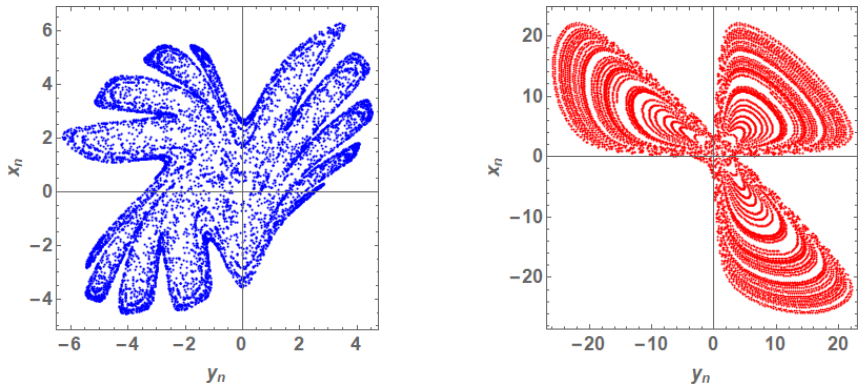

(a) (b)

Figure 25: (a) Chaotic behavior of the simplified Gumowski-Mira map A (244). Parameters: $a = -0.8$, $b = 0.1$. Initial conditions: $y_0 = 0.1$, $x_0 = 0.1$. (b) Chaotic behavior of the simplified Gumowski-Mira map B (248). Parameters: $a = -0.99$, $b = 0.008$. Initial conditions: $y_0 = 0.1$, $x_0 = 0.5$.

4.1.7 Ikeda map

Assume that the $v-i$ characteristic of the voltage-controlled extended memristor is given by

$v-i$ characteristic of the extended memristor

$$\left.\begin{array}{rcl} i &=& -\rho\Big(h\big(x,\ \ln\mid v\mid\big)-\ln\mid v\mid\Big)v, \\ \dfrac{dx}{dt} &=& \mu\Big(g\big(x,\ \ln\mid v\mid\big)-x\Big), \end{array}\right\} \tag{249}$$

where

$$\left.\begin{array}{rcl} h(x,\ \ln\mid v\mid) &=& a+b\big\{\ln\mid v\mid\cos(\xi)-x\sin(\xi)\big\}, \\ g(x,\ \ln\mid v\mid) &=& b\big\{\ln\mid v\mid\sin(\xi)+x\cos(\xi)\big\}, \end{array}\right\} \tag{250}$$

and

$$\xi = c-\frac{d}{1+\ln\mid v\mid^2+x^2}, \tag{251}$$

and $a,\ b,\ c$ and d are constants. Substituting Eq. (250) into Eq. (249), we obtain

$$\left.\begin{array}{rcl} i &=& -\rho\Big(a+b\big\{\ln\mid v\mid\cos(\xi)-x\sin(\xi)\big\}-\ln\mid v\mid\Big)v, \\ \dfrac{dx}{dt} &=& \mu\bigg(b\Big\{\ln\mid v\mid\sin(\xi)+x\cos(\xi)\Big\}-x\bigg). \end{array}\right\} \tag{252}$$

The voltage-controlled extended memristor (252) is an active element, since the instantaneous power consumed by the memristor satisfies

$$P(t)\triangleq v(t)\,i(t)=-\rho\Big(a+b\big\{\ln\mid v\mid\cos(\xi)-x\sin(\xi)\big\}-\ln\mid v\mid\Big)v(t)^2<0, \tag{253}$$

since we can choose $x(t)$ and $v(t)$ such that $a+b\big\{\ln\mid v\mid\cos(\xi)-x\sin(\xi)\big\}-\ln\mid v\mid$ is sufficiently large.

To study the non-volatility property, we drive the voltage-controlled extended memristor (252) by the voltage source $v_s(t)$ where we set $v_s(t)=v(t)\to 0$ for $t\geq t_0$. If $0<\mid v\mid\ll 1$, then $\big\mid\ln\mid v\mid\big\mid$ is sufficiently large and $\xi\approx c$. Furthermore, the resistive-fuse function $\mu(s)$ satisfies Eq. (155). Thus, we obtain

$$\frac{dx}{dt}=\mu\bigg(b\Big\{\ln\mid v\mid\sin(\xi)+x\cos(\xi)\Big\}-x\bigg)=0. \tag{254}$$

It has the solution $x(t)=r$, where r is a constant.

Similarly, considering that the saturation function $\rho(s)$ satisfies Eq. (154), we get

$$\lim_{v\to 0} i=\lim_{v\to 0}-\rho\Big(a+b\big\{\ln\mid v\mid\cos(\xi)-x\sin(\xi)\big\}-\ln\mid v\mid\Big)v\to 0. \tag{255}$$

Thus, without loss of generality, we can define

$$i\,\Big|_{v=0}=0. \tag{256}$$

Since the state $x(t)$ is a constant in the neighborhood of $v=0$, the behavior of the two-terminal device (249) is similar to that of non-volatile memristors.

The dynamics of the circuit in Fig. 18 is given by

The dynamics of the circuit

$$\left.\begin{array}{rcl} C\dfrac{dv}{dt} &=& \rho\Big(a+b\big\{\ln\mid v\mid\cos(\xi)-x\sin(\xi)\big\}-\ln\mid v\mid\Big)v, \\ \dfrac{dx}{dt} &=& \mu\bigg(b\Big\{\ln\mid v\mid\sin(\xi)+x\cos(\xi)\Big\}-x\bigg), \end{array}\right\} \tag{257}$$

where $C = 1$. If $\mid v \mid$ is not sufficiently small and if $\mid x \mid$ is not sufficiently large, then this equation is recast into the form

$$\left.\begin{array}{rcl} \dfrac{d \ln \mid v \mid}{dt} &=& a + b\Big\{\ln \mid v \mid \cos(\xi) - x \sin(\xi)\Big\} - \ln \mid v \mid, \\ \dfrac{dx}{dt} &=& b\Big\{\ln \mid v \mid \sin(\xi) + x \cos(\xi)\Big\} - x. \end{array}\right\} \tag{258}$$

Setting $y \triangleq \ln \mid v \mid$, we obtain

$$\left.\begin{array}{rcl} \dfrac{dy}{dt} &=& a + b\Big\{y \cos(\xi) - x \sin(\xi)\Big\} - y, \\ \dfrac{dx}{dt} &=& b\Big\{y \sin(\xi) + x \cos(\xi)\Big\} - x, \end{array}\right\} \tag{259}$$

$$\xi = c - \frac{d}{1 + y^2 + x^2}. \tag{260}$$

Using Euler method, we obtain from Eq. (259)

$$\boxed{\left.\begin{array}{rcl} y_{n+1} - y_n &=& a + b\Big\{y_n \cos(\xi_n) - x_n \sin(\xi_n)\Big\} - y_n, \\ x_{n+1} - x_n &=& b\Big\{y_n \sin(\xi) + x_n \cos(\xi_n)\Big\} - x_n, \end{array}\right\}} \tag{261}$$

where

$$\xi_n = c - \frac{d}{1 + {y_n}^2 + {x_n}^2}. \tag{262}$$

It can be recast into the Ikeda map [22, 23]

Ikeda map

$$\left.\begin{array}{rcl} y_{n+1} &=& a + b\Big\{y_n \cos(\xi_n) - x_n \sin(\xi_n)\Big\}, \\ x_{n+1} &=& b\Big\{y_n \sin(\xi_n) + x_n \cos(\xi_n)\Big\}. \end{array}\right\} \tag{263}$$

The chaotic behavior of the Ikeda map (263) is shown in Fig. 26.

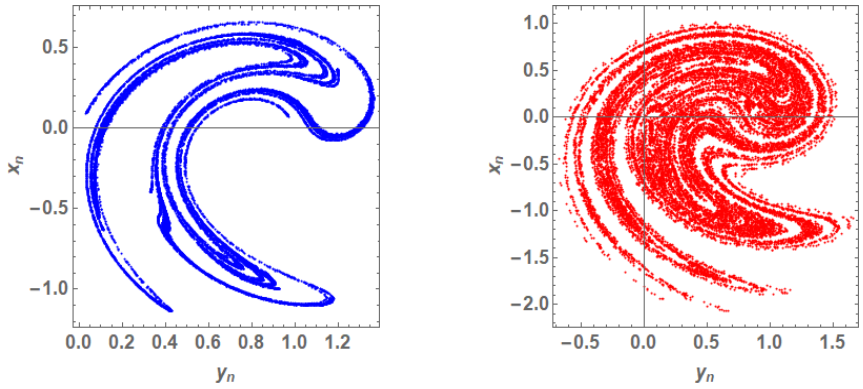

(a) (b)

Figure 26: Chaotic behavior of the Ikeda map (263) for two different parameters. (a) Parameters: $a = 1$, $b = 0.8, c = 0.4$, $d = 6$. Initial conditions: $y_0 = 0$, $x_0 = 0$. (b) Parameters: $a = 0.84$, $b = 0.95, c = 0.4$, $d = 6$. Initial conditions: $y_0 = 0$, $x_0 = 0$.

4.1.8 Peter de Jong map

Assume that the $v-i$ characteristic of the voltage-controlled extended memristor is given by

$v-i$ characteristic of the extended memristor

$$\left.\begin{array}{rcl} i &=& -\rho\Big(h\big(x,\ \ln\mid v\mid\big)-\ln\mid v\mid\Big)v, \\ \dfrac{dx}{dt} &=& \mu\Big(g\big(x,\ \ln\mid v\mid\big)-x\Big), \end{array}\right\} \tag{264}$$

where

$$\left.\begin{array}{rcl} h\big(x,\ \ln\mid v\mid\big) &=& \sin(a\pi x)-\cos(b\pi\ln\mid v\mid), \\ g\big(x,\ \ln\mid v\mid\big) &=& \sin(c\pi\ln\mid v\mid)-\cos(d\pi x), \end{array}\right\} \tag{265}$$

and $a,\ b,\ c$ and d are constants. Substituting Eq. (265) into Eq. (264), we obtain

$$\left.\begin{array}{rcl} i &=& -\rho\Big(\sin(a\pi x)-\cos(b\pi\ln\mid v\mid)-\ln\mid v\mid\Big)v, \\ \dfrac{dx}{dt} &=& \mu\Big(\sin(c\pi\ln\mid v\mid)-\cos(d\pi x)-x\Big). \end{array}\right\} \tag{266}$$

The voltage-controlled extended memristor (266) is an active element, since the instantaneous power consumed by the memristor satisfies

$$P(t)\triangleq v(t)\,i(t)=-\rho\Big(\sin(a\pi x(t))-\cos(b\pi\ln\mid v(t)\mid)-\ln\mid v(t)\mid\Big)v(t)^2<0, \tag{267}$$

when $-\ln\mid v(t)\mid$ is sufficiently large.

To study the non-volatility property, we drive the voltage-controlled extended memristor (266) by the voltage source $v_s(t)$ where we set $v_s(t)=v(t)\to 0$ for $t\geq t_0$. If $\mid x\mid$ becomes sufficiently large, then

$$\frac{dx}{dt}=0, \tag{268}$$

since the resistive-fuse function $\mu(s)$ satisfies Eq. (155). Thus $x(t)$ remains in finite region.

Similarly, in the neighborhood of $v=0$, we obtain

$$\lim_{v\to 0} i=\lim_{v\to 0}-\rho\Big(\sin(a\pi x)-\cos(b\pi\ln\mid v\mid)-\ln\mid v\mid\Big)v\to 0, \tag{269}$$

since $\mid\ln\mid v\mid\mid$ is sufficiently large and the saturation function $\rho(s)$ satisfies Eq. (154). Thus, without loss of generality, we can define

$$i\ \Big|_{v=0}=0. \tag{270}$$

Assume that $x(t)$ is not large and therefore $\dfrac{dx}{dt}\neq 0$. Then the state $x(t)$ changes with time even if Eq. (270) is satisfied. Thus the behavior of the two-terminal device (266) is a volatile memristor.

The dynamics of the circuit in Fig. 18 is given by

The dynamics of the circuit

$$\left.\begin{array}{rcl} C\dfrac{dv}{dt} &=& \rho\Big(\sin(a\pi x)-\cos(b\pi\ln\mid v\mid)-\ln\mid v\mid\Big)v, \\ \dfrac{dx}{dt} &=& \mu\Big(\sin(c\pi\ln\mid v\mid)-\cos(d\pi x)-x\Big), \end{array}\right\} \tag{271}$$

where $C = 1$.

If $\mid v \mid$ is not sufficiently small and if $\mid x \mid$ is not sufficiently large, then this equation is rewritten in the form

$$\left.\begin{array}{rcl} \dfrac{d \ln \mid v \mid}{dt} & = & \Big(\sin(a\pi x) - \cos(b\pi \ln \mid v \mid) - \ln \mid v \mid\Big), \\ \dfrac{dx}{dt} & = & \Big(\sin(c\pi \ln \mid v \mid) - \cos(d\pi x) - x\Big). \end{array}\right\} \tag{272}$$

Setting $y \triangleq \ln \mid v \mid$, we obtain

$$\left.\begin{array}{rcl} \dfrac{dy}{dt} & = & \sin(a\pi x) - \cos(b\pi y) - y, \\ \dfrac{dx}{dt} & = & \sin(c\pi y) - \cos(d\pi x) - x. \end{array}\right\} \tag{273}$$

Using Euler method, we obtain from Eq. (273)

$$\boxed{\left.\begin{array}{rcl} y_{n+1} - y_n & = & \sin(a\pi x_n) - \cos(b\pi y_n) - y_n, \\ x_{n+1} - x_n & = & \sin(c\pi y_n) - \cos(d\pi x_n) - x_n. \end{array}\right\}} \tag{274}$$

It can be recast into the Peter de Jong map [20]

Peter de Jong map

$$\left.\begin{array}{rcl} y_{n+1} & = & \sin(a\pi x_n) - \cos(b\pi y_n), \\ x_{n+1} & = & \sin(c\pi y_n) - \cos(d\pi x_n). \end{array}\right\} \tag{275}$$

The chaotic behavior of the Peter de Jong map (275) is shown in Fig. 27.

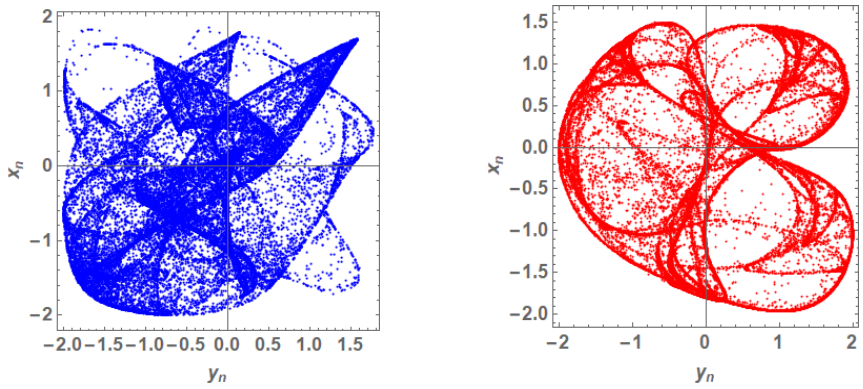

(a) (b)

Figure 27: Chaotic behavior of the Peter de Jong map (275) for two different parameters. (a) Parameters: $a = 0.854$, $b = 0.404, c = 0.742. d = 0.51$. Initial conditions: $v_0 = 1$, $x_0 = 1$. (b) Parameters: $a = 0.56$, $b = 0.54, c = -0.29. d = 0.54$. Initial conditions: $v_0 = 1$, $x_0 = 1$.

5 Two Element Nonlinear Resistor Circuits

Consider the two-element circuit in Fig. 28, which consists of a linear capacitor C and a nonlinear resistor with a characteristic curve defined by

$$i_R = f(v_R), \tag{276}$$

where i_R and v_R are the current through and voltage across the nonlinear resistor, respectively. The dynamics of the circuit in Fig. 28 is given by

Dynamics of the nonlinear resistor circuit

$$C\frac{dv}{dt} = -f(v), \tag{277}$$

where v is the voltage across the capacitor with the capacitance C.

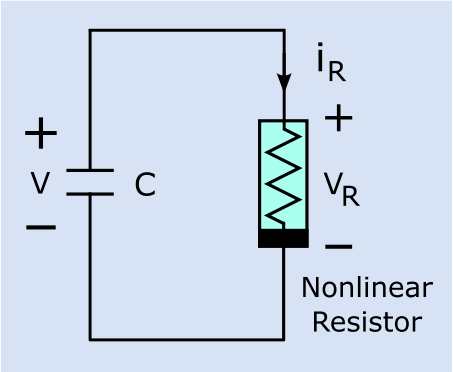

Figure 28: Two-element nonlinear resistor circuit consisting of a capacitor and a nonlinear resistor with the characteristic curve $i_R = f(v_R)$, where i_R and v_R are the current through and voltage across the nonlinear resistor, respectively, and v is the voltage across the capacitor with the capacitance C.

We discretize Eq. (277) using the Euler method defined by

Euler method

$$\frac{dv}{dt} \approx \frac{v(t+\Delta t) - v(t)}{\Delta t}, \tag{278}$$

where Δt is the time step size. Then we can approximate Eq. (277) by

$$C\frac{v(t+\Delta t) - v(t)}{\Delta t} = -f\big(v(t)\big). \tag{279}$$

If we set $v_n \triangleq v(t + n\Delta t)$ (where n is an integer), then we obtain

$$\left.\begin{aligned} v_1 - v_0 &= -\frac{\Delta t}{C} f(v_0), \\ v_2 - v_1 &= -\frac{\Delta t}{C} f(v_1), \\ &\vdots \\ v_{n+1} - v_n &= -\frac{\Delta t}{C} f(v_n). \end{aligned}\right\} \tag{280}$$

We can simply write

$$v_{n+1} - v_n = -\frac{\Delta t}{C} f(v_n), \tag{281}$$

where $n = 0, 1, 2, \cdots$. Furthermore, it can be written as

$$v_{n+1} = -\frac{\Delta t}{C} f(v_n) + v_n. \tag{282}$$

If we set $\Delta t = 1$ and $C = 1$, we obtain from Eq. (282)

$$v_{n+1} = -f(v_n) + v_n. \tag{283}$$

5.1 Examples of the two-element nonlinear resistor circuit generating chaotic behavior

In this section we show the examples of the nonlinear resistor circuits, which can be transformed into the one-dimensional chaotic maps.

5.1.1 Quadratic polynomial nonlinearity

Let us first consider the nonlinear resistor with a quadratic polynomial nonlinearity, that is, the characteristic curve of the nonlinear resistor is given by

$$i_R = f(v_R) = \alpha v_R^2 + \beta v_R + \gamma, \tag{284}$$

where α, β, and γ are constants.

(1) Logistic map

Assume that the $v - i$ characteristic of the nonlinear resistor is given by

$$i_R = f(v_R) = -a\, v_R(1 - v_R) + v_R, \tag{285}$$

where $a > 0$. Then the nonlinear resistor is an active element, since the instantaneous power consumed by the nonlinear resistor satisfies

$$P_R(t) \triangleq v_R(t)\, i_R(t) = -a\, v_R(t)^2 \left(1 - \frac{1}{a} - v_R(t)\right) < 0, \tag{286}$$

when $v_R(t) < 1 - \dfrac{1}{a}$.

The dynamics of the nonlinear resistor circuit shown in Fig. 28 is given by

Dynamics of the nonlinear resistor circuit

$$\frac{dv}{dt} = -f(v) = av(1 - v) - v = -av\left(v - 1 + \frac{1}{a}\right), \tag{287}$$

where $C = 1$ and $f(v) = -av(1 - v) + v$. Assume that $a > 1$. Then Eq. (287) has the unstable equilibrium point at origin and the asymptotically stable point at $v = 1 - \dfrac{1}{a} > 0$. If the initial condition $v(0)$ is positive, then $v(t) \to 1 - \dfrac{1}{a}$ for $t > 0$ and if the initial condition $v(0)$ is negative, then $v(t) \to -\infty$ for $t > 0$.

From Eq. (283), we obtain the discretized equation for Eq. (287)

Logistic map

$$v_{n+1} = a\, v_n(1 - v_n), \tag{288}$$

where $\Delta t = 1$. Thus we obtain the well-known logistic map [14]. The chaotic behavior of the logistic map (288) is shown in Fig. 29. The correlation between v_n and v_{n+20} is very weak as shown in Fig. 29(b).

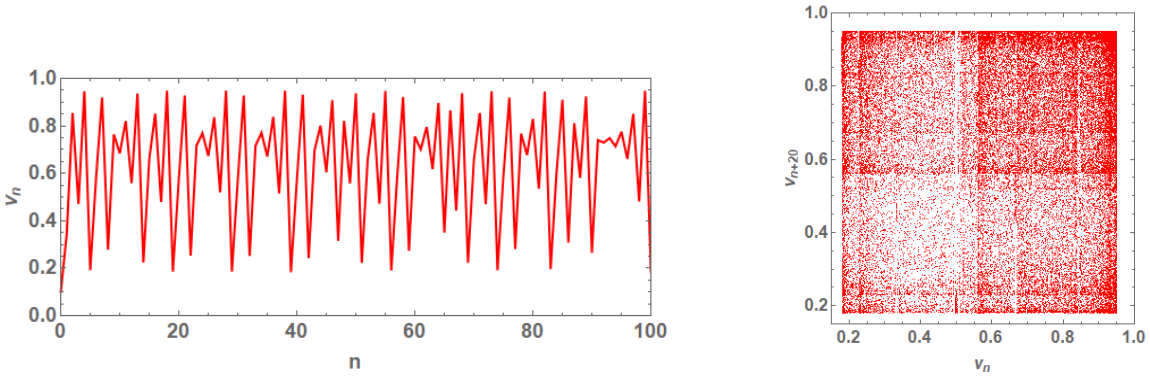

(a) Time series plot of v_n vs. n.

(b) Plot for v_n vs. v_{n+20}.

Figure 29: Chaotic behavior of the logistic map (288). Parameter: $a = 3.8$. Initial condition: $v_0 = 0.1$.

(2) Kawakami one-dimensional map

Assume that the $v - i$ characteristic of the nonlinear resistor is given by

$$i_R = f(v_R) = a - {v_R}^2 + v_R, \tag{289}$$

where $a > 0$. The nonlinear resistor is an active element, since the instantaneous power consumed by the nonlinear resistor satisfies

$$P_R(t) \triangleq v_R(t)\, i_R(t) = (a - {v_R(t)}^2 + v_R(t))v_R(t) < 0, \tag{290}$$

when $v_R(t)$ is sufficiently large.

The dynamics of the nonlinear resistor circuit shown in Fig. 28 is given by

Dynamics of the nonlinear resistor circuit

$$\frac{dv}{dt} = -f(v) = v^2 - v - a, \tag{291}$$

where $C = 1$ and $f(v) = -v^2 + v + a$. It has the stable equilibrium point $p_1 = \dfrac{1 - \sqrt{1 + 4a}}{2}$ and the unstable equilibrium point $p_2 = \dfrac{1 + \sqrt{1 + 4a}}{2}$, where $p_1 < p_2$. Thus, if the initial condition $v(0) < p_2$, then $v(t) \to p_1$ for $t > 0$, and if the initial condition $v(0) > p_2$, then $v(t) \to \infty$ for $t > 0$.

From Eq. (283), we obtain the discretized equation for Eq. (291)

Kawakami one-dimensional map

$$v_{n+1} = {v_n}^2 - a, \tag{292}$$

where $\Delta t = 1$. Thus we obtain the Kawakami one-dimensional map [33]. The chaotic behavior of the Kawakami one-dimensional map (292) is shown in Fig. 30. The correlation between v_n and v_{n+20} is very weak as shown in Fig. 30(b).

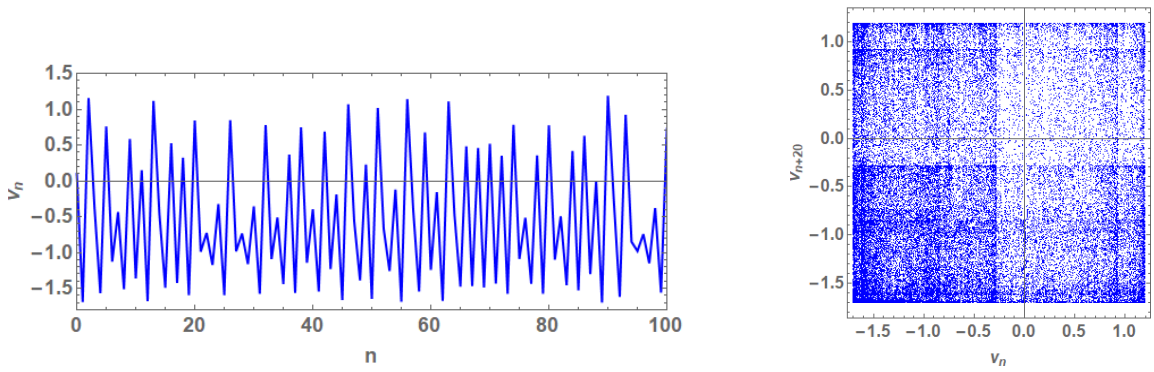

(a) Time series plot of v_n vs. n.

(b) Plot for v_n vs. v_{n+20}.

Figure 30: Chaotic behavior of the Kawakami one-dimensional map (292). Parameter: $a = 1.7$. Initial condition: $v_0 = 0.1$.

(3) One-dimensional map

Assume that the $v - i$ characteristic of the nonlinear resistor is given by

$$i_R = f(v_R) = (v_R - a)(v_R - b), \qquad (293)$$

where a and b are constants which satisfy $a < 0 < b$. The nonlinear resistor is an active element, since the instantaneous power consumed by the nonlinear resistor satisfies

$$P_R(t) \triangleq v_R(t)\, i_R(t) = (v_R(t) - a)(v_R(t) - b)v_R(t) < 0, \qquad (294)$$

when $a < v_R(t) < b$.

The dynamics of the nonlinear resistor circuit shown in Fig. 28 is given by

Dynamics of the nonlinear resistor circuit

$$\frac{dv}{dt} = -(v - a)(v - b), \qquad (295)$$

where $C = 1$ and $f(v) = (v - a)(v - b)$. This equation has the unstable equilibrium point p_a at $v = a$ and the asymptotically stable equilibrium point p_b at $v = b$. Thus, if the initial condition $v(0) > a$, then $v(t) \to b$ and if the initial condition $v(0) < a$, then $v(t) \to -\infty$.

The discretized equation for Eq. (295) is given by

One-dimensional map A

$$v_{n+1} = -(v_n - a)(v_n - b) + v_n, \qquad (296)$$

where $\Delta t = 1$. In our computer simulations, Eq. (296) exhibits chaotic behavior for $a = -1$ and $b = 1.8$ as shown in Fig. 31. The correlation between v_n and v_{n+20} is very weak as shown in Fig. 31(b).

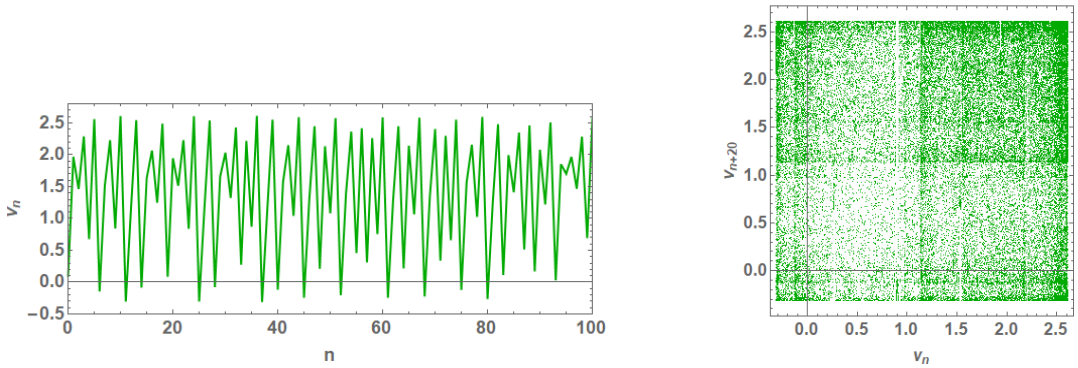

(a) Time series plot of v_n vs. n.

(b) Plot for v_n vs. v_{n+20}.

Figure 31: Chaotic behavior of the one-dimensional map A (296). Parameters: $a = -1$, $b = 1.8$. Initial condition: $v_0 = 0.1$.

5.1.2 Piecewise-linear nonlinearity

Consider the nonlinear resistors with piecewise-linear nonlinearity composed of straight-line segments.

(1) Piecewise-linear map A

Assume that the $v - i$ characteristic of the nonlinear resistor is given by

$$i_R = f(v_R) = -a \mid v_R \mid + b + v_R, \tag{297}$$

where $a > 0$ and $b > 0$ are constants. The nonlinear resistor is an active, since the instantaneous power consumed by the nonlinear resistor satisfies

$$P_R(t) \triangleq v_R(t)\, i_R(t) = \Big(-a \mid v_R(t) \mid + b + v_R(t) \Big)\, v_R(t) < 0, \tag{298}$$

when $v_R(t) < 0$ and $\mid v_R(t) \mid \ll 1$. The dynamics of the circuit is given by

Dynamics of the nonlinear resistor circuit

$$\frac{dv}{dt} = a \mid v \mid - b - v. \tag{299}$$

If $a > 1$, then it has a stable equilibrium point $p_1 = -\dfrac{b}{a+1}$ and an unstable equilibrium point $p_2 = \dfrac{b}{a-1}$, where $p_1 < p_2$. Thus, if the initial condition $x(0) < p_2$, then $x(t) \to p_1$ for $t > 0$, and if the initial condition $x(0) > p_2$, then $x(t) \to \infty$ for $t > 0$.

The discretized equation for Eq. (299) is given by

Piecewise-linear map A

$$v_{n+1} = a \mid v_n \mid - b, \tag{300}$$

where $\Delta t = 1$. This is the piesewise-linear version of the Kawakami one-dimensional map (292).

In our computer simulations, Eq. (300) exhibits chaotic behavior for $a = 1.5$ and $b = 0.5$ as shown in Fig. 32. The correlation between v_n and v_{n+20} is very weak as shown in Fig. 32(b).

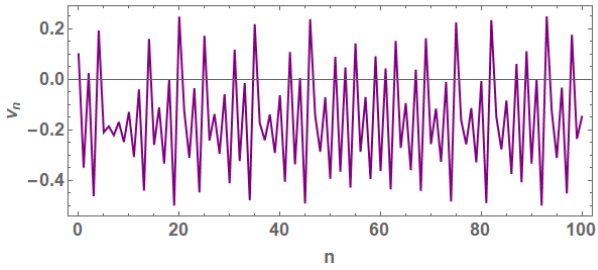

(a) Time series plot of v_n vs. n.

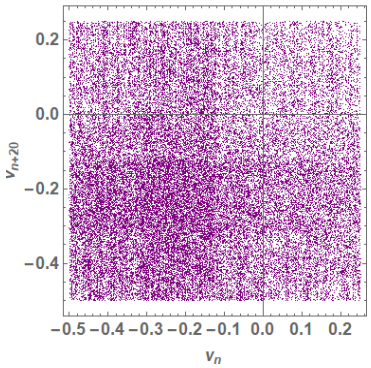

(b) Plot for v_n vs. v_{n+20}.

Figure 32: Chaotic behavior of the piecewise-linear map A (296). Parameters: $a = 1.5$, $b = 0.5$. Initial condition: $v_0 = 0.1$.

(1) Piecewise-linear map B

Assume that the $v - i$ characteristic of the nonlinear resistor is given by

$$i_R = f(v_R) = -av_R - 0.5(b-a)\big(\mid v_R + 0.5 \mid - \mid v_R - 0.5 \mid\big) + v_R, \quad (301)$$

where a and b are constants. Assume that $a = -1.98$ and $b = 1.98$. The nonlinear resistor is an active, since the instantaneous power consumed by the nonlinear resistor satisfies

$$P_R(t) \triangleq v_R(t)\, i_R(t) = \Big[-av_R(t) - 0.5(b-a)\big(\mid v_R(t) + 0.5 \mid - \mid v_R(t) - 0.5 \mid\big) + v_r(t)\Big]\, v_R(t) \le 0, \quad (302)$$

when $\mid v_R(t) \mid \ll 1$. The dynamics of the circuit is given by

Dynamics of the nonlinear resistor circuit

$$\frac{dv}{dt} = av + 0.5(b-a)\big(\mid v + 0.5 \mid - \mid v - 0.5 \mid\big) - v. \quad (303)$$

The origin is the unstable equilibrium point, and the points $p_1 \approx -0.664$ and $p_2 \approx 0.664$ are the asymptotically stable equilibrium points. Thus, if the initial condition $v(t_0)$ is positive, then $v(t) \to p_2$, and if the initial condition $v(t_0)$ is negative, then $v(t) \to p_1$.

The discretized equation for Eq. (299) is given by

Piecewise-linear map B

$$v_{n+1} = av_n + 0.5(b-a)\big(\mid v_n + 0.5 \mid - \mid v_n - 0.5 \mid\big), \quad (304)$$

where $\Delta t = 1$. If Eq. (304) is defined on the interval $0 \le v_n \le 1$, then it is equivalent to the tent map (tent transformation) [13, 27].

In our computer simulations, Eq. (304) exhibits chaotic behavior for $a = -1.98$ and $b = 1.98$ as shown in Fig. 33[4]. The correlation between v_n and v_{n+20} is much more weaker than in other examples (see Fig. 33(b)).

[4]Note that if for $a = -2$ and $b = 2$, then we cannot get the expected result in our computer simulations. In floating point calculations, the errors will accumulate and the calculation will not be able to be performed correctly.

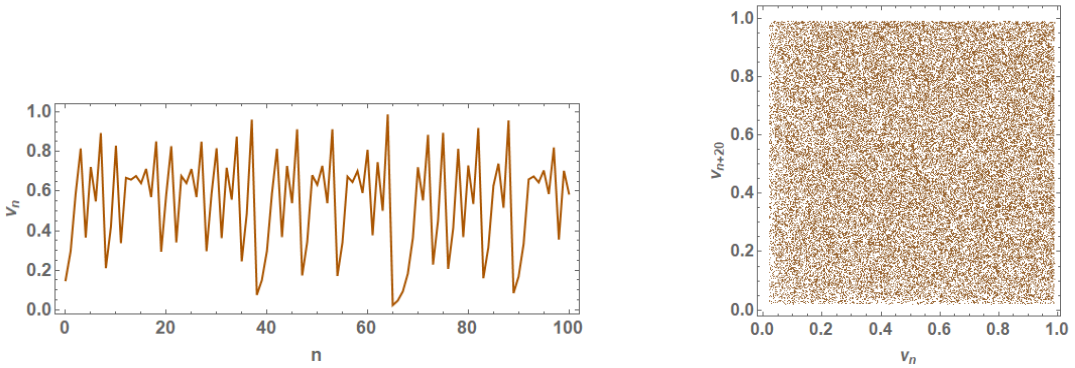

(a) Time series plot of v_n vs. n.

(b) Plot for v_n vs. v_{n+20}.

Figure 33: Chaotic behavior of the piecewise-linear map B (tent map) (296). Parameters: $a = -1.98$, $b = 1.98$. Initial condition: $v_0 = 0.15$.

(1) Piecewise-linear map C

Define the function $g(x)$ by

$$g(x) = \begin{cases} ax & \text{if} \quad x \le 0.5, \\ a(x - 0.5) & \text{if} \quad x > 0.5, \end{cases} \tag{305}$$

where $a > 1$ is a positive constant. Assume that the $v - i$ characteristic of the nonlinear resistor is given by

$$i_R = f(v_R) = -g(v_R) + v_R. \tag{306}$$

Since $a > 1$, the nonlinear resistor is an active, since the instantaneous power consumed by the nonlinear resistor satisfies

$$P_R(t) \triangleq v_R(t)\, i_R(t) = \Big[-g(v_R(t)) + v_R(t) \Big]\, v_R(t) \le 0, \tag{307}$$

when $v_R(t) \le 0.5$.

The dynamics of the circuit is given by

Dynamics of the nonlinear resistor circuit

$$\frac{dv}{dt} = g(v) - v. \tag{308}$$

It has the two unstable equilibrium points, $p_1 = 0$ and $p_2 = \dfrac{a}{2(a-1)}$.

The discretized equation for Eq. (299) is given by

Piecewise-linear map C

$$v_{n+1} = g(v_n), \tag{309}$$

where $\Delta t = 1$. If $a = 2$ and Eq. (309) is defined on the interval $0 \le v_n \le 1$, then it is equivalent to the doubling map (also known as the doubling transformation, Bernoulli shift map, or sawtooth map) [27].

In our computer simulations, Eq. (304) exhibits chaotic behavior for $a = 1.99$, as shown in Fig. 33[5]. The correlation between v_n and v_{n+20} is very weak as shown in Fig. 34(b), which is similar to that in Fig. 33(b).

[5]Note that if for $a = 2$, then we cannot get the expected result in our computer simulations. In floating point calculations, the errors will accumulate and the calculation will not be able to be performed correctly.

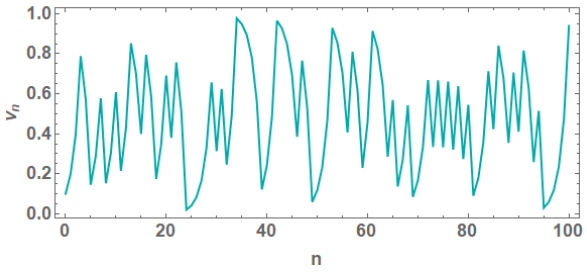

(a) Time series plot of v_n vs. n.

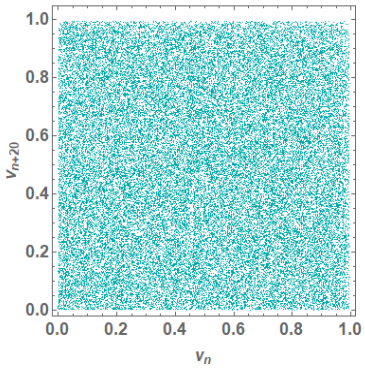

(b) Plot for v_n vs. v_{n+20}.

Figure 34: Chaotic behavior of the piecewise-linear map C (309). Parameter: $a = 1.99$. Initial condition: $v_0 = 0.1$.

6 Five Element Nonlinear Resistor Circuits

Consider the five-element circuit in Fig. 35, which consists of five elements, i.e., a linear inductor L, a linear capacitor C, a DC voltage source E, a linear resistor r, and a nonlinear resistor with the characteristic curve

$$i_R = f(v_R), \tag{310}$$

where $f(v_R)$ is a scaler function of v_R. The dynamics of the circuit is given by

Dynamics of the nonlinear resistor circuit

$$\left.\begin{aligned} C\frac{dv}{dt} &= i - f(v), \\ L\frac{di}{dt} &= -v - ri - E, \end{aligned}\right\} \tag{311}$$

where v and i denote the voltage of the capacitor and the current of the inductor, respectively.

We discretize it using the Euler method defined by

Euler method

$$\left.\begin{aligned} \frac{dv}{dt} &\approx \frac{v(t+\Delta t) - v(t)}{\Delta t}, \\ \frac{di}{dt} &\approx \frac{i(t+\Delta t) - i(t)}{\Delta t}, \end{aligned}\right\} \tag{312}$$

where Δt is the time step size. Then we can approximate Eq. (311) by

$$\left.\begin{aligned} C\frac{v(t+\Delta t) - v(t)}{\Delta t} &= i(t) - f\big(v(t)\big), \\ L\frac{x(t+\Delta t) - x(t)}{\Delta t} &= -v(t) - ri(t) - E. \end{aligned}\right\} \tag{313}$$

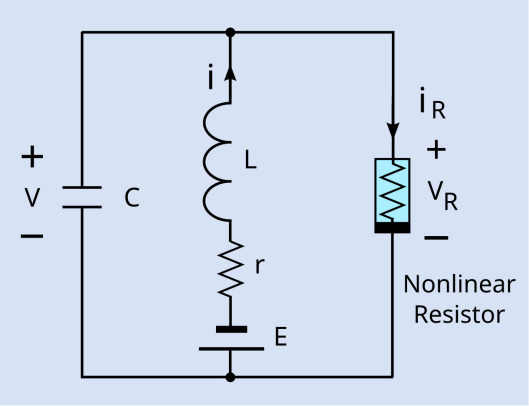

Figure 35: Five-element circuit, which consists of a linear inductor L, a linear capacitor C, a DC voltage source E, a linear resistor r, and a nonlinear resistor with the characteristic curve $i_R = f(v_R)$, where i_R and v_R are the current through and voltage across the nonlinear resistor, respectively, v is the voltage across the capacitor with the capacitance C, and i is the current through the inductor with the inductance L.

If we set $v_n \triangleq v(t + n\Delta t)$, and $i_n \triangleq i(t + n\Delta t)$, then we get from Eq. (313)

$$\left.\begin{aligned} v_{n+1} - v_n &= \frac{\Delta t}{C}\left\{i_n - f(v_n)\right\}, \\ i_{n+1} - i_n &= \frac{\Delta t}{L}\left\{-v_n - r i_n - E\right\}, \end{aligned}\right\} \tag{314}$$

where $n = 0, 1, 2, \cdots$. We can rewrite Eq. (314) in the following form

Two-dimensional map

$$\left.\begin{aligned} v_{n+1} &= \frac{\Delta t}{C}\left\{i_n - f(v_n)\right\} + v_n, \\ i_{n+1} &= \frac{\Delta t}{L}\left\{-v_n - r\, i_n - E\right\} + i_n. \end{aligned}\right\} \tag{315}$$

6.1 Examples of the nonlinear resistor circuits generating chaotic maps

In this section we show some examples of the nonlinear resistor circuits. They can be transformed into the two-dimensional chaotic maps.

6.1.1 Van der Pol chaotic map

Assume that the parameters of Eq. (311) are given by

$$C = 1,\ L = 1,\ r = 0,\ E = 0, \tag{316}$$

and $v - i$ characteristic of the nonlinear resistor is given by

$$i_R = f(v_R) = \frac{{v_R}^3}{3} - v_R. \tag{317}$$

The nonlinear resistor defined by Eq. (317) is eventually passive, meaning that for a large enough $\mid v_R(t) \mid$, the instantaneous power

$$P_R(t) \triangleq v_R(t)\, i_R(t) = \left(\frac{v_R(t)^2}{3} - 1 \right) v_R(t)^2, \tag{318}$$

is positive, which is consumed by the nonlinear resistor. From Eq. (311), we obtain the following Van der Pol equation

Dynamics of the nonlinear resistor circuit

$$\left.\begin{aligned} \frac{dv}{dt} &= i - \frac{v^3}{3} + v, \\ \frac{di}{dt} &= -v. \end{aligned}\right\} \tag{319}$$

Thus, from Eq.(315), we can obtain the discretized equation for Eq. (319)

Discretized Van der Pol equation

$$\left.\begin{aligned} v_{n+1} &= \Delta t \left(i_n - \frac{v_n^3}{3} + v_n \right) + v_n, \\ i_{n+1} &= -\Delta t\, v_n + i_n. \end{aligned}\right\} \tag{320}$$

The chaotic behavior of the discretized Van der Pol equation is shown in Fig. 36.

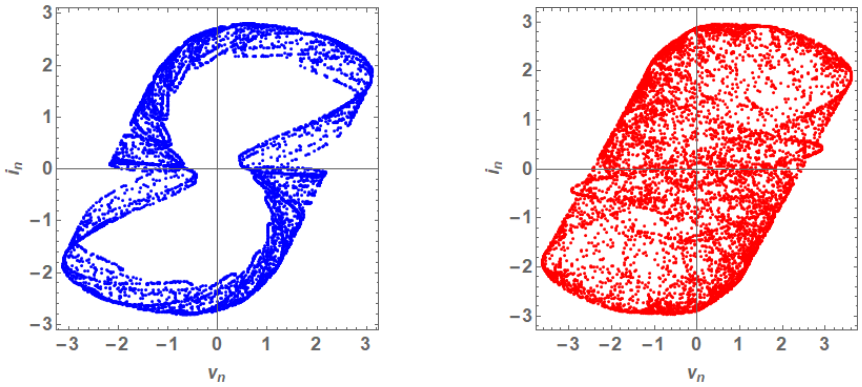

(a) (b)

Figure 36: Chaotic behavior of the discretized Van der Pol equation (320) for two different parameters. (a) Parameter: $\Delta t = 0.52$. Initial conditions: $v_0 = 0.01$, $i_0 = 0.02$. (b) Parameter: $\Delta t = 0.64$. Initial conditions: $v_0 = 0.01$, $i_0 = 0.02$.

6.1.2 Hopalong Map

Assume next that the parameters in Eq. (311) are given by

$$C = 1,\ L = 1,\ r = 1,\ E = -a, \tag{321}$$

and $v - i$ characteristic of the nonlinear resistor is defined by

$$f(v_R) = v_R + \mathrm{sgn}(v_R)\,\sqrt{|\,bv_R - c\,|}, \qquad (322)$$

where c is a constant. The nonlinear resistor defined by Eq. (322) is passive, since the instantaneous power $P_R(t)$ consumed by the nonlinear resistor is given by

$$P_R(t) \triangleq v_R(t)\,i_R(t) = {v_R}^2 + v_R\ \mathrm{sgn}(v_R(t))\,\sqrt{|\,bv_R(t) - c\,|} \geq 0. \qquad (323)$$

However, the DC voltage source E (which is an active element) powers the nonlinear circuit.

From Eq. (311), we obtain

Dynamics of the nonlinear resistor circuit

$$\left.\begin{aligned} \frac{dv}{dt} &= i - v - \mathrm{sgn}(v)\,\sqrt{|\,bv - c\,|}, \\ \frac{di}{dt} &= -v - i + a. \end{aligned}\right\} \qquad (324)$$

Similarly, from Eq.(315), we obtain its discretized equation

Hopalong Map

$$\left.\begin{aligned} v_{n+1} &= i_n - \mathrm{sgn}(v_n)\,\sqrt{|\,bv_n - c\,|}, \\ i_{n+1} &= -v_n + a, \end{aligned}\right\} \qquad (325)$$

where $\Delta t = 1$. Thus we obtain the Hopalong map [31]. The chaotic behavior of the Hopalong map is shown in Fig. 37.

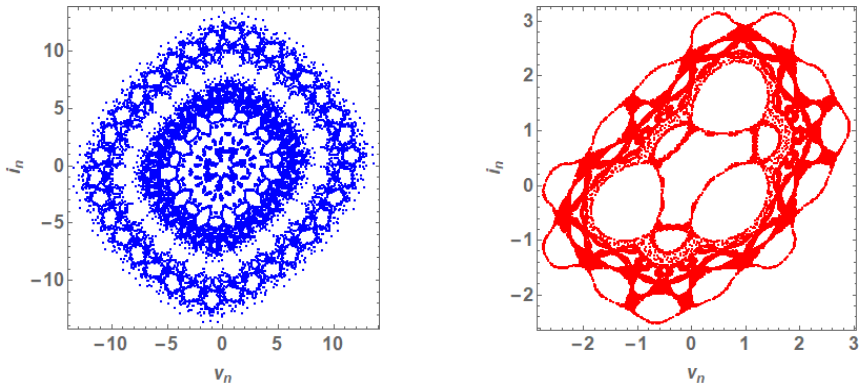

(a) (b)

Figure 37: Chaotic behavior of the Hopalong map (325) for two different parameters. (a) Parameters: $a = -0.1$, $b = 0.3$, $c = 0.3$. Initial conditions: $v_0 = 0$, $i_0 = 0$. (b) Parameters: $a = 0.4$, $b = 1$, $c = -0.01$. Initial conditions: $v_0 = 0$, $i_0 = 0$.

6.1.3 Gingerbreadman Map

Assume next that the parameters in Eq. (311) are given by

$$C = 1,\ L = 1,\ r = 1,\ E = 0, \qquad (326)$$

and the $v - i$ characteristic of the nonlinear resistor is defined by

$$f(v_R) = v_R - a \mid v_R \mid -1, \qquad (327)$$

where $a > 0$ is constant. The nonlinear resistor defined by Eq. (327) is active, since the instantaneous power $P_R(t)$ for $a \neq 1$ satisfies

$$P_R(t) \triangleq v_R(t)\, i_R(t) = v_R\,(v_R(t) - a \mid v_R(t) \mid -1) < 0, \qquad (328)$$

when $0 < v_R(t) < \dfrac{1}{1-a}$. If $a = 1$, then $P_R(t) < 0$ when $v_R(t) > 0$.

From Eq. (311), we obtain

Dynamics of the nonlinear resistor circuit

$$\left.\begin{aligned} \frac{dv}{dt} &= i - v + a \mid v \mid +1, \\ \frac{di}{dt} &= -v - i. \end{aligned}\right\} \qquad (329)$$

If we replace the variable i with $-j$, we get

$$\left.\begin{aligned} \frac{dv}{dt} &= -j - v + a \mid v \mid +1, \\ \frac{dj}{dt} &= v - j. \end{aligned}\right\} \qquad (330)$$

From Eq.(315), the discretized equation for Eq. (330) is given by

Modified Gingerbreadman Map

$$\left.\begin{aligned} v_{n+1} &= 1 - j_n + a \mid v_n \mid, \\ j_{n+1} &= v_n, \end{aligned}\right\} \qquad (331)$$

where $\Delta t = 1$. If $a = 1$, then Eq. (331) is equivalent to the Gingerbreadman map (see [32]). The chaotic behavior of Eq. (331) is shown in Fig. 38.

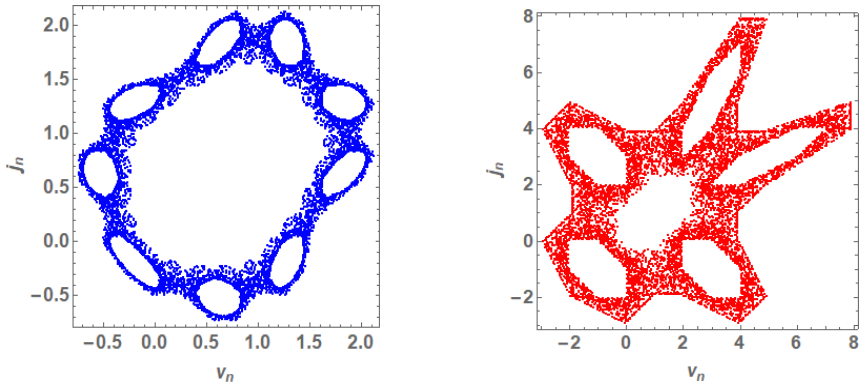

(a) (b)

Figure 38: Chaotic behavior of the Modified Gingerbreadman map (331) for two different parameters. (a) Parameter $a = 0.5$. Initial conditions: $v_0 = -0.1$, $j_0 = 0$. (b) Parameter $a = 1$. Initial conditions: $v_0 = -0.1$, $j_0 = 0$.

6.1.4 Lozi Map

Assume next that the parameters in Eq. (311) are given by

$$C = 1,\ L = -\frac{1}{b},\ r = -\frac{1}{b},\ E = 0, \tag{332}$$

and $v - i$ characteristic of the nonlinear resistor is defined by

$$f(v_R) = v_R - a \mid v_R \mid -1, \tag{333}$$

where $a > 0$ is a constant. The nonlinear resistor defined by Eq. (333) is active, since the instantaneous power $P_R(t)$ consumed by the nonlinear resistor

$$P_R(t) \triangleq v_R(t)\, i_R(t) = v_R(t)\,(v_R - a \mid v_R(t) \mid -1), \tag{334}$$

becomes negative when $v_R(t) > 0$. The linear resistor with the negative resistance $r = -\frac{1}{b}$ is also active.

From Eq. (311), we obtain

$$\left.\begin{array}{rcl} \dfrac{dv}{dt} & = & i - v + a \mid v \mid +1, \\ \left(-\dfrac{1}{b}\right)\dfrac{di}{dt} & = & -v + \dfrac{i}{b}. \end{array}\right\} \tag{335}$$

It can be written as

Dynamics of the nonlinear resistor circuit

$$\left.\begin{array}{rcl} \dfrac{dv}{dt} & = & i - v + a \mid v \mid +1, \\ \dfrac{di}{dt} & = & bv - i. \end{array}\right\} \tag{336}$$

From Eq.(315), the discretized equation for Eq. (336) is given by

Lozi Map

$$\left.\begin{array}{rcl} v_{n+1} & = & 1 - a \mid v_n \mid +i_n, \\ i_{n+1} & = & bv_n, \end{array}\right\} \tag{337}$$

where $\Delta t = 1$. Thus we obtain the Lozi map [27], which is also obtained from the generalized extended memristor circuit (see Sec. 4.1.3). We have shown the chaotic behavior of the Lozi map(337) in Fig. 21 of Sec. 4.1.3.

6.1.5 Hénon map

In this section, we derive the Hénon map from the different elements. Assume next that the parameters in Eq. (311) are given by

$$C = -\frac{1}{b},\ L = 1,\ r = 1,\ E = 0, \tag{338}$$

and $v - i$ characteristic of the nonlinear resistor is defined by

$$f(v_R) = -\frac{v_R}{b} + \frac{a{v_R}^2}{b^2} - 1, \tag{339}$$

where $a = 1.4$ and $b = 0.3$. The nonlinear resistor defined by Eq. (339) is active, since the instantaneous power $P_R(t)$ consumed by the nonlinear resistor

$$P_R(t) \triangleq v_R(t)\, i_R(t) = v_R \left(-\frac{v_R(t)}{b} + \frac{a{v_R(t)}^2}{b^2} - 1 \right), \tag{340}$$

becomes negative when $0 < v_R(t) < \dfrac{b + b\sqrt{1+4a}}{2a}$. Furthermore, the linear capacitor has a negative capacitance, that is, $C = -\dfrac{1}{b}$. In this case, the energy $W(0,t)$ stored in the capacitor

$$W(0,t) = \int_0^t v_C(\tau)\, i_C(\tau) d\tau = \int_0^t v_C(\tau) \left\{ C \frac{dv_C(\tau)}{d\tau} \right\} d\tau = \int_0^t \frac{d}{d\tau} \left\{ C \frac{{v_C(\tau)}^2}{2} \right\} d\tau = C \frac{{v_C(\tau)}^2}{2} \Big|_0^t = C \frac{{v_C(t)}^2}{2}, \tag{341}$$

becomes negative, where $v_C(\tau)$ and $i_C(\tau)$ are the voltage and the current of the capacitor, respectively, and we assumed that $v_C(0) = 0$ for simplicity. Thus, it is an active element.

From Eq. (311), we obtain

Dynamics of the nonlinear resistor circuit

$$\left.\begin{aligned} -\frac{dv}{dt} &= i + \frac{v}{b} - \frac{av^2}{b^2} + 1, \\ \frac{di}{dt} &= -v - i. \end{aligned}\right\} \tag{342}$$

If we replace the variable v with $-bx$, we get

$$\left.\begin{aligned} \frac{dx}{dt} &= i - x - ax^2 + 1, \\ \frac{di}{dt} &= bx - i. \end{aligned}\right\} \tag{343}$$

The discretized equation for Eq. (343) is given by

Hénon map

$$\left.\begin{aligned} x_{n+1} &= i_n - a{x_n}^2 + 1, \\ i_{n+1} &= bx_n. \end{aligned}\right\} \tag{344}$$

where $\Delta t = 1$. Thus we obtain the Hénon map [19], which is also obtained from the generalized extended memristor circuit (see Sec. 4.1.2). We have shown the chaotic behavior of the Hénon map (344) in Fig. 20 of Sec. 4.1.2.

6.1.6 Yamaguti-Ushiki map

In this section, we derive the Yamaguti-Ushiki map. Assume next that the parameters in Eq. (311) are given by

$$C = -1,\ L = 1,\ r = 1,\ E = 0, \tag{345}$$

and $v - i$ characteristic of the nonlinear resistor is defined by

$$f(v_R) = (2h-1)\,v_R + 2h\,{v_R}^2, \qquad (346)$$

where $h > 0$ is a constant. The nonlinear resistor defined by Eq. (346) is active, since the instantaneous power $P_R(t)$ consumed by the nonlinear resistor

$$P_R(t) \triangleq v_R(t)\,i_R(t) = v_R\left\{(2h-1)\,v_R(t) + 2h\,v_R(t)^2\right\}, \qquad (347)$$

becomes negative when $v_R(t) \ll 0$, that is, when $v_R(t)$ is sufficiently small, and $0 < h < 0.5$. Furthermore, the linear capacitor has the negative capacitance, that is, $C = -1$.

From Eq. (311), we obtain

Dynamics of the nonlinear resistor circuit

$$\left.\begin{aligned} -\frac{dv}{dt} &= i - (2h-1)v - 2htv^2, \\ \frac{di}{dt} &= -v - i. \end{aligned}\right\} \qquad (348)$$

If we replace the variable v with $-x$, then we get from Eq. (348)

$$\left.\begin{aligned} \frac{dx}{dt} &= i + (2h-1)x - 2htx^2, \\ \frac{di}{dt} &= x - i. \end{aligned}\right\} \qquad (349)$$

The discretized equation for Eq. (349) is given by

$$\left.\begin{aligned} x_{n+1} &= i_n + 2h\,x_n - 2h{x_n}^2, \\ i_{n+1} &= x_n. \end{aligned}\right\} \qquad (350)$$

It can be written as

Yamaguti-Ushiki map

$$\left.\begin{aligned} x_{n+1} &= 2h\,x_n(1-x_n) + i_n, \\ i_{n+1} &= x_n. \end{aligned}\right\} \qquad (351)$$

Thus, we obtain the Yamaguti-Ushiki map, which is obtained by the discretization of the logistic differential equation using the central difference method [1]. Let us briefly explain the above. The logistic differential equation is given by

$$\frac{dy}{dt} = y(1-y). \qquad (352)$$

Using the central difference method for $\dfrac{dy}{dt}$, we obtain

$$\frac{y_{n+1} - y_{n-1}}{2\Delta t} = y_n(1-y_n), \qquad (353)$$

where $y_n = y(t + n\Delta t)$ and $y_1 = y_0 + \Delta t y_0(1-y_0)$ and Δt is the time step size. If we set $z_{n+1} = y_n$, Eq. (353) can be transformed into the form

$$\left.\begin{aligned} y_{n+1} &= 2\Delta t\,y_n(1-y_n) + z_n, \\ z_{n+1} &= y_n. \end{aligned}\right\} \qquad (354)$$

Thus, Eq. (354) is equivalent to Eq. (351), if $h = \Delta t$. The chaotic behavior of Yamaguti-Ushiki map (351) is shown in Fig. 39. Note that if the initial condition is given by $x_0 = 0.525$ and $i_0 = 0.0$, then the overflow occurred in computation when n exceeds 4080.

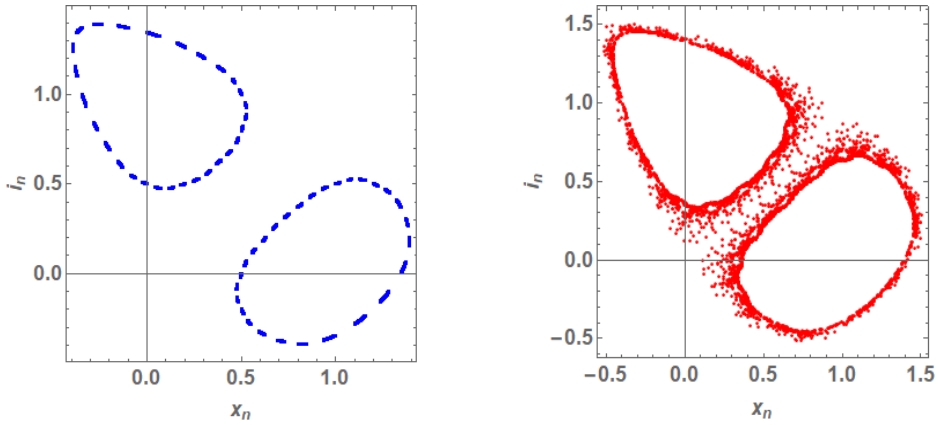

(a) (b)

Figure 39: Behavior of the Yamaguti-Ushiki map (351) for different initial conditions. (a) Parameter: $h = 0.402$. Initial conditions: $x_0 = 0.5$, $i_0 = 0.0$. (b) Parameter: $h = 0.402$. Initial conditions: $x_0 = 0.5$, $i_0 = 0.525$.

6.1.7 Helleman map

Assume next that the parameters in Eq. (311) are given by

$$C = \frac{1}{b},\ L = 1,\ r = 1,\ E = 0, \tag{355}$$

and $v - i$ characteristic of the nonlinear resistor is defined by

$$f(v_R) = -\frac{(2a-1)v_R}{b} - \frac{2a{v_R}^2}{b^2}, \tag{356}$$

where $a = 1.64$ and $b = -0.21$. The nonlinear resistor defined by Eq. (356) is active, since the instantaneous power $P_R(t)$ consumed by the nonlinear resistor

$$P_R(t) \triangleq v_R(t)\, i_R(t) = v_R(t) \left(-\frac{(2a-1)v_R(t)}{b} - \frac{2a{v_R(t)}^2}{b^2} \right), \tag{357}$$

becomes negative when $v_R(t)$ is sufficiently large. Furthermore, the linear capacitor C has a negative capacitance, i.e.,

$$C = \frac{1}{b} = -\frac{1}{0.21}. \tag{358}$$

From Eq. (311), we obtain

Dynamics of the nonlinear resistor circuit

$$\left.\begin{aligned} \left(\frac{1}{b}\right)\frac{dv}{dt} &= i + \frac{(2a-1)v}{b} + \frac{2av^2}{b^2}, \\ \frac{di}{dt} &= -v - i. \end{aligned}\right\} \tag{359}$$

If we replace the variable v with bx, we get

$$\left.\begin{aligned} \frac{dx}{dt} &= i + (2a-1)x + 2ax^2, \\ \frac{di}{dt} &= -bx - i. \end{aligned}\right\} \tag{360}$$

Furthermore, if we replace the variable i with $-j$, we get

$$\left.\begin{aligned} \frac{dx}{dt} &= -j + (2a-1)x + 2ax^2, \\ \frac{dj}{dt} &= bx - j. \end{aligned}\right\} \tag{361}$$

The discretized equation for Eq. (361) is given by

$$\left.\begin{aligned} x_{n+1} &= \left\{-j_n + (2a-1)x_n + 2a{x_n}^2\right\}\Delta t + x_n, \\ j_{n+1} &= (bx_n - j_n)\Delta t + j_n, \end{aligned}\right\} \tag{362}$$

where Δt is the time step size. If $\Delta t = 1$, then Eq. (362) can be recast into the Helleman map [34]:

Helleman Map

$$\left.\begin{aligned} x_{n+1} &= -j_n + 2ax_n + 2a{x_n}^2, \\ j_{n+1} &= bx_n. \end{aligned}\right\} \tag{363}$$

The chaotic behavior of the Helleman map (363) is shown in Fig. 40. Its attractor is very similar to that of the Hénon map (188). Note that the chaotic attractors of Eqs. (362) and (363) are quite different, even though the parameter value of a is different.

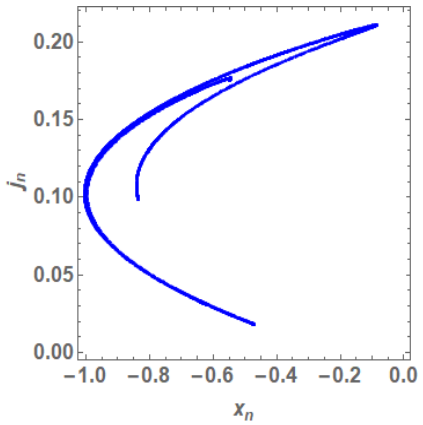

(a)

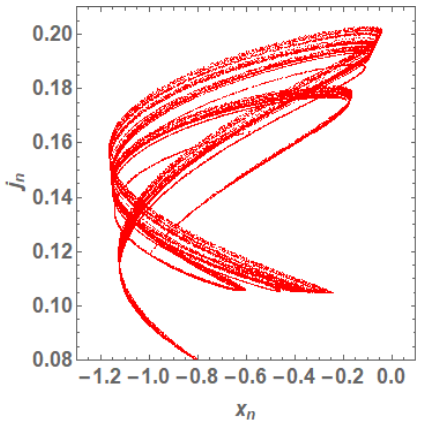

(b)

Figure 40: (a) Chaotic behavior of the Helleman map (363). Parameters: $a = 1.64$, $b = -0.21$. Initial conditions: $x_0 = -0.5$, $j_0 = 0.1$. (b) Chaotic behavior of the discretized equation (362). Parameters: $a = 3.2$, $b = -0.21$. Initial conditions: $x_0 = -0.5$, $j_0 = 0.1$, $\Delta t = 0.5$.

6.1.8 Kawakami Maps

Many interesting examples of two-dimensional chaotic maps are given by Kawakami [33]. In this section we derive some of their examples using Eq. (311). In these examples, the $v-i$ characteristics of the nonlinear resistors are quite similar, but the associated chaotic maps are quite different.

Example 1.

Assume next that the parameters in Eq. (311) are given by

$$C = 1,\ L = 1,\ r = 1,\ E = 0, \tag{364}$$

and $v-i$ characteristic of the nonlinear resistor is defined by

$$f(v_R) = (1-a)v_R - \frac{5}{1+{v_R}^2}, \tag{365}$$

where a is a constant. The nonlinear resistor defined by Eq. (365) is active, since the instantaneous power $P_R(t)$ consumed by the nonlinear resistor satisfies

$$P_R(t) \triangleq v_R(t)\, i_R(t) = v_R \left\{ (1-a)v_R(t) - \frac{5}{1+{v_R(t)}^2} \right\} < 0, \tag{366}$$

for some $v_R(t)$, which depends on the parameter a. Suppose $a = -1.03$. Then $P_R(t) < 0$ when $v_R(t) = 0.5$.

From Eq. (311), we obtain

Dynamics of the nonlinear resistor circuit

$$\left.\begin{aligned} \frac{dv}{dt} &= i - (1-a)v + \frac{5}{1+v^2}, \\ \frac{di}{dt} &= -v - i. \end{aligned}\right\} \tag{367}$$

From Eq.(315), the discretized equation for Eq. (367) is given by

Kawakami Map A

$$\left.\begin{aligned} v_{n+1} &= i_n + av_n + \frac{5}{1+{v_n}^2}, \\ i_{n+1} &= -v_n, \end{aligned}\right\} \tag{368}$$

where $\Delta t = 1$. Thus, we get the chaotic map of Kawakami [33]. The chaotic behavior of the Kawakami Map A (368) is shown in Fig. 41.

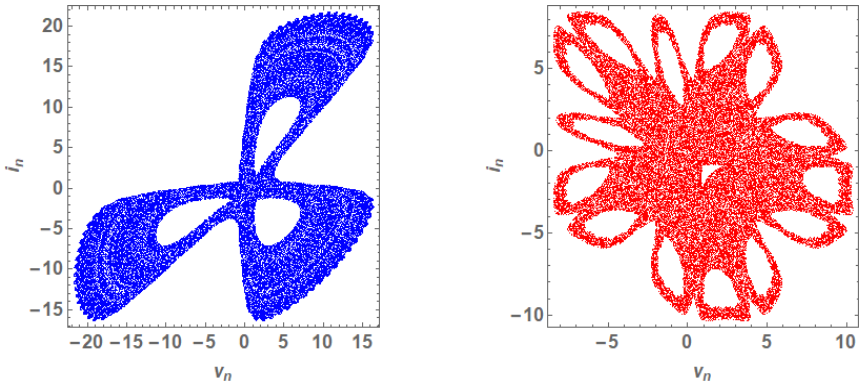

(a) (b)

Figure 41: Chaotic behavior of the Kawakami Map A (368) for two different parameters. (a) Parameter: $a = -1.03$. Initial conditions: $v_0 = 4.0$, $i_0 = 0$. (b) Parameter: $a = 0.46$. Initial conditions: $v_0 = 4.0$, $i_0 = 0$.

Example 2.

Assume next that the parameters in Eq. (311) are given by

$$C = 1,\ L = 1,\ r = 1,\ E = 0, \tag{369}$$

and $v - i$ characteristic of the nonlinear resistor is defined by

$$f(v_R) = (1-a)v_R - \frac{5v_R}{1+{v_R}^2}, \tag{370}$$

where a is a constant.

If $a < 1$, then the nonlinear resistor defined by Eq. (370) is eventually passive, since for a large enough $\mid v_R \mid$, the instantaneous power $P_R(t)$ satisfies

$$P_R(t) \triangleq v_R(t)\, i_R(t) = v_R \left\{ (1-a)v_R - \frac{5v_R(t)}{1+v_R(t)^2} \right\} = (1-a)v_R(t)^2 - \frac{5v_R(t)^2}{1+v_R(t)^2} > 0, \tag{371}$$

and $P_R(t) < 0$ for $0 <\mid v_R \mid \ll 1$ and for some parameter a (for example, $a > -1.5$).

If $a > 1$, then the nonlinear resistor defined by Eq. (370) is active, since the instantaneous power $P_R(t)$ consumed by the nonlinear resistor satisfies

$$P_R(t) \triangleq v_R(t)\, i_R(t) = (1-a)v_R(t)^2 - \frac{5v_R(t)^2}{1+v_R(t)^2} \leq 0. \tag{372}$$

From Eq. (311), we obtain

Dynamics of the nonlinear resistor circuit

$$\left.\begin{aligned} \frac{dv}{dt} &= i - (1-a)v + \frac{5v}{1+v^2}, \\ \frac{di}{dt} &= -v - i. \end{aligned}\right\} \tag{373}$$

From Eq.(315), the discretized equation for Eq. (373) is given by

Kawakami Map B

$$\left.\begin{aligned} v_{n+1} &= i_n + a v_n + \frac{5 v_n}{1 + {v_n}^2}, \\ i_{n+1} &= -v_n. \end{aligned}\right\} \tag{374}$$

where $\Delta t = 1$. Thus, we get the chaotic map of Kawakami [33]. The chaotic behavior of the Kawakami Map B (374) is shown in Fig. 42.

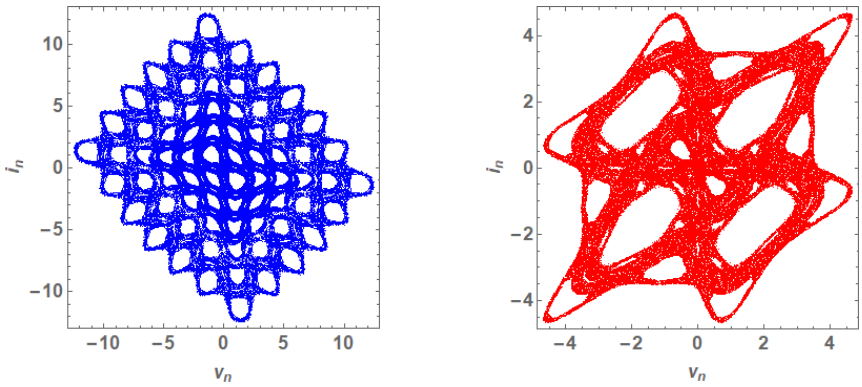

(a) (b)

Figure 42: Chaotic behavior of the Kawakami Map B (374) for two different parameters. (a) Parameter: $a = 0.2$. Initial conditions: $v_0 = 0.1$, $i_0 = 0$. (b) Parameter: $a = -1.0$. Initial conditions: $v_0 = 0.1$, $i_0 = 0$.

Example 3.

Assume next that the parameters in Eq. (311) are given by

$$C = 1,\ L = 1,\ r = 1,\ E = 0, \tag{375}$$

and $v - i$ characteristic of the nonlinear resistor is defined by

$$f(v_R) = (1 - a) v_R + \frac{5}{1 + {v_R}^2} - 6, \tag{376}$$

where a is a constant. The nonlinear resistor defined by Eq. (376) is active, since the instantaneous power $P_R(t)$ consumed by the nonlinear resistor satisfies

$$P_R(t) \triangleq v_R(t)\, i_R(t) = v_R \left\{ (1 - a) v_R(t) + \frac{5}{1 + v_R(t)^2} - 6 \right\} < 0, \tag{377}$$

for some $v_R(t)$, which depends on the parameter a. Suppose $a = -1.32$. Then $P_R(t) < 0$ when $v_R(t) = 1$.

From Eq. (311), we obtain

Dynamics of the nonlinear resistor circuit

$$\left.\begin{aligned} \frac{dv}{dt} &= i - (1 - a) v - \frac{5}{1 + v^2} + 6, \\ \frac{di}{dt} &= -v - i. \end{aligned}\right\} \tag{378}$$

From Eq.(315), the discretized equation for Eq. (378) is given by

Kawakami Map C

$$\left.\begin{aligned} v_{n+1} &= i_n + a v_n - \frac{5}{1+{v_n}^2} + 6, \\ i_{n+1} &= -v_n. \end{aligned}\right\} \tag{379}$$

where $\Delta t = 1$. Thus, we get the chaotic map of Kawakami [33]. The chaotic behavior of the Kawakami Map C (379) is shown in Fig. 43.

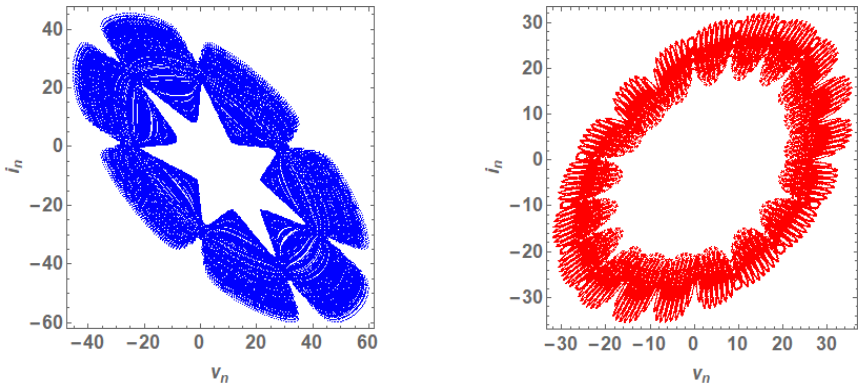

(a) (b)

Figure 43: Chaotic behavior of the Kawakami Map C (379) for two different parameters. (a) Parameter: $a = 1.25$. Initial conditions: $v_0 = 30.0$, $i_0 = 0$. (b) Parameter: $a = -0.8$. Initial conditions: $v_0 = 26.0$, $i_0 = 0$.

Example 4.

Assume next that the parameters in Eq. (311) are given by

$$C = 1,\ L = 1,\ r = 1,\ E = 0, \tag{380}$$

and $v - i$ characteristic of the nonlinear resistor is defined by

$$f(v_R) = (1-a)v_R - \frac{4\tan^{-1}(v_R)}{1+{v_R}^2}, \tag{381}$$

where $a = 0.55$ or 0.95. The nonlinear resistor defined by Eq. (365) is eventually passive, since the instantaneous power $P_R(t) \leq 0$ when $v_R(t) \approx 0$, however, when $\mid v_R(t) \mid$ is sufficiently large, the instantaneous power $P_R(t) > 0$. Here, $P_R(t)$ is defined by

$$P_R(t) \triangleq v_R(t)\, i_R(t) = v_R \left\{ (1-a)v_R(t) - \frac{4\tan^{-1}(v_R(t))}{1+{v_R(t)}^2} \right\}. \tag{382}$$

From Eq. (311), we obtain

Dynamics of the nonlinear resistor circuit

$$\left.\begin{aligned} \frac{dv}{dt} &= i-(1-a)v+\frac{4\tan^{-1}(v)}{1+v^2}, \\ \frac{di}{dt} &= -v-i. \end{aligned}\right\} \tag{383}$$

From Eq.(315), the discretized equation for Eq. (367) is given by

Kawakami Map D

$$\left.\begin{aligned} v_{n+1} &= i_n+av_n+\frac{4\tan^{-1}(v_n)}{1+{v_n}^2}, \\ i_{n+1} &= -v_n, \end{aligned}\right\} \tag{384}$$

where $\Delta t = 1$. Thus, we get the chaotic map of Kawakami [33]. The chaotic behavior of the Kawakami Map D (384) is shown in Fig. 44.

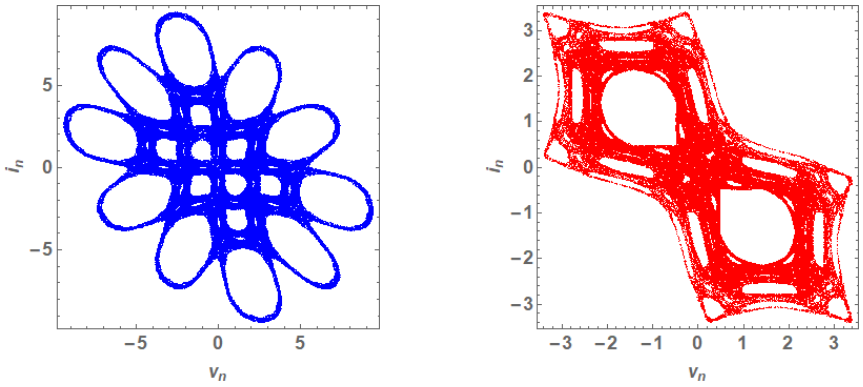

(a) (b)

Figure 44: Chaotic behavior of the Kawakami Map D (384) for two different parameters. (a) Parameter: $a = 0.55$. Initial conditions: $v_0 = 0.1$, $i_0 = 0$. (b) Parameter: $a = 0.95$. Initial conditions: $v_0 = 0.1$, $i_0 = 0$.

Example 5.

Assume next that the parameters in Eq. (311) are given by

$$C = 1,\ L = \frac{1}{0.995},\ r = \frac{1}{0.995},\ E = 0, \tag{385}$$

and $v - i$ characteristic of the nonlinear resistor is defined by

$$f(v_R) = av_R - \frac{5}{1+{v_R}^2} + 5. \tag{386}$$

The nonlinear resistor defined by Eq. (386) is active, since the instantaneous power $P_R(t)$ consumed by the nonlinear resistor satisfies

$$P_R(t) \triangleq v_R(t)\, i_R(t) = v_R \left\{ av_R(t) - \frac{5}{1+{v_R(t)}^2} + 5 \right\} < 0, \tag{387}$$

for some $v_R(t)$, which depends on the parameter a. Suppose $a = 1.97$ or $a = 1.7$. Then $P_R(t) < 0$ when $v_R(t) = -2$.

From Eq. (311), we obtain

Dynamics of the nonlinear resistor circuit

$$\left.\begin{aligned} \frac{dv}{dt} &= i - av + \frac{5}{1+v^2} - 5, \\ \frac{di}{dt} &= -0.995v + i. \end{aligned}\right\} \tag{388}$$

From Eq.(315), the discretized equation for Eq. (388) is given by

Kawakami Map E

$$\left.\begin{aligned} v_{n+1} &= i_n + (1-a)v_n + \frac{5}{1+{v_n}^2} - 5, \\ i_{n+1} &= -0.995v_n, \end{aligned}\right\} \tag{389}$$

where $\Delta t = 1$. Thus, we get the chaotic map of Kawakami [33]. The chaotic behavior of the Kawakami Map E (389) is shown in Fig. 45.

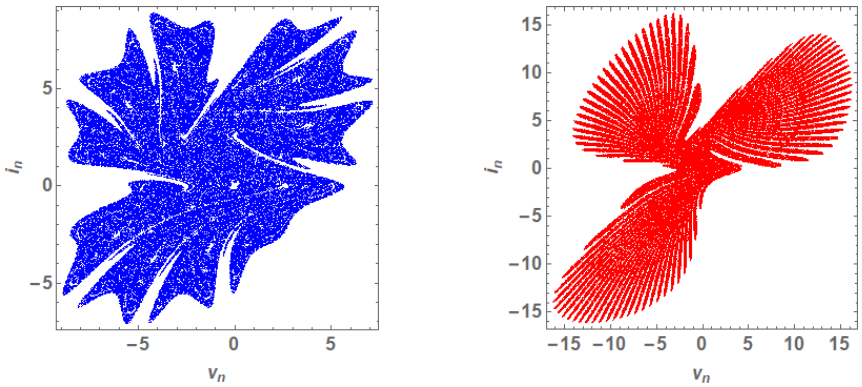

(a) (b)

Figure 45: Chaotic behavior of the Kawakami Map E (389) for two different parameters. (a) Parameter: $a = 1.7$. Initial conditions: $v_0 = 4$, $i_0 = 0$. (b) Parameter: $a = 1.97$. Initial conditions: $v_0 = 4$, $i_0 = 0$.

Example 6.

Assume next that the parameters in Eq. (311) are given by

$$C = \frac{1}{b},\ L = 1,\ r = 1,\ E = 0, \tag{390}$$

and $v - i$ characteristic of the nonlinear resistor is defined by

$$f(v_R) = \left(\frac{1}{b}\right)\left\{(1-a)v_R - \frac{5}{1+{v_R}^2} - 1\right\}, \tag{391}$$

where $a < 0$ and $b > 0$ are constants. The nonlinear resistor defined by Eq. (376) is active, since the instantaneous power $P_R(t)$ consumed by the nonlinear resistor satisfies

$$P_R(t) \triangleq v_R(t)\, i_R(t) = \left(\frac{v_R(t)}{b}\right) \left\{(1-a)v_R(t) - \frac{5}{1+{v_R(t)}^2} - 1\right\} < 0, \tag{392}$$

for some $v_R(t)$, which depends on the parameter a. Suppose $a = -1.11$. Then $P_R(t) < 0$ when $v_R(t) = 0.5$.

From Eq. (311), we obtain

Dynamics of the nonlinear resistor circuit

$$\left.\begin{aligned} \left(\frac{1}{b}\right)\frac{dv}{dt} &= i - \left(\frac{1}{b}\right)\left\{(1-a)v - \frac{5}{1+v^2} - 1\right\}, \\ \frac{di}{dt} &= -v - i. \end{aligned}\right\} \tag{393}$$

It can be recast into the form

Dynamics of the nonlinear resistor circuit

$$\left.\begin{aligned} \frac{dv}{dt} &= bi - (1-a)v + \frac{5}{1+v^2} + 1, \\ \frac{di}{dt} &= -v - i. \end{aligned}\right\} \tag{394}$$

From Eq.(315), the discretized equation for Eq. (394) is given by

Kawakami Map F

$$\left.\begin{aligned} v_{n+1} &= bi_n + av_n + \frac{5}{1+{v_n}^2} + 1, \\ i_{n+1} &= -v_n, \end{aligned}\right\} \tag{395}$$

where $\Delta t = 1$. Thus, we get the chaotic map of Kawakami [33]. The chaotic behavior of the Kawakami Map F (395) is shown in Fig. 46.

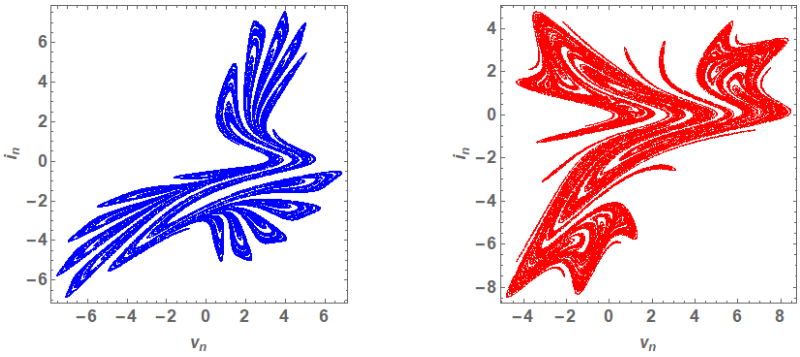

(a) (b)

Figure 46: Chaotic behavior of the Kawakami Map F (395) for two different parameters. (a) Parameters: $a = -1.11$, $b = 0.95$. Initial conditions: $v_0 = 0.1$, $i_0 = 0$. (b) Parameters: $a = -0.7$, $b = 0.95$. Initial conditions: $v_0 = 0.1$, $i_0 = 0$.

6.2 Chua circuit

Consider the Chua circuit in Fig. 47 which exhibits chaotic behavior (see [35] for moredetails). It contains the five circuit elements: two linear capacitors C_1 and C_2, one linear inductor L, one linear resistor R, and one nonlinear resistor. The dynamics of this circuit is given by

$$\left.\begin{aligned} C_1 \frac{dv_1}{dt} &= \frac{v_2 - v_1}{R} - f(v_1), \\ C_2 \frac{dv_2}{dt} &= y - \frac{v_2 - v_1}{R}, \\ L \frac{di}{dt} &= -v_2, \end{aligned}\right\} \tag{396}$$

where the symbols v_1, v_2, and i denote the voltage across the capacitor C_1, the voltage across the capacitor C_2, and the current through the inductor L, respectively. The $v - i$ characteristic of the nonlinear resistor is given by

$$i_R = f(v_R) = \frac{1}{16} {v_R}^3 - \frac{7}{6} v_R, \tag{397}$$

where i_R and v_R are the current through and voltage across the nonlinear resistor.

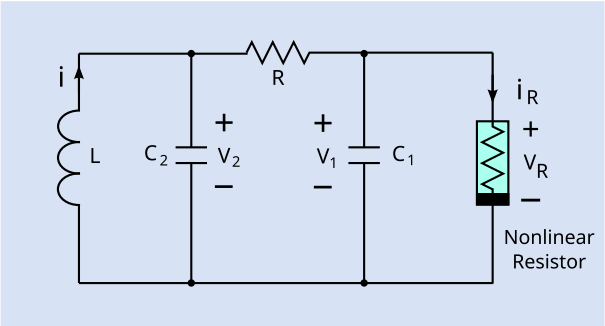

Figure 47: Chua circuit, which contains five circuit elements: two linear capacitors C_1 and C_2, one linear inductor L, one linear resistor R, and one nonlinear resistor, where v_1, v_2, and i denote the voltage across the capacitor C_1, the voltage across the capacitor C_2, and the current through the inductor L, respectively. The $v - i$ characteristic of the nonlinear resistor is given by $i_R = f(v_R) = \frac{1}{16} {v_R}^3 - \frac{7}{6} v_R$, where i_R and v_R are the current through and voltage across the nonlinear resistor.

The nonlinear resistor defined by Eq. (397) is active, since the instantaneous power $P_R(t)$ consumed by the nonlinear resistor satisfies

$$P_R(t) \triangleq v_R(t)\, i_R(t) = v_R(t) \left(\frac{1}{16} v_R(t)^3 - \frac{7}{6} v_R(t) \right) < 0, \tag{398}$$

when $0 <\mid v_R(t) \mid< \sqrt{\frac{112}{6}} \approx 4.32$.

If we set

$$\left.\begin{aligned} C_1 = \frac{1}{\alpha}, \quad C_2 = 1, \quad L = \frac{1}{\beta}, \quad R = 1, \\ x = v_1, \quad y = v_2, \quad i = z, \end{aligned}\right\} \tag{399}$$

then the dynamics of the Chua circuit is defined by [35, 36]

$$\left.\begin{aligned} \frac{dx}{dt} &= \alpha\big(y - x - f(x)\big), \\ \frac{dy}{dt} &= x - y + z, \\ \frac{dz}{dt} &= -\beta y, \end{aligned}\right\} \tag{400}$$

where $f(x)$ is given by

$$f(x) = \frac{1}{16}x^3 - \frac{7}{6}x. \tag{401}$$

Equation (400) exhibits chaotic behavior and many well-known bifurcation phenomena (see [35, 36] for more details). We discretize Eq. (400) using the Euler method. Then we obtain the following equation:

Discretized Chua circuit equation

$$\left.\begin{aligned} x_{n+1} &= \alpha\big(y_n - x_n - f(x_n)\big)\Delta t + x_n, \\ y_{n+1} &= \big(x_n - y_n + z_n\big)\Delta t + y_n, \\ z_{n+1} &= -\beta y_n \Delta t + z_n, \end{aligned}\right\} \tag{402}$$

where Δt is the time step size, $x_n \triangleq x(t + n\Delta t)$, $y_n \triangleq y(t + n\Delta t)$, and $z_n \triangleq z(t + n\Delta t)$ $(n = 0, 1, 2, \cdots)$.

We show the chaotic behavior of Eq. (402) in Fig. 48, which clearly shows the topological structure (see the paper-sheet model of Ref. [24]) of the chaotic behavior. We have observed the similar topological structure in Figs. 11, 12, 13, 14, and 17. Note that in the computer simulations, Eq. (400) has no chaotic attractor when we use the parameter values shown in Fig. 48.

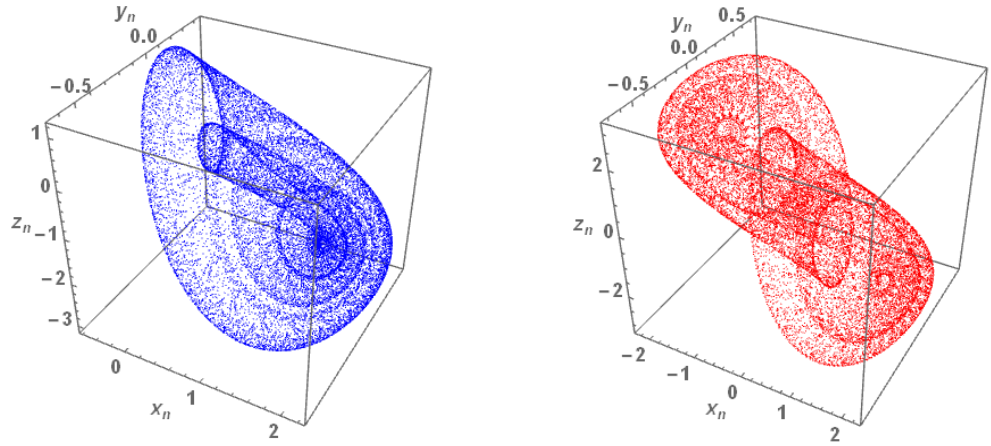

(a) (b)

Figure 48: Chaotic behavior of the discretized Chua circuit equation (402) for two different parameters. (a) Parameters: $\alpha = 3$, $\beta = 5$, $\Delta t = 0.226$. Initial conditions: $x_0 = 0.1$, $y_0 = 0.1$, $z_0 = 0.1$. (b) Parameters: $\alpha = 3$, $\beta = 5$, $\Delta t = 0.25$. Initial conditions: $x_0 = 0.1$, $y_0 = 0.1$, $z_0 = 0.1$.

7 Controlled Source Circuits

Consider the controlled source circuit in Fig. 49, which consists of a linear inductor L, a linear capacitor C, a linear resistor r, a controlled current source, and an independent voltage source $e(t)$. The controlled current source is define by

$$i_c = f_c(v,\, i), \tag{403}$$

where v and i are the voltage across the capacitor and the current through the inductor, respectively and i_c is the output current of the controlled current source. The controlled current source and the independent voltage source are usually active elements.

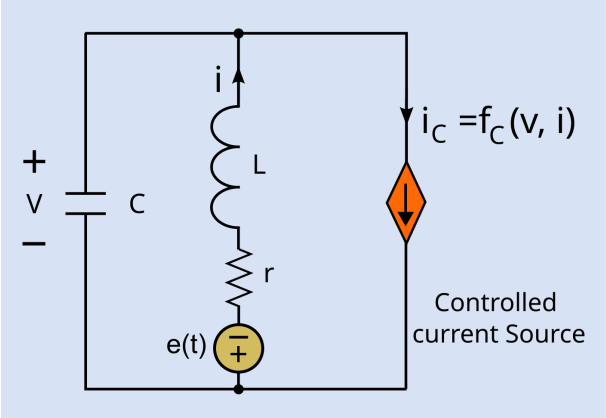

Figure 49: Controlled Source Circuit, which consists of a linear inductor L, a linear capacitor C, a linear resistor r, a controlled current source defined by $i_c = f_c(v,\, i)$, and an independent voltage source $e(t)$, where v is the voltage across the capacitor with the capacitance C and i is the current through the inductor with the inductance L, and i_c is the output current of the controlled current source.

The dynamics of this circuit is given by

Dynamics of the controlled circuit

$$\left.\begin{aligned} C\frac{dv}{dt} &= i - f_c(v,i), \\ L\frac{di}{dt} &= -v - ri - e(t), \end{aligned}\right\} \tag{404}$$

where v and i are the voltage of the capacitor and the current of the inductor. We discretize it using the Euler method defined by

Euler method

$$\left.\begin{aligned} \frac{dv}{dt} &\approx \frac{v(t+\Delta t) - v(t)}{\Delta t}, \\ \frac{di}{dt} &\approx \frac{i(t+\Delta t) - i(t)}{\Delta t}, \end{aligned}\right\} \tag{405}$$

where Δt is the time step size. Then we can approximate Eq. (404) by

$$\left.\begin{aligned} C\frac{v(t+\Delta t)-v(t)}{\Delta t} &= i(t)-f_c\big(v(t),\, i(t)\big), \\ L\frac{x(t+\Delta t)-x(t)}{\Delta t} &= -v(t)-ri(t)-e(t). \end{aligned}\right\} \tag{406}$$

If we set $v_n \triangleq v(t+n\Delta t)$, and $i_n \triangleq i(t+n\Delta t)$, then we get from Eq. (406)

$$\left.\begin{aligned} v_{n+1}-v_n &= \frac{\Delta t}{C}\left\{i_n - f_c(v_n,\, i_n)\right\}, \\ i_{n+1}-i_n &= \frac{\Delta t}{L}\left\{-v_n - ri_n - e(t+n\Delta t)\right\}, \end{aligned}\right\} \tag{407}$$

where $n = 0, 1, 2, \cdots$. We can rewrite Eq. (407) in the following form

Two-dimensional map

$$\left.\begin{aligned} v_{n+1} &= \frac{\Delta t}{C}\left\{i_n - f_c(v_n,\, i_n)\right\} + v_n, \\ i_{n+1} &= \frac{\Delta t}{L}\left\{-v_n - r\, i_n - e(n\Delta t)\right\} + i_n. \end{aligned}\right\} \tag{408}$$

Example 1.

Assume next that the parameters in Eq. (311) are given by

$$C = \frac{1}{b},\ L = 1,\ r = 1,\ e(t) = 0, \tag{409}$$

and the controlled current source $f_c(v, i)$ is defined by

$$f_c(v,\, i) = (1-a)\left(\frac{v}{b}\right) + \frac{5}{1+\left(\frac{v}{b}\right)^2} - 6 - 0.2\, e^{-i^2}, \tag{410}$$

where a is a constant.

Substituting Eqs. (409) and (410) into Eq. (404), we obtain

Dynamics of the controlled source circuit

$$\left.\begin{aligned} \left(\frac{1}{b}\right)\frac{dv}{dt} &= i - (1-a)\left(\frac{v}{b}\right) - \frac{5}{1+\left(\frac{v}{b}\right)^2} + 6 + 0.2\, e^{-i^2}, \\ \frac{di}{dt} &= -v - i. \end{aligned}\right\} \tag{411}$$

If we set $v = bx$, we obtain

$$\left.\begin{aligned} \frac{dx}{dt} &= i - (1-a)x - \frac{5}{1+x^2} + 6 + 0.2\, e^{-i^2}, \\ \frac{di}{dt} &= -bx - i. \end{aligned}\right\} \tag{412}$$

Using the Euler method, the discretized equation for Eq. (412) is given by

Kawakami Map G

$$\left.\begin{aligned} x_{n+1} &= i_n + a x_n - \frac{5}{1+{x_n}^2} + 6 + 0.2\, e^{-{i_n}^2}, \\ i_{n+1} &= -b x_n, \end{aligned}\right\} \quad (413)$$

where $\Delta t = 1$. Thus, we get the chaotic map of Kawakami shown in [33]. The chaotic behavior of the Kawakami Map G (413) is shown in Fig. 50.

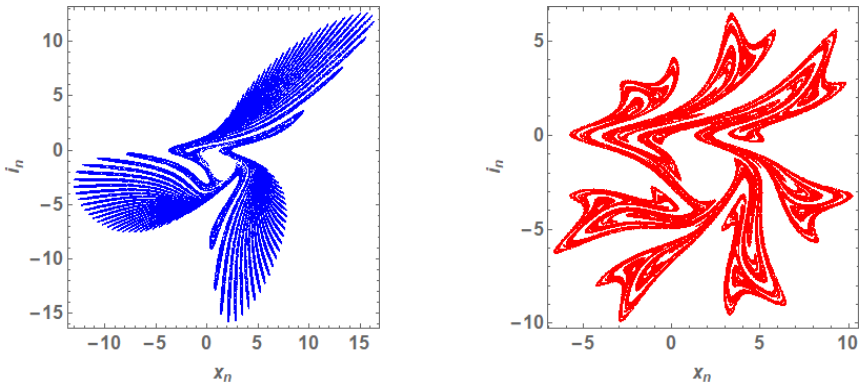

(a) (b)

Figure 50: Chaotic behavior of the Kawakami Map G (413) for two different parameters. (a) Parameters: $a = -0.96$, $b = 0.97$. Initial conditions: $x_0 = 0.1$, $i_0 = 0$. (b) Parameters: $a = -0.55$, $b = 0.97$. Initial conditions: $x_0 = 0.1$, $i_0 = 0$.

Example 2.

Assume that the parameters in Eq. (311) are given by

$$C = \frac{1}{b},\ L = 1,\ r = 1,\ e(t) = 0, \quad (414)$$

and the controlled current source $f_c(v, i)$ is defined by

$$f_c(v,\, i) = (1-a)\left(\frac{v}{b}\right) - \frac{5\left\{\left(\frac{v}{b}\right)^2 - 1\right\}}{\left(\frac{v}{b}\right)^2 + 1} - \tan^{-1}\left(\frac{v}{b} + i\right), \quad (415)$$

where a is a constant.

Substituting Eqs. (414) and (415) into Eq. (404), we obtain

Dynamics of the controlled source circuit

$$\left.\begin{aligned}\left(\frac{1}{b}\right)\frac{dv}{dt} &= i-(1-a)\left(\frac{v}{b}\right)+\frac{5\left\{\left(\frac{v}{b}\right)^2-1\right\}}{\left(\frac{v}{b}\right)^2+1}+\tan^{-1}\left(\frac{v}{b}+i\right),\\ \frac{di}{dt} &= -v-i.\end{aligned}\right\} \tag{416}$$

If we set $v = bx$, we obtain

$$\left.\begin{aligned}\frac{dx}{dt} &= i-(1-a)x+\frac{5(x^2-1)}{x^2+1}+\tan^{-1}(x+i),\\ \frac{di}{dt} &= -bx-i.\end{aligned}\right\} \tag{417}$$

Using the Euler method, the discretized equation for Eq. (417) is given by

Kawakami map H

$$\left.\begin{aligned}x_{n+1} &= i_n+ax_n+\frac{5({x_n}^2-1)}{{x_n}^2+1}+\tan^{-1}(x_n+i_n),\\ i_{n+1} &= -bx_n,\end{aligned}\right\} \tag{418}$$

where $\Delta t = 1$. Thus, we get the chaotic map of Kawakami shown in [33]. The chaotic behavior of the Kawakami Map H (418) is shown in Fig. 51.

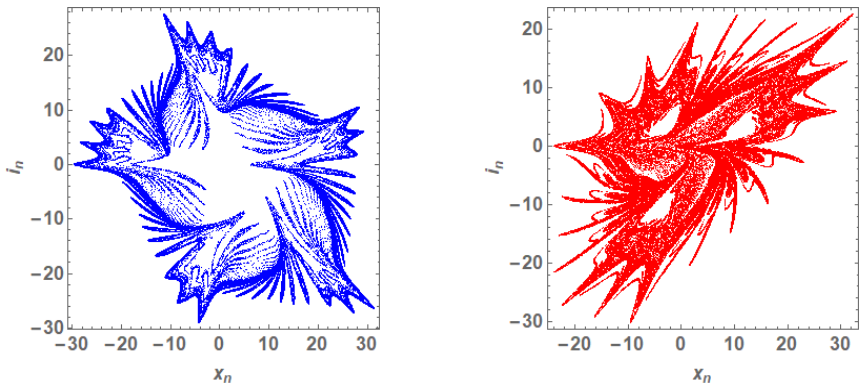

(a) (b)

Figure 51: Chaotic behavior of the Kawakami Map H (418) for two different parameters. (a) Parameters: $a = 0.5$, $b = 0.93$. Initial conditions: $x_0 = 0.1$, $i_0 = 0$. (b) Parameters: $a = -1.2$, $b = 0.94$. Initial conditions: $x_0 = 0.1$, $i_0 = 0$.

Example 3.

Assume next that the parameters in Eq. (311) are given by

$$C = \frac{1}{b},\ L = 1,\ r = 1,\ e(t) = d\cos(\pi t), \tag{419}$$

and the controlled current source $f_c(v, i)$ is defined by

$$f_c(v,\, i) = (1-a)\left(\frac{v}{b}\right) - \frac{5\left(\frac{v}{b}\right)^2}{1+\left(\frac{v}{b}\right)^2} - 1 + 0.2\, e^{-y^2}, \qquad (420)$$

where a and b are constants.

Substituting Eqs. (419) and (420) into Eq. (404), we obtain

Dynamics of the controlled source circuit

$$\left.\begin{aligned} \left(\frac{1}{b}\right)\frac{dv}{dt} &= i - (1-a)\left(\frac{v}{b}\right) + \frac{5\left(\frac{v}{b}\right)^2}{1+\left(\frac{v}{b}\right)^2} + 1 - 0.2\, e^{-y^2}, \\ \frac{di}{dt} &= -v - i - e(t). \end{aligned}\right\} \qquad (421)$$

If we set $v = bx$ and $e(t) = -c\cos(\pi t)$, we obtain

$$\left.\begin{aligned} \frac{dx}{dt} &= i - (1-a)x + \frac{5x^2}{1+x^2} + 1 - 0.2\, e^{-y^2}, \\ \frac{di}{dt} &= -bx - i + c\cos(\pi t). \end{aligned}\right\} \qquad (422)$$

Using the Euler method, the discretized equation for Eq. (422) is given by

Kawakami Map I

$$\left.\begin{aligned} x_{n+1} &= i_n + a x_n + \frac{5{x_n}^2}{1+{x_n}^2} + 1 - 0.2\, e^{-{y_n}^2}, \\ i_{n+1} &= -b x_n + c\cos(n\pi) = -b x_n + c(-1)^n, \end{aligned}\right\} \qquad (423)$$

where $\Delta t = 1$. Thus, we get the chaotic map of Kawakami shown in [33]. The chaotic behavior of the Kawakami Map I (423) is shown in Fig. 52 (Note that a different plotting method is used in [33]).

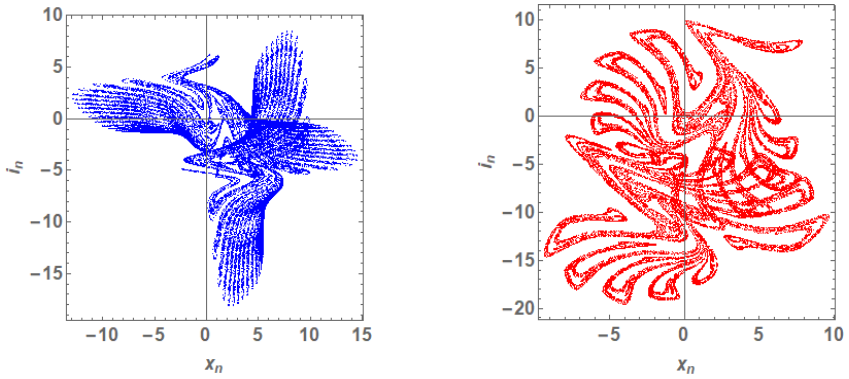

(a) (b)

Figure 52: Chaotic behavior of the Kawakami Map I (423) for two different parameters. (a) Parameters: $a = 0.01$, $b = 0.97$, $c = 4$. Initial conditions: $x_0 = 0.1$, $i_0 = 0$. (b) Parameters: $a = 0.18$, $b = 0.96$, $c = 5$. Initial conditions: $x_0 = 0.1$, $i_0 = 0$.

Example 4.

Assume that the parameters in Eq. (311) are given by

$$C = -\frac{1}{b},\ L = 1,\ r = 1,\ e(t) = 0, \tag{424}$$

and the controlled current source $f_c(v, i)$ is defined by

$$f_c(v,\, i) = -\left(\frac{v}{b}\right) + a\left|\,\frac{v}{b}\,\right| - 1, \tag{425}$$

where a and b are constants. Note that the capacitor has a negative capacitance $C = -\frac{1}{b}$.

Substituting Eqs. (424) and (425) into Eq. (404), we obtain

Dynamics of the controlled source circuit

$$\left.\begin{aligned} -\left(\frac{1}{b}\right)\frac{dv}{dt} &= i + \left(\frac{v}{b}\right) - a\left|\,\frac{v}{b}\,\right| + 1, \\ \frac{di}{dt} &= -v - i. \end{aligned}\right\} \tag{426}$$

If we set $v = -bx$, we obtain

$$\left.\begin{aligned} \frac{dx}{dt} &= i - x - a \mid x \mid +1, \\ \frac{di}{dt} &= bx - i. \end{aligned}\right\} \tag{427}$$

Using the Euler method, the discretized equation for Eq. (427) is given by

Lozi Map

$$\left.\begin{aligned} x_{n+1} &= 1 - a \mid x_n \mid + i_n, \\ i_{n+1} &= bx_n, \end{aligned}\right\} \tag{428}$$

where $\Delta t = 1$. That is, we get the Lozi Map [27], which is also obtained from the generalized extended memristor circuit (see Sec. 4.1.3) and the nonlinear resistor circuit (see Sec. 6.1.4). We have shown the chaotic behavior of the Lozi map in Fig. 21 of Sec. 4.1.3.

Example 5.

Assume next that the parameters in Eq. (311) are given by

$$C = -\frac{1}{b},\ L = 1,\ r = 1,\ e(t) = 0, \tag{429}$$

and the controlled current source $f_c(v, i)$ is defined by

$$f_c(v,\, i) = -\left(\frac{v}{b}\right) + a\left(\frac{v}{b}\right)^2 - 1, \tag{430}$$

where a and b are constants. Note that the capacitor has a negative capacitance $C = -\frac{1}{b}$.

Substituting Eqs. (429) and (430) into Eq. (404), we obtain

Dynamics of the controlled source circuit

$$\left.\begin{aligned} -\left(\frac{1}{b}\right)\frac{dv}{dt} &= i + \left(\frac{v}{b}\right) - a\left(\frac{v}{b}\right)^2 + 1, \\ \frac{di}{dt} &= -v - i. \end{aligned}\right\} \tag{431}$$

If we set $v = -bx$, we obtain

$$\left.\begin{aligned} \frac{dx}{dt} &= i - x - ax^2 + 1, \\ \frac{di}{dt} &= bx - i. \end{aligned}\right\} \tag{432}$$

Using the Euler method, the discretized equation for Eq. (432) is given by

Hénon Map

$$\left.\begin{aligned} x_{n+1} &= 1 - a{x_n}^2 + i_n, \\ i_{n+1} &= bx_n, \end{aligned}\right\} \tag{433}$$

where $\Delta t = 1$. That is, we get the Hénon Map [19], which is also obtained from the generalized extended memristor circuit (see Sec. 4.1.2) and the nonlinear resistor circuit (see Sec. 6.1.5). We have shown the chaotic behavior of the Hénon map in Fig. 20 of Sec. 4.1.2.

Example 6.

Assume next that the parameters in Eq. (311) are given by

$$C = 1,\ L = 1,\ r = 1,\ e(t) = 0, \tag{434}$$

and the controlled current source $f_c(v, i)$ is defined by

$$f_c(v,\, i) = -b(1 - 0.05i^2)\, i - F(v) + v, \tag{435}$$

where $F(v)$ is given by

$$F(v) = av + \frac{2(1-a)v^2}{1+v^2}, \tag{436}$$

and a and b are constants.

Substituting Eqs. (434) and (435) into Eq. (404), we obtain

Dynamics of the controlled source circuit

$$\left.\begin{aligned} \frac{dv}{dt} &= i + b(1 - 0.05i^2)\, i + F(v) - v, \\ \frac{di}{dt} &= -v - i. \end{aligned}\right\} \tag{437}$$

Using the Euler method, the discretized equation for Eq. (438) is given by

Simplified Gumowski-Mira map B

$$\left.\begin{aligned} v_{n+1} &= i_n + b(1 - 0.05{i_n}^2)i_n + F(v_n), \\ i_{n+1} &= -v_n, \end{aligned}\right\} \tag{438}$$

where $\Delta t = 1$. We get the simplified Gumowski-Mira map B, which is also obtained from the generalized extended memristor circuit (see Sec. 4.1.6). We have shown the chaotic behavior of the simplified Gumowski-Mira map B in Fig. 25(b) of Sec. 4.1.6.

8 Hamiltonian Circuits

Consider the circuit in Fig. 53, which consists of a frequency-dependent negative resistor (FNDR) and a nonlinear resistor. The FNDR is a two-terminal linear element defined by

$$i = G\left(\frac{d^2v}{dt^2}\right), \tag{439}$$

where G is the conductance, and i and v are the current through and the voltage across the FNDR. It is a higher-order circuit element. The $v - i$ characteristic of the nonlinear resistor is given by

$$i_R = f(v_R), \tag{440}$$

where i_R and v_R are the current through and voltage across the nonlinear resistor, respectively, and $f(v_R)$ is a scaler function of v_R.

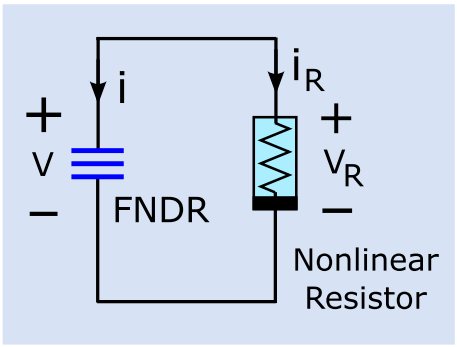

Figure 53: Hamiltonian circuit, which consists of a frequency-dependent negative resistor (FNDR) defined by $i = G\left(\frac{d^2v}{dt^2}\right)$ and a nonlinear resistor with the characteristic curve $i_R = f(v_R)$. Here, G is the conductance, i and v are the current through and the voltage across the FNDR, respectively, and i_R and v_R are the current through and the voltage across the nonlinear resistor, respectively.

We next examine whether the FNDR is active or passive. Let us drive the FNDR by the voltage source $v_s(t)$ where we set $v_s(t) = v(t) = \sin(t)$ for $t \geq t_0$. The instantaneous power of the FNDR is given by

$$P(t) \triangleq v(t)\, i(t) = v(t) \left(G \frac{d^2 v}{dt^2} \right) = \sin(t) \left(G \frac{d^2}{dt^2} \sin(t) \right) = -G \left(\sin(t) \right)^2 < 0. \tag{441}$$

Thus, the FNDR is an active element. In the case of the non-linear resistor, the $v-i$ characteristic determines whether it is active or passive.

The dynamics of this circuit is given by

Dynamics of the Hamiltonian circuit

$$\frac{d^2 v}{dt^2} = -f(v), \tag{442}$$

where v denotes the voltage across the FNDR and we assumed that $G = 1$.

If we set $p = \dfrac{dv}{dt}$, Eq. (442) can be rewritten as Hamilton's equation:

Hamilton's equation

$$\left.\begin{array}{rcl} \dfrac{dx}{dt} & = & \dfrac{\partial H(x,\, p)}{\partial p} = p, \\ \dfrac{dp}{dt} & = & -\dfrac{\partial H(x,\, p)}{\partial x} = -f(x), \end{array}\right\} \tag{443}$$

where the Hamiltonian $H(x,\, p)$ is given by

Hamiltonian

$$H(x,\, p) = \frac{p^2}{2} + \int f(x) dx. \tag{444}$$

Next we obtain the discretized equation of (442). Using a second-order central difference for the time derivatives, we obtain:

Second-order central difference

$$\frac{d^2 v}{dt^2} \approx \frac{v(t + \Delta t) - 2v(t) + v(t - \Delta t)}{(\Delta t)^2}, \tag{445}$$

where Δt is the time step size. Then Eq. (442) can be approximated by

$$\frac{v(t + \Delta t) - 2v(t) + v(t - \Delta t)}{(\Delta t)^2} = -f(v(t)). \tag{446}$$

If we set $\Delta t = 1$ and $v_n \triangleq v(t + n\Delta t)$, then we obtain from Eq. (457)

Discretized equation for the Hamiltonian circuit equation (442)

$$v_{n+1} - 2v_n + v_{n-1} + f(v_n) = 0. \tag{447}$$

If we set $y_n = -v_{n-1}$, then Eq. (447) can be written as

Two-dimensional map A

$$\left.\begin{aligned} v_{n+1} &= y_n + 2v_n - f(v_n), \\ y_{n+1} &= -v_n. \end{aligned}\right\} \tag{448}$$

Furthermore, if we define $F(v_n) \triangleq f(v_n) - 2v_n$, then Eq. (448) can be recast int the form

Two-dimensional map B

$$\left.\begin{aligned} v_{n+1} &= y_n - F(v_n), \\ y_{n+1} &= -v_n. \end{aligned}\right\} \tag{449}$$

8.1 Kawakami maps

Consider the two-dimensional map B (449). If we replace the variable y_n by i_n in Eq. (449), then the following four types of Kawakami maps are described by using the form of Eq. (449). That is, they can be obtained from the discretized Hamiltonian circuit equations.

Kawakami Map A

$$\left.\begin{aligned} v_{n+1} &= i_n + av_n + \frac{5}{1+{v_n}^2}, \\ i_{n+1} &= -v_n. \end{aligned}\right\} \tag{450}$$

Kawakami Map B

$$\left.\begin{aligned} v_{n+1} &= i_n + av_n + \frac{5v_n}{1+{v_n}^2}, \\ i_{n+1} &= -v_n. \end{aligned}\right\} \tag{451}$$

Kawakami Map C

$$\left.\begin{aligned} v_{n+1} &= i_n + av_n - \frac{5}{1+{v_n}^2} + 6, \\ i_{n+1} &= -v_n. \end{aligned}\right\} \tag{452}$$

Kawakami Map D

$$\left.\begin{aligned} v_{n+1} &= i_n + av_n + \frac{4\tan^{-1}(v_n)}{1+{v_n}^2}, \\ i_{n+1} &= -v_n. \end{aligned}\right\} \tag{453}$$

Note that these four Kawakami maps (450)-(450) are also obtained from the nonlinear resistor circuit equations (see Sec. 6.1.8 for more details).

8.2 Yamaguti-Ushiki map

Consider the Hamiltonian circuit in Fig. 53, where the $v-i$ characteristic of the nonlinear resistor is given by

$$i_R = f(v_R) = b{v_R}^3 - av_R, \tag{454}$$

where $a \geq 0$ and $b > 0$. If $a > 0$, the nonlinear resistor is eventually passive since the instantaneous power $P_R(t)$ consumed by the nonlinear resistor satisfies

$$P_R(t) \triangleq v_R(t)\, i_R(t) = v_R(t)\, \Big\{ b{v_R(t)}^3 - av_R(t) \Big\} = b\, {v_R(t)}^2\, \Big\{ {v_R(t)}^2 - \frac{a}{b} \Big\} \leq 0, \tag{455}$$

for $\mid v_R(t) \mid < \sqrt{\frac{a}{b}}$. However, if $\mid v_R(t) \mid > 0$, then $P_R(t) > 0$. In the case where $a = 0$, the nonlinear resistor is passive since the instantaneous power $P_R(t)$ satisfies

$$P_R(t) \triangleq v_R(t)\, i_R(t) = b{v_R(t)}^4 \geq 0. \tag{456}$$

The dynamics of this circuit is given by

Dynamiccs of the Hamiltonian circuit

$$\frac{d^2v}{dt^2} + bv^3 - av = 0, \tag{457}$$

where v denotes the voltage across the FNDR and we assume that $G = 1$. By setting $p = \dfrac{dv}{dt}$, Eq. (457) can be transformed into the form

Hamilton's equation

$$\left.\begin{array}{rcl} \dfrac{dx}{dt} & = & \dfrac{\partial H(x,\, p)}{\partial p} = p, \\ \dfrac{dp}{dt} & = & -\dfrac{\partial H(x,\, p)}{\partial x} = -f(x) = -bx^3 - ax, \end{array}\right\} \tag{458}$$

where the Hamiltonian $H(x,\, p)$ is given by

Hamiltonian

$$H(x,\, p) = \frac{p^2}{2} + \int f(x)dx = \frac{p^2}{2} + \frac{bx^4}{4} - \frac{ax^2}{2}, \tag{459}$$

where $f(x)$ is given by

$$f(x) = bx^3 - ax. \tag{460}$$

Note that if $a > 0$, the Hamiltonian $H(x,\, p)$ has a saddle point at $(x,\, p) = (0,\, 0)$.

Assume that $\Delta t = 1$ and define $v_n \triangleq v(t + n\Delta t)$. Then we obtain from Eqs. (447) and (457

Discretized equation for the Hamiltonian circuit equation (457)

$$v_{n+1} - 2v_n + v_{n-1} + b{v_n}^3 - av_n = 0. \tag{461}$$

By setting $y_n = -v_{n-1}$, Eq. (461) can be written as

Two-dimensional map

$$\left.\begin{aligned} v_{n+1} &= y_n + 2v_n - b{v_n}^3 + av_n, \\ y_{n+1} &= -v_n. \end{aligned}\right\} \tag{462}$$

If we set $a = 0$, $b = 1$, and $y_n = v_{n-1}$, then Eq. (461) is transformed into the two-dimensional Yamaguti-Ushiki map [1]

Two-dimensional Yamaguti-Ushiki map

$$\left.\begin{aligned} v_{n+1} &= -y_n + 2v_n - {v_n}^3, \\ y_{n+1} &= v_n. \end{aligned}\right\} \tag{463}$$

The chaotic behavior of Eqs. (462) and (463) is shown in Fig. 54.

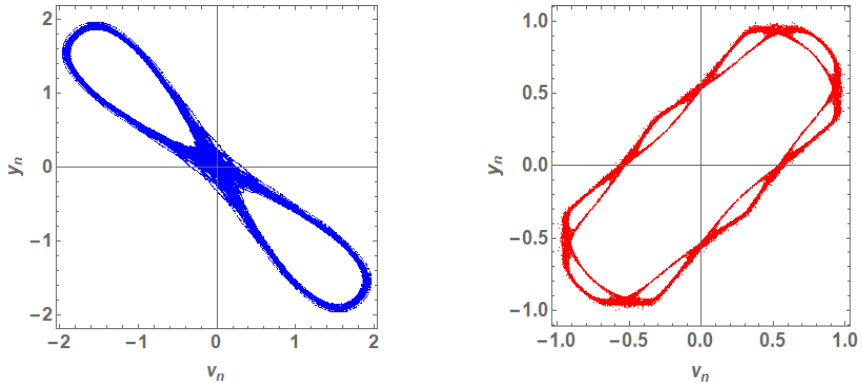

(a) (b)

Figure 54: (a) Chaotic behavior of the two-dimensional map (462). Parameters: $a = 0.34$, $b = 0.2$. Initial conditions: $v_0 = 0.01$, $y_0 = 0.01$. (b) Chaotic behavior of the two-dimensional Yamaguti-Ushiki map (463). Initial conditions: $v_0 = 0.3105$, $y_0 = -0.3105$. Note that when n exceeds 34770, the overflow occurred in the calculation of Eq. (463).

8.3 Chirikov standard map

Consider the Hamiltonian circuit in Fig. 53, where the $v - i$ characteristic of the nonlinear resistor is given by

$$i_R = f(v_R) = k \sin(v_R), \tag{464}$$

where $k > 0$ is a constant. The nonlinear resistor is active since the instantaneous power $P_R(t)$ consumed by the nonlinear resistor satisfies

$$P_R(t) \triangleq v_R(t)\, i_R(t) = v_R(t)\, \{k \sin(v_R(t))\} < 0, \tag{465}$$

for $\pi < v_R(t) < 3\pi$.

The dynamics of this circuit is given by

Dynamiccs of the Hamiltonian circuit

$$\frac{d^2v}{dt^2} - k\sin(v) = 0, \tag{466}$$

where v denotes the voltage across the FNDR and we assume that $G = 1$.

By setting $p = \dfrac{dv}{dt}$, Eq. (466) can be transformed into the form

Hamilton's equation

$$\left.\begin{aligned} \frac{dv}{dt} &= \frac{\partial H(x,\, p)}{\partial p} = p, \\ \frac{dp}{dt} &= -\frac{\partial H(x,\, p)}{\partial v} = k\sin(v). \end{aligned}\right\} \tag{467}$$

Using the Euler method, we can approximate Eq. (467) by

$$\left.\begin{aligned} \frac{v(t+\Delta t) - v(t)}{\Delta t} &= p(t), \\ \frac{p(t+\Delta t) - p(t)}{\Delta t} &= k\sin(v(t)). \end{aligned}\right\} \tag{468}$$

If we set $\Delta t = 1$, $v_n \triangleq v(t + n\Delta t)$, and $p_n \triangleq p(t + n\Delta t)$, then we obtain from Eq. (468)

Discretized equation

$$\left.\begin{aligned} v_{n+1} - v_n &= p_n, \\ p_{n+1} - p_n &= k\sin(v_n), \end{aligned}\right\} \tag{469}$$

where $n = 0, 1, 2, \cdots$. We can rewrite Eq. (469) in the following form

Modified Chirikov standard map

$$\left.\begin{aligned} v_{n+1} &= v_n + p_n, \\ p_{n+1} &= p_n + k\sin(v_n), \end{aligned}\right\} \tag{470}$$

where we take v_n and p_n modulo 2π. This equation is considered to be a modified version of the standard Chirikov map. If we replace p_n on the right hand side of the first equation with p_{n+1}, then we obtain the original Chirikov standard map [37], which is defined by

Chirikov standard map

$$\left.\begin{aligned} v_{n+1} &= v_n + p_{n+1}, \\ p_{n+1} &= p_n + k\sin(v_n), \end{aligned}\right\} \tag{471}$$

where we also take v_n and p_n modulo 2π. Compare the the right-hand side of the first equation in Eqs. (470) and (471). The chaotic behaviors of Eqs. (470) and (470) are shown in Figs. 55 and 56, respectively.

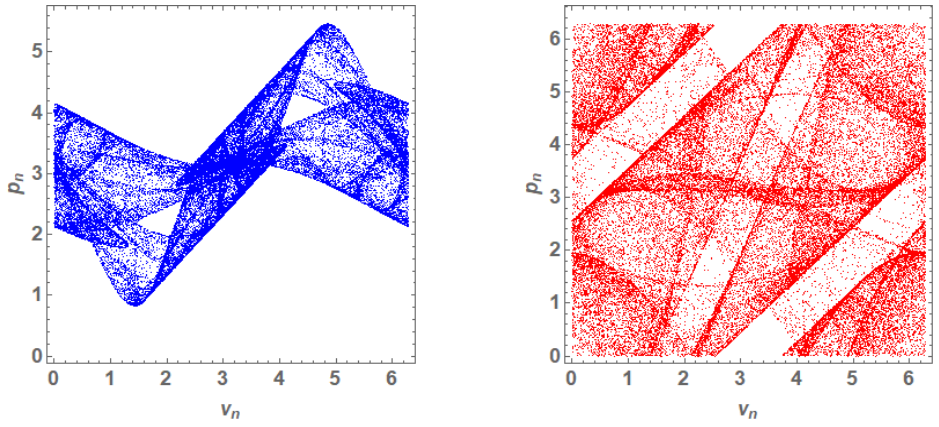

(a) (b)

Figure 55: Chaotic behavior of the modified Chirikov standard map (470) for two different parameters. (a) Parameter: $k = 2$. Initial conditions: $v_0 = 5$, $p_0 = 3.65$. (b) Parameter: $k = 4$. Initial conditions: $v_0 = 5$, $p_0 = 3.65$.

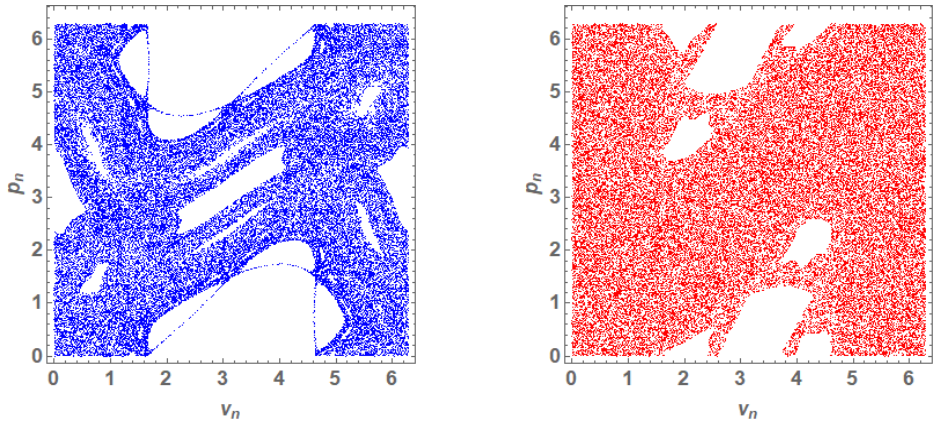

(a) (b)

Figure 56: Chaotic behavior of the original Chirikov standard map (471) for two different parameters. (a) Parameter: $k = 1.5$. Initial conditions: $v_0 = 5$, $y_0 = 3.65$. (b) Parameter: $k = 2.5$. Initial conditions: $v_0 = 5$, $y_0 = 3.65$.

8.4 Hénon-Heiles system.

Consider the circuit in Fig. 57, which consists of two frequency-dependent negative resistors (FNDRs) and two controlled current sources. The dynamics of the circuit is given by

Dynamics of the controlled circuit

$$\left.\begin{aligned} \frac{d^2v_1}{dt^2} + f_1(v_1,\, v_2) = 0, \\ \frac{d^2v_2}{dt^2} + f_2(v_1,\, v_2) = 0, \end{aligned}\right\} \tag{472}$$

where v_1 and v_2 are the voltages across the left FNDR and the right FNDR, respectively, and $f_1(v_1,\, v_2)$ and $f_2(v_1,\, v_2)$ are scaler functions of v_1 and v_2.

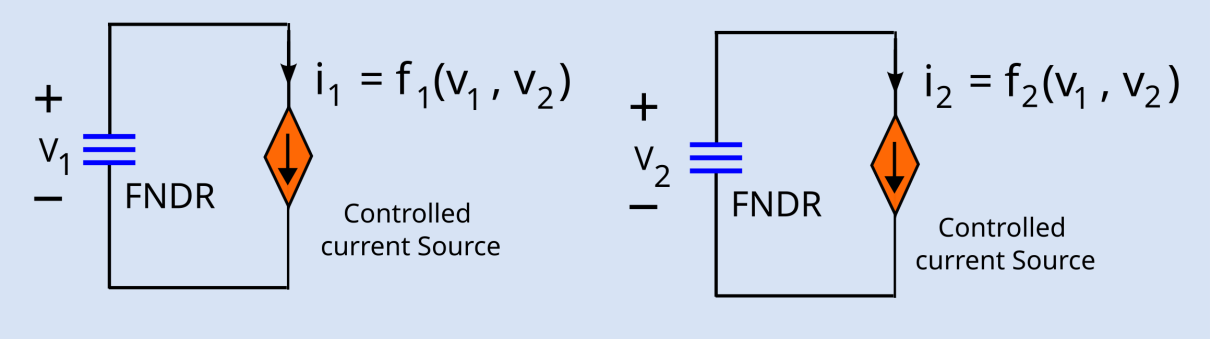

Figure 57: Hamiltonian circuit, which consists of two frequency-dependent negative resistors (FNDRs) and two controlled current sources, where v_1 and v_2 are the voltages across the left FNDR and the right FNDR, respectively, and i_1 and i_2 are the output currents of the left controlled current source and the right controlled current source which are defined by $f_1(v_1,\, v_2)$ and $f_2(v_1,\, v_2)$, respectively.

If we set $p_1 = \dfrac{dv_1}{dt}$ and $p_2 = \dfrac{dv_2}{dt}$, then Eq. (472) can be written as

$$\left.\begin{aligned} \frac{dv_1}{dt} &= p_1, \\ \frac{dp_1}{dt} &= -f_1(v_1,\, v_2), \\ \frac{dv_2}{dt} &= p_2, \\ \frac{dp_2}{dt} &= -f_2(v_1,\, v_2). \end{aligned}\right\} \tag{473}$$

Assume that $f_1(v_1,\, v_2)$ and $f_2(v_1,\, v_2)$ satisfy the relation

$$\left.\begin{aligned} f_1(v_1,\, v_2) = \frac{\partial V(v_1,\, v_2)}{\partial v_1}, \\ f_2(v_1,\, v_2) = \frac{\partial V(v_1,\, v_2)}{\partial v_2}, \end{aligned}\right\} \tag{474}$$

where $V(v_1,\, v_2)$ is the scaler function of v_1 and v_2. Then, Eq, (473) becomes Hamilton's equation

Hamilton's equation

$$\left.\begin{aligned} \frac{dv_1}{dt} &= p_1 \\ \frac{dp_1}{dt} &= -\frac{\partial V(v_1,\, v_2)}{\partial v_1}, \\ \frac{dv_2}{dt} &= p_2 \\ \frac{dp_2}{dt} &= -\frac{\partial V(v_1,\, v_2)}{\partial v_2}, \end{aligned}\right\} \tag{475}$$

where the Hamiltonian $H(v_1,\, v_2,\, p_1,\, p_2)$ is given by

Hamiltonian

$$H(v_1,\, v_2,\, p_1,\, p_2) = \frac{p_1^2}{2} + \frac{p_2^2}{2} + V(v_1,\, v_2). \tag{476}$$

Assume that $V(v_1,\, v_2)$ is given by

$$V(v_1,\, v_2) = \frac{{v_1}^2 + {v_2}^2}{2} + {v_1}^2 v_2 - \frac{{v_2}^3}{3}. \tag{477}$$

Then $f_1(v_1,\, v_2)$ and $f_2(v_1,\, v_2)$ are described by

$$\left.\begin{aligned} f_1(v_1,\, v_2) &= \frac{\partial V(v_1,\, v_2)}{\partial v_1} &&= v_1 + 2v_1 v_2, \\ f_2(v_1,\, v_2) &= \frac{\partial V(v_1,\, v_2)}{\partial v_2} &&= v_2 + {v_1}^2 - {v_2}^2, \end{aligned}\right\} \tag{478}$$

and Eq. (475) is equivalent to the Hénon-Heiles equation:

Hénon-Heiles equation

$$\left.\begin{aligned} \frac{dv_1}{dt} &= p_1 \\ \frac{dp_1}{dt} &= -v_1 - 2v_1 v_2, \\ \frac{dv_2}{dt} &= p_2, \\ \frac{dp_2}{dt} &= -v_2 - {v_1}^2 + {v_2}^2. \end{aligned}\right\} \tag{479}$$

Substituting Eq. (478) into Eq. (472), we obtain the dynamics of the circuit

Dynamics of the controlled circuit

$$\left.\begin{aligned} &\frac{d^2x}{dt^2} + x + 2xy = 0, \\ &\frac{d^2y}{dt^2} + y + x^2 - y^2 = 0, \end{aligned}\right\} \tag{480}$$

where we set $x = v_1$ and $y = v_2$.

In this paper, we descretize the above equation using a second-order central difference. That is, we obtain the following discretized equation from Eq. (480)

$$\left.\begin{aligned} &\frac{x(t+\Delta t) - 2x(t) + x(t-\Delta t)}{(\Delta t)^2} + x(t) + 2x(t)y(t) = 0, \\ &\frac{y(t+\Delta t) - 2y(t) + y(t-\Delta t)}{(\Delta t)^2} + y(t) + x(t)^2 - y(t)^2 = 0. \end{aligned}\right\} \tag{481}$$

If we set $\Delta t = 1$, $x_n \triangleq x(t + n\Delta t)$, and $y_n \triangleq y(t + n\Delta t)$, then we obtain

$$\left.\begin{aligned} &x_{n+1} - 2x_n + x_{n-1} + x_n + 2x_n y_n = 0, \\ &y_{n+1} - 2y_n + y_{n-1} - 2y_n + y_n + {x_n}^2 - {y_n}^2 = 0. \end{aligned}\right\} \tag{482}$$

Define $w_{n+1} = x_n$ and $z_{n+1} = y_n$. Then we get the discretized Hënon-Heiles equation [38]:

Discretized Hénon-Heiles equation

$$\left.\begin{aligned} w_{n+1} &= x_n, \\ x_{n+1} &= x_n - 2x_n y_n - w_n, \\ z_{n+1} &= y_n, \\ y_{n+1} &= y_n - z_n + y_n - {x_n}^2 + {y_n}^2. \end{aligned}\right\} \tag{483}$$

The chaotic behavior of the discretized Hénon-Heiles equation (483) is shown in Fig. 58.

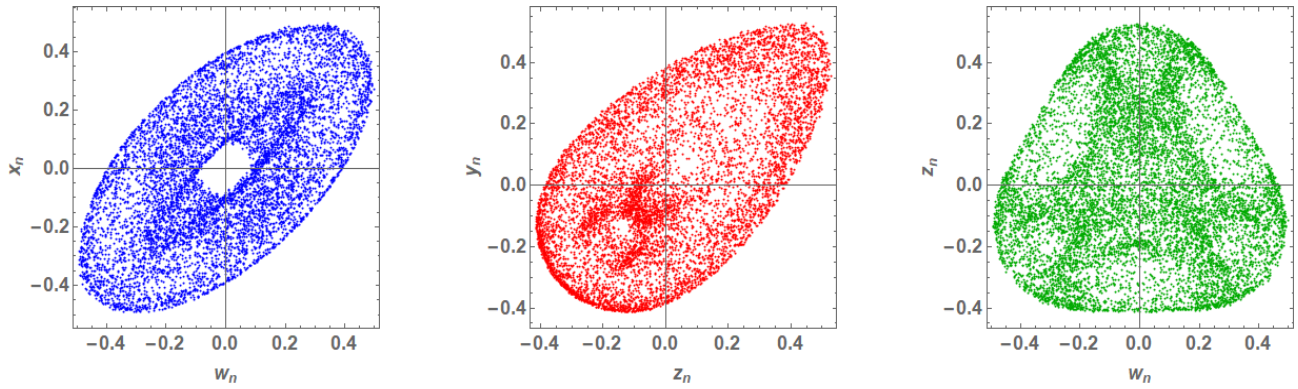

(a) (w_n, x_n)-plane (b) (z_n, y_n)-plane (c) (w_n, z_n)-plane

Figure 58: Chaotic behavior of the discretized Hénon-Heiles equation (483). Initial conditions: $w_0 = 0.28$, $x_0 = 0$, $y_0 = 0$, $z_0 = 0.28$.

Consider next the function $V(v_1, v_2)$ is given by

$$V(v_1, v_2) = \frac{2{v_1}^2 + {v_2}^2}{2} + {v_1}^2 v_2 - \frac{{v_2}^3}{3}. \tag{484}$$

Then the the discretized Hamilton's equation is given by

Discretized Hamiton's equation

$$\left.\begin{aligned} w_{n+1} &= x_n, \\ x_{n+1} &= -2x_n y_n - w_n, \\ z_{n+1} &= y_n, \\ y_{n+1} &= y_n - z_n + y_n - {x_n}^2 + {y_n}^2. \end{aligned}\right\} \tag{485}$$

Note the difference between the second equation of (483) and (485). The chaotic behavior of the discretized Hamilton's equation (485) is shown in Fig. 59.

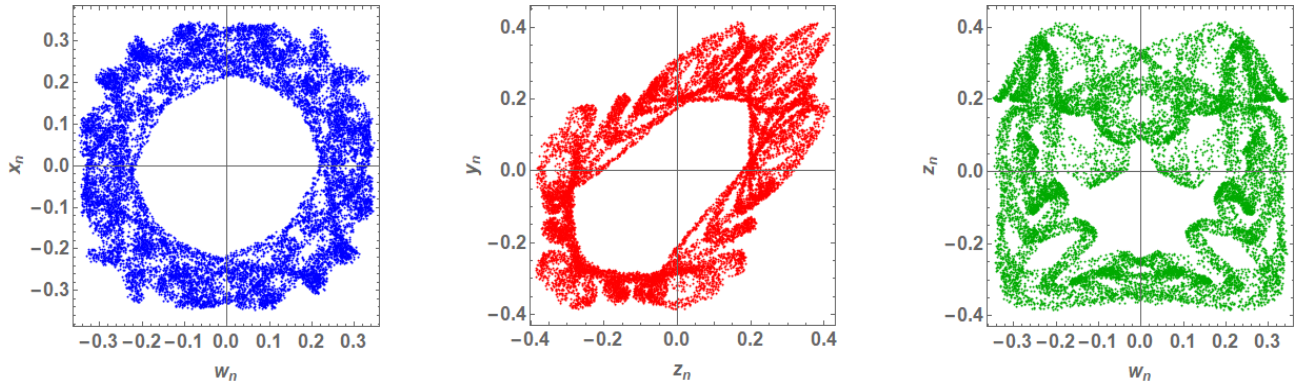

(a) (w_n, x_n)-plane (b) (z_n, y_n)-plane (c) (w_n, z_n)-plane

Figure 59: Chaotic behavior of the discretized Hamilton's equation (485). Initial conditions: $w_0 = 0.2$, $x_0 = 0.2$, $y_0 = 0.2$, $z_0 = 0.2$.

9 Conclusion

We have shown that many well-known chaotic maps can be generated by discretizing the equations of memristor or nonlinear resistor circuits using the Euler method or the central difference method. We have also shown that a wide variety of nonlinear maps, such as those found in engineering, physics, chemistry, biology, and ecological systems, are closely related to discretized memristor or nonlinear resistor circuit equations. These circuits usually contain the active element. It seems that discretizing the memristor or nonlinear resistor circuit equations is one of the most promising methods to find interesting chaotic maps.

Acknowledgment

I would like to thank Professor Leon Chua (University of California, Berkeley) for sending me many important papers on the classification of memristors more than 10 years ago.

References

[1] Yamaguti, M. & Ushiki, S. [1981] "Chaos in numerical analysis of ordinary differential equations," *Physica D* **3**(3), 618-626.

[2] Chua, L.O. [1971] "Memristor–The missing circuit element", *IEEE Trans. Circuit Th.* **CT-18** (5), 507-519.

[3] Chua, L.O. & Kang, S.M. [1976] "Memristive devices and systems," *Proc. IEEE* **64**(2), 209-223.

[4] Chua, L.O. [2012] "The fourth element," *Proc. IEEE* **100**(6), 1920-1927.

[5] Strukov, D., Snider, G., Stewart, D., & Williams, R.S. [2008] "The missing memristor found," *Nature* **453**, 80-83.

[6] Chua, L. [2015] "Everything you want to know about memristors, but are afraid to ask," *Radioengineering* **24**(2), 319-368.

[7] Itoh, M. [2023] "Non-Volatility Property and Pinched Hysteresis Loops of 2-terminal Devices and Memristors," *viXra*: 2302.0055 [Category: Mathematical Physics].

[8] Itoh M. & Chua, L.O. [2016] "Parasitic Effects on Memristor Dynamics," *International Journal of Bifurcation and Chaos* **26**(6), (1630014-1)-(1630014-55).

[9] Wang, R., Yang, J.-Q., Mao, J.-Y., Wang, Z.-P., Wu, S., Zhou, M., Chen, T., Zhou, Y. & Han, S.-T. [2020] "Recent advances of volatile memristors: Devices, mechanisms, and applications," *JAdv. Intell. Syst.* **2**(9), 2000055.

[10] Yu, Y., Wang, C., Wen, Y., Jiang, C., Abrahams, I., Du,Z., Sun, J., & Huang, X. [2022] "Realization of volatile and non-volatile resistive switching with N-TiO2 nanorod arrays based memristive devices through compositional control," *Journal of Alloys and Compounds* **909**, 164743.

[11] Deleanu, D.N. [2014] "On the selective synchronization of some dynamical systems that exhibit chaos," *Proc. of CHAOS2014*, 81-90, Lisbon, Portugal.

[12] Anh, N.H.T., Liet, D.V., & Kawamoto, S. [2016] "Nonlinear dynamics of two-dimensional chaos Map and fractal set for snow crystal," *Chaotic Modeling and Simulation (CMSIM)* **1**: 21-31.

[13] Hayama, S. [1994] "Fundamentals of Chaotic Dynamics," Gendai-Sugakusha (in Japanese).

[14] Hayama, S. [1999] "A New Qualitative Change in Chaotic Dynamics under Basin Riddling," *Progress of Theoretical Physics* **101**(3), 519-539.

[15] Zhao, M., Xuan, Z. & Li, C. [2016] "Dynamics of a discrete-time predator-prey system," *Advances in Continuous and Discrete Models* **2016**(1), 191.

[16] Wua, Y., Yang, G., Jin, H., & Noonanaa, J.P. [2012] "Image encryption using the two-dimensional logistic chaotic map," *Journal of Electronic Imaging* **21**(1), 013014.

[17] Chua, L. [2011] "Resistance switching memories are memristors," *Appl. Phys. A* **102**, 765-783.

[18] Chossat, P. & Golubitsky, M. [1988] "Symmetry increasing bifurcation of chaotic attractors," *Physica D* **32**, 423–436.

[19] Hénon, M. [1976] "A two-dimensional mapping with a strange attractor," *Comm. Math. Phys.* **50(1)**, 69-77.

[20] Pickover, C.A. [1995] "The Pattern Book: Fractals, Art, and Nature," *World Scientific Publishing Company, Hackensack, NJ* 197-198.

[21] Lorenz, E.N. [1963] "Deterministic nonperiodic flow," *Journal of the Atmospheric Sciences* **20**(2) 130–141.

[22] Ikeda, K. [1979] "Multiple-valued stationary state and its instability of the transmitted light by a ring cavity system," *Optics Communications* **30**(2), 257–261.

[23] Hammel, S.M., Jones, C.K.R.T., & Moloney, J.V. [1985] "Global dynamical behavior of the optical field in a ring cavity," *Journal of the Optical Society of America B* **2**(4), 552-564.

[24] Rössler, O.E. [1976], "An Equation for Continuous Chaos," *Physics Letters* **57A** (5), 397–398.

[25] Itoh M. & Chua, L.O. [2017] "Dynamics of Hamiltonian Systems and Memristor Circuits," *International Journal of Bifurcation and Chaos* **27**(2), (1630014-1)-(1630014-55).

[26] Ouannas, A. & Abu-Saris, R. [2016] "On Matrix Projective Synchronization and Inverse Matrix Projective Synchronization for Different and Identical Dimensional Discrete-Time Chaotic Systems," *Journal of Chaos* **2016**, 1-7.

[27] Peitgen, H.-O., Jürgens, H., & Saupe, D. [1992] "Chaos and Fractals: New Frontiers of Science," New York: Springer-Verlag, 672.

[28] Bremer, C.L. & Kaplan, D.T. [2001] "Markov chain Monte Carlo estimation of nonlinear dynamics from time series," *Physica D* **160**, 116–126.

[29] Jouini L., Ouannas, A., Khennaoui, A.A., Wang, X., Grassi, G., & Pham, V.T. [2019] "The fractional form of a new three-dimensional generalized Hénon map," *Advances in Difference Equations* **2019** 122.

[30] Mira C. [2014]. ABOUT WHAT IS CALLED "GUMOWSKI-MIRA MAP," Technical Report, ResearchGate. https://www.researchgate.net/publication/263469351.

[31] Martin, B. [1989] "Graphic Potential of Recursive Functions," in *Computers in Art, Design and Animation* (Landsdown J. and Earnshaw, R. A. eds.), New York: Springer–Verlag, 109–129.

[32] Devaney, R.L., [1984] "A Piecewise Linear Model for the Zones of Instability of an Area Preserving Map," *Physica D* **10**, 387-393.

[33] Kawakami, H. [1990] "Chaos CG Collection," Saiensu-Sha (in Japanese).

[34] Bao-long, C. [1987] "Chaotic behavior in the Helleman mapping," *Applied Mathematics and Mechanics* **8**, 649–653.

[35] Madan, R.N. (1993) *Chua's Circuit: A Paradigm for Chaos* (World Scientific, Singapore).

[36] Hirsch, M.W., Smale, S., and Devaney, R.L. (2003) *Differential Equations, Dynamical Systems, and an Introduction to Chaos, Second Edition* (Elsevier Academic Press, Amsterdam).

[37] Chirikov, B. & Shepelyansky, D. (2008) "Chirikov standard map," *Scholarpedia* **3**(3):3550.

[38] Hénon, M. & Heiles, C. [1964]. "The applicability of the third integral of motion: Some numerical experiments," *The Astronomical Journal* **69** 73–79.

Appendix

Classification of Memristors

A voltage-controlled memristor can be classified into four classes [6, 7]:

- voltage-controlled ideal memristor

$$\left.\begin{array}{rcl} i & = & G(\varphi)v, \\ \dfrac{d\varphi}{dt} & = & v. \end{array}\right\} \tag{486}$$

- voltage-controlled ideal generic memristor

$$\left.\begin{array}{rcl} i & = & G(x)v, \\ \dfrac{dx}{dt} & = & \hat{g}(x)v. \end{array}\right\} \tag{487}$$

- voltage-controlled generic memristor

$$\left.\begin{array}{rcl} i & = & \tilde{G}(\boldsymbol{x})v, \\ \dfrac{d\boldsymbol{x}}{dt} & = & \tilde{\boldsymbol{g}}(\boldsymbol{x},\ v). \end{array}\right\} \tag{488}$$

- voltage-controlled extended memristor

$$\left.\begin{array}{rcl} i & = & \hat{G}(\boldsymbol{x},\ v)v, \\ & & \mid \hat{G}(\boldsymbol{x},\ 0) \mid < \infty, \\ \dfrac{d\boldsymbol{x}}{dt} & = & \tilde{\boldsymbol{g}}(\boldsymbol{x},\ v). \end{array}\right\} \tag{489}$$

  Here, i, v, φ, and $\boldsymbol{x}$ indicate the terminal current, the terminal voltage, the flux, and the state variable of the voltage-controlled memristor, respectively, $G(\cdot)$, $\tilde{G}(\cdot)$, $\hat{G}(\cdot)$, and $\hat{g}(\cdot)$ are continuous scalar-valued functions, $\boldsymbol{x} = (x_1,\ x_2,\ \cdots,\ x_n) \in \mathbb{R}^n$, and $\tilde{\boldsymbol{g}} = (\tilde{g}_1,\ \tilde{g}_2,\ \cdots,\ \tilde{g}_n) : \mathbb{R}^n \to \mathbb{R}^n$.

Similarly, a current-controlled memristor can be classified into four classes [6]:

- current-controlled ideal memristor

$$\left.\begin{array}{rcl} v & = & R(q)i, \\ \dfrac{dq}{dt} & = & i. \end{array}\right\} \tag{490}$$

- current-controlled ideal generic memristor

$$\left.\begin{array}{rcl} v & = & R(x)i, \\ \dfrac{dx}{dt} & = & \hat{f}(x)i. \end{array}\right\} \tag{491}$$

- current-controlled generic memristor

$$\left.\begin{array}{rcl} v & = & \tilde{R}(\boldsymbol{x})i, \\ \dfrac{d\boldsymbol{x}}{dt} & = & \tilde{\boldsymbol{f}}(\boldsymbol{x},\ i). \end{array}\right\} \tag{492}$$

- current-controlled extended memristor

$$\left.\begin{array}{rcl} v & = & \hat{R}(\boldsymbol{x},\ i)i, \\ & & |\ \hat{R}(\boldsymbol{x},\ 0)\ | < \infty, \\ \dfrac{d\boldsymbol{x}}{dt} & = & \tilde{\boldsymbol{f}}(\boldsymbol{x},\ i). \end{array}\right\} \tag{493}$$

Here, $R(\cdot)$, $\tilde{R}(\cdot)$, $\hat{R}(\cdot)$, and $\hat{f}(\cdot)$ are continuous scalar-valued functions, $\boldsymbol{x} = (x_1,\ x_2,\ \cdots,\ x_n) \in \mathbb{R}^n$, and $\tilde{\boldsymbol{f}} = (\tilde{f}_1,\ \tilde{f}_2,\ \cdots,\ \tilde{f}_n) : \mathbb{R}^n \to \mathbb{R}^n$.